Antimicrobial Peptides – Structure, Function and Resistance

Thomas Vargues

Doctor of Philosophy

The University of Edinburgh

2009

Declaration

I, Thomas Vargues, hereby certify that this thesis has been composed by myself, and that it is a record of my work, and that it ahs not been accepted in partial or complete fulfilment of any other degree or professional qualification.

Thomas Vargues

University of Edinburgh

2009

Acknowledgements

First of all I would like to thank Dr Dominic Campopiano for giving me the opportunity to do a PhD in this very interesting field. His constant supervision and his scientific “flair” kept me motivated and focused.

I would like to thanks Prof John Govan for allowing me to study in his laboratory at little France and for sharing very interesting discussions in this research field.

I have to thank Dr Derek Macmillan from University College London and Dr Dusan Uhrin for their help and technical support in research fields I was not familiar with.

A special thank for Emily Seo who helped me a lot when things were not at their best. I would like to thank Dave Clarke and Gareth Morrison for their team support but also Marine, Jon and Karin for all the help provided and all members of Lab 229, past and present.

I don’t know where to start to thank my cousin Julien Valton for priceless help and “positive thinking” towards this thesis. I am also grateful to Gregory Vernier for his advices and experience regarding many topics linked to this study. I really enjoyed such endless and helpless discussions across the ocean. We will meet for sure around a good “Whiskass chaton”. I would also like to thank Carole Mathevon for all the advices provided and nice chats over the phone.

An enormous thank for all my family for things only they know. Florent, Guillaume, Augustin, Mum, Dad and Mam. I think my grandfather would have been proud of this also…

Finally, a very special thank will go for a tricky “weegie” girl, Aileen who gave me joy and hope for these last two years. Your humour and constant support were priceless to me.

And thanks for the one I forgot…….

Higher eukaryotes produce a vast range of antimicrobial peptides (AMPs) that play important roles in their defence against microbial infection. Beta defensins are small (3-5 kDa), cationic peptides that display broad, potent antimicrobial activity against a range of microbes and also act as chemoattractants of important immunomodulatory cells. To generate highly pure peptides for structural and functional studies, we developed a method to prepare recombinant human beta defensin-2 (HBD2). The *HBD2* gene was synthesised by recursive PCR with codons optimised for expression in *Escherichia coli.* HBD2 was expressed as an insoluble fusion to a His-tagged ketosteroid isomerase. After cleavage from the fusion with cyanogen bromide, ^{1}H NMR spectroscopy and mass spectrometry confirmed that the oxidised HBD2 was folded and possessed the correct β-defensin disulfide bond topology. The recombinant HBD2 was active against *E. coli*, *P. aeruginosa*, *S. aureus* and *C. albicans* and was also a chemoattractant against HEK293 cells expressing the chemokine receptor CCR6. ^{15}N-labelled HBD2 was also prepared and was highly suitable for future structural studies. Since defensins are thought to interact with bacterial membranes we also tested the recombinant HBD2 in biophysical studies (surface plasmon resonance, SPR, Biacore). We observed different binding to artificial model membranes containing either *E. coli* Kdo_2-lipid A or phospholipids.

Bacterial resistance to AMPs has been linked to the covalent modification of the outer membrane lipid A by 4-amino-4-deoxy-L-arabinose (L-Ara4N). This neutralises the charge of the LPS, thereby decreasing the electrostatic attraction of cationic peptides to the bacterial membrane. The pathogen *Burkholderia cenocepacia* displays extremely high resistance to AMPs and other antibiotics and the Ara4N pathway appears to be essential. To explore this further we expressed recombinant forms of two enzymes (ArnB and ArnG) from the *B. cenocepacia* Ara4N pathway. Purified ArnB is a pyridoxal 5'-phosphate (PLP)-dependent transaminase and we tested its ability to bind amino acid substrates. We investigated the binding of inhibitors L- and D-cycloserine to ArnB and tested their antibiotic activity against *Burkholderia* strains. We also studied the *B. cenocepacia* ArnG – a proposed membrane protein undecaprenyl-L-Ara4N flippase – and showed that the protein behaved as a dimer by non-denaturing gel analysis. The *B. cenocepacia* ArnG failed to complement *E. coli* knock-out strains encoding the equivalent flippase proteins ArnE and ArnF, suggesting that ArnG is a *Burkholderia*-specific protein.

Abbreviations

Aa	Amino acid(s)
AMP	Antimicrobial peptide
APS	Ammonium persulfate
ArnT	L-Ara4N transferase
Bcc	Burkholderia cepacia complex
CF	Cystic fibrosis
CFTR	Cystic fibrosis transmembrane conductance regulator
cfu	Colony forming units
Da	Dalton
DDM	n-Dodecyl-β-maltoside
DDT	Dithiothreitol
EDTA	Ethylenediaminetetracetic acid
ESI-MS	Electrospray ionisation mass spectroscopy
FPLC	Fast protein liquid chromatography
FT-ICR	Fourier transform ion cyclotron resonance
HBD1	Human β-defensin-1
HBD2	Human β-defensin-2
HBD3	Human β-defensin-3
HBD4	Human β-defensin-4
g	Gravity (centrifugal force)
HEPES	N-(2-Hydroxyethyl)piperazine-N`-(2-ethanesulfonic acid)
IMAC	Immobilized metal affinity chromatography
IPTG	Isopropyl-1-thio-β–D-galactopyranoside
ISA	Isosensitest agar

ISB	Isosensitest broth
kDa	Kilo daltons
Kdo	3-deoxy-D-manno-oct-2-ulosonic acid
Ko	D-*glycero*-α-D-talo-oct-2-ulosonic acid
L-Ara4N	4-amino-4-deoxy-β-L-arabinose
LB	Luria Bertani
LC-MS	Liquid chromatography mass spectrometry
LD	Lethal dose
LPS	Lipopolysaccharide
MIC	Minimum inhibitory concentration
PAGE	Polyacrylamide gel electrophoresis
PLP	Pyridoxal 5'-phosphate
PMP	Pyridoxamine phosphate
PBS	Phosphate buffered solution
PCR	Polymerase chain reaction
PET	Phospoethanolamine
PMB	Polymyxin B
SDS	Sodium dodecylsulfate
SPR	Surface plasmon resonance
SPPS	Solid Phase Peptide Synthesis
TB	Terrific broth
TCEP	Tris carboxyethylphosphine
TFA	Trifluoroacetic acid
Tris	Tris [hydroxymethyl] aminomethane

Ugd	UDP-glucose dehydrogenase
UV-Vis	Ultraviolet- visible spectroscopy

Table of Contents

Attached publications:

Vargues T, Morrison GJ, Seo ES, Clarke DJ, Fielder HL, Bennani J, Pathania U, Kilanowski F, Dorin JR, Govan JR, Mackay CL, Uhrín D, Campopiano DJ. (2009) Efficient production of human beta-defensin 2 (HBD2) in Escherichia coli. *Protein Pept. Lett.* **16** 668-676.

Seo ES, **Vargues T**, Clarke DJ, Uhrín D, Campopiano DJ. (2009) Preparation of isotopically labelled recombinant beta-defensin for NMR studies. *Protein Expr. Purif.* **65** 179-184.

List of Figures

Chapter 1: Defensins - Multifaceted Peptides of the Innate and Adaptive

Chapter 2: Expression, Purification and Characterisation of the Mature Recombinant Human β-Defensin 2 (HBD2).

Chapter 3: Comparison of Synthetic and Recombinant Production of Defensins

Chapter 4: Into the Resistance

Chapter 5: Characterisation of Enzymes Involved in Ara4N biosynthesis in *Burkholderia cenocepacia*

Chapter 6:

List of Tables

Chapter 1: Defensins - Multifaceted Peptides of the Innate and Adaptive Immune System

Chapter 2: Expression, Purification and Characterisation of the Mature Recombinant Human β-Defensin 2 (HBD2).

Chapter 5: Characterisation of Enzymes Involved in Ara4N biosynthesis in *Burkholderia cenocepacia*.

Chapter 6: Materials & Methods

Chapter 1: Defensins - Multifaceted Peptides of the Innate and Adaptive Immune System

“There is probably no chemotherapeutic drug to which in suitable circumstances the bacteria cannot react by in some way acquiring ‘fastness’ [resistance]”
- Alexander Fleming, 1946

1.1 The Expanding Diversity of The Antimicrobial Peptide Family

Defensins belong to a large family of small molecules called antimicrobial peptides (AMPs). To date more than 900 examples of such AMPs have been reported and classified [1]. This classification is divided into different categories based on their structures and topologies. They are spread throughout all kingdoms and phylum and display a well-recognized broad-spectrum antimicrobial activity at physiological concentrations. Growing interest within this field has also allowed the observations of their potent action towards fungi and viruses. AMPs are therefore considered as important components of the innate immune system and are also effective modulators of the adaptive immune system. An online database for antimicrobial peptides is available at http://aps.unmc.edu/AP/main.php [2]. The majority of peptides found in this database (97%) are less than 50 amino acids long and have an average length of 28 residues. Other common traits associated with this family (96%) are the net positive charge shared by such peptides (also known as cationic antimicrobial peptides, cAMPS) and also their ability to adopt an organised fold with hydrophobic patches [3]. These two characteristics define of their amphipathic nature. Interestingly, small anionic pro-peptides have been described and their antimicrobial activities have been tested against both Gram-negative and Gram-positive bacteria. However such peptides remain marginal in comparison with their cationic homologues and are restricted to a few animal species [4]. Different groups of peptides within the cAMPs family have emerged in the last few decades; these include the epidermal cathelicidins [5] and defensins [6] which are human peptides. Other classes of AMPs have been isolated, characterised and classified mainly under their structural differences. Examples of their diversity are given in Table 1.1.

The growing interest in AMPs over the years has encouraged researchers to investigate their potential use as new therapeutics [7, 8, 9]. For example their structural and functional diversity has made such peptides ideal candidates for novel antibiotics. It is thought that resistance towards AMPs requires more than a simple genetic “trick” to counterfeit their action as a drastic modification of the lipid membrane composition and topology is required [10, 11].

Type	AMPs	Characteristics
Linear α-helical peptides	Cathelicidin (LL37) (*human*) Cecropin, melittin, andropin, ceratotoxin (*insect*) Maiganin 2 (*frog*) Buforin II (*amphibian*) CAP18 (*rabbit*)	No cysteine, adopt an amphipathic α-helical structure when they enter a membrane
Linear non α-helical peptides	Histatin 5 (*human*) PR39 (*pig*) Indolicidin (*cow*) Apidaecins, abaecin, (*honeybee*)	Proline, arginine, histidine or tryptophane-rich peptides
One or two disulfide bonds	Bactenecin 1 (*cow*) Protegrin 1 (*pig*)	
Three or more disulfide bonds	α-Defensins, β-Defensins, (*human*) θ-Defensins (*monkey*) Spheniscins (*king pinguin*) Hepcidin (*human*)	Rigid framework constituted with an antiparallel β-sheets motif (except for θ-Def.)

Table 1.1. Examples of AMPs diversity. A non-exhaustive list of AMPs organised according to their structure and S-S bond topology.

1.2 Defensins

1.2.1 Structural Classification

Defensins are a subset of the larger and expanding AMPs family and are characterised by a triple β-sheet fold held together by six conserved cysteine residues that oxidise to form three disulfide (S-S) bonds. Two main subgroups of defensins have been defined according to the topology of these three S-S bonds. Hence the alpha (α-) defensins display a S-S connectivity of Cys_1-Cys_6, Cys_2-Cys_4 and Cys_3-Cys_5 whereas beta (β-) defensins share a Cys_1-Cys_5, Cys_2-Cys_4, Cys_3-Cys_6 S-S connectivity (Fig. 1.1). The α-defensins contain ~29-35 residues while β-defensins present a longer primary sequence that comprises ~40-50 residues. An additional class of defensins have been described, the θ-defensins. θ-Defensins are the most recently identified subfamily of defensins. Rhesus theta-defensins (RTDs), also known as retrocyclins, were isolated from macaque leucocytes [12].

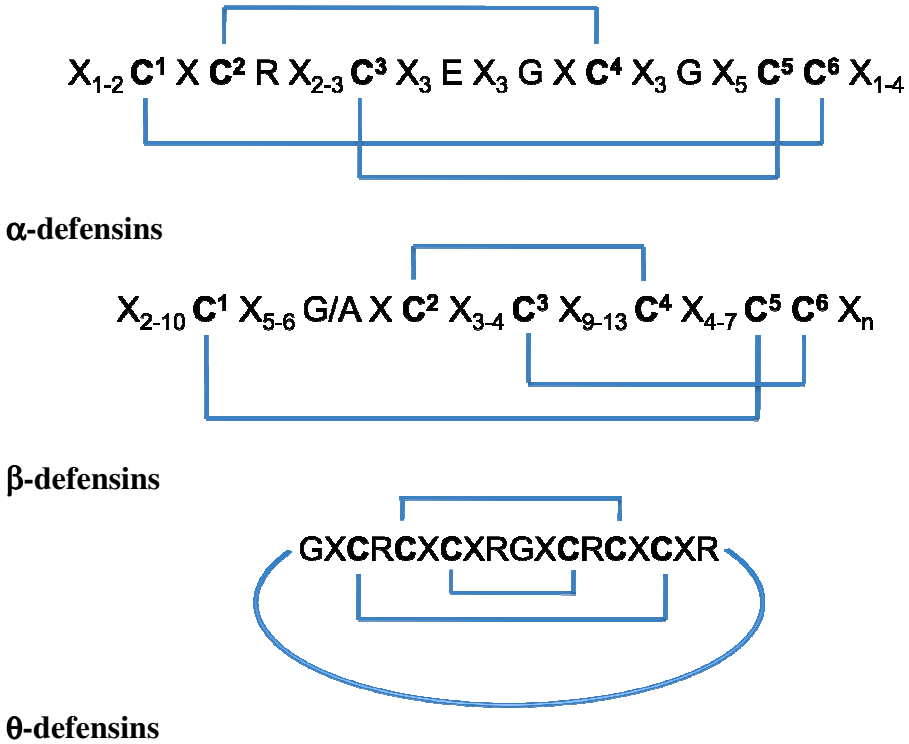

Figure 1.1 The disulfide bridging connectivity in α, β, and θ-defensins. The S-S bond connectivites are indicated with the blue connectors.

This peptide was isolated from the rhesus monkey polymorphonuclear leucocytes (PMNs) [13]. θ-Defensins are cyclic peptides fused at their N- and C- termini but also display three disulfide bridges. The three different disulfide bridge topologies found in the three defensin classes are described in figure 1.1.

1.2.2 From the Innate to the Adaptive immune system

Despite the fact that the antimicrobial function of defensins (discussed later) has been extensively studied and still remains the main focus for a large number of research groups, additional properties have been described and attributed to such molecules.

Mammals share their environment with numerous potentially pathogenic microorganisms. Natural barriers such as mucous membranes and skin protect them from microbial disease. However, when the epithelial "shield" is weakened or breached, invading pathogens are eliminated by the innate immune system, the first protective mechanism employed [14]. This first reaction is followed by a second protective phenomenon called the adaptive immune response.

In the mammalian innate immune response, a rapid mobilised host defence is activated at a basal level in a time quick enough to avoid any microbial replication and therefore an imminent invasion. It includes different cells effectors such as epithelial cells, mast cells, neutrophils, macrophage cells or natural killer cells [15]. Components from invading pathogens (known as Pathogen-associated molecular patterns, PAMPs) activate cell-surface receptors such as Toll-like receptors (TLRs), which results in the release of various mediators such as the complement cascade, cytokines, chemokines and antimicrobial peptides including defensins and cathelicidin. Cathelicidin (LL37/hCAP-18), stored by specific (secondary) granules, is encoded by one gene [16] and expressed on all epithelial areas [17]. When these mediators are released, they recruit and activate PMNs. In humans, α-defensins, also known as human neutrophil peptides (HNP1 to HNP4) are localised in high concentrations in azurophilic granules (primary) and paneth cell granules [18, 19]. Neutrophils in contact with the ingested microorganism release α-defensins into the surroundings such that they reach a high localised concentration of peptides (over 10

mg/ml). Other peptides related to the α-defensin family, human defensin 5 and 6 (HD5 and HD6) are constitutively expressed in the Paneth cells located in the small intestine. From the intestinal crypt HD5 and HD6 are excreted to the lumen [20, 21]. In 2003, Salzman and coworkers demonstrated that transgenic mice expressing HD5 appear to be more resistant against virulent, orally-injected *Salmonella typhimurium* bacteria than non-transgenic candidates [22].

The second major group of defensins, the β-defensins, are also involved in the host defense system. In humans, only four β-defensins (HBD1 to HBD4) have been described and studied in detail to date, however more than 30 loci have been identified in the human genome [23]. HBD1 is constitutively expressed in various tissues [24, 25] in the epithelial cells of the respiratory and urinary tracts [26, 27]. Bals and coworkers have demonstrated that the lack of the mouse β-defensin-1 gene (mBD1), the murine homologue of HBD1, resulted in delayed clearance of *Haemophilus influenzae* from the lungs in a knock-out mouse model [28] and an associated increased load of *Staphylococcus* in the bladder [29]. In contrast to the constitutively expressed HBD1, defensins HBD2, 3 and 4 are inducible peptides produced by epithelial and keratinocytes cells in response to proinflammatory stimuli. This production can be stimulated by various elements such as lipopolysaccharides (LPS), interleukins (IL), tumour necrosis factor (TNF) or histamines [30, 31].

There is no doubt that defensins play a key role in the innate immune system but recent studies have also pointed out their involvement in the adaptive immune response [32]. This response differs from the innate defense response as it is a delayed physiological mechanism that occurs for weeks after a host invasion. If the innate immune reaction is clinically “silent”, the adaptive response always triggers an inflammatory process. However, despite the fact that these two systems have usually been opposed or complemented, recent studies have shown that the immune system could be described as a continuum organisation rather than the dichotomic paradigm by which it is usually referred [33]. Antimicrobial peptides such as defensins could play an important role in this continuum organisation as growing evidence highlights their ability to link the innate to the adaptive immune system.

Various studies have shed light on the interaction of defensins with receptors located on lymphocytes and immature dendritic cells (DCs) that lead to the activation of an adaptive response. Almost 20 years ago Territo and coworkers showed that

HNP1 and HNP2 were chemotactic for human monocytes *in vitro* [34]. The migration of some human T lymphocytes including naïve CD4 and CD8 T cells by human α-defensins was observed. Such peptides were also able to recruit human dendritic cells [35]. Human β-defensins 1, 2 and 3 were reported to be chemotactic for CD4 memory T cells, immature (but not mature) DCs but also for human TNF-α-treated neutrophils [36, 37, 38]. The β-defensins in these studies appear to bind and activate a G-protein-coupled receptor (GPCR), the chemokine-coupled receptor 6 (CCR6). This receptor was previously shown to bind the chemokine MIP-3α (also known as CCL20), but β-defensins display similar structured motifs and charge distribution with this "natural" CCR6 ligand despite very low homology sequences [39]. Interestingly, MIP-3α has also been shown to be microbicidal [40]. The resemblance between the two molecules has led β-defensins to be considered as chemokine-like peptides.

1.2.3 Antiviral Properties

In addition to their biological action in both innate and adaptive systems, defensins have been reported to display antiviral activities. In the mid 1980's, human NP1, NP2 and NP3 were tested against a range of viruses including herpes simplex types 1 and 2 viruses (HSV-1 and HSV-2), influenza A virus, cytomegalovirus and vesicular stomatitis virus. Studies showed that these viruses when preincubated with such peptides have the capacity to lose their property to infect target cells [41]. Similar conclusions were reached with rabbit NP1 and NP2 with the exception of cytomegalovirus and two non-enveloped viruses which retained their infectivity [42]. More recently, the inactivation mechanism of NP1 towards HSV-2 was analysed in detail. This study revealed that despite the fact that NP1 did not prevent glycoproteins from the viral envelope binding to the heparan sulfate receptors located on the host cell, it did prohibit cell-to-cell spreading and viral entry [43]. Moreover, the ability of many defensins to bind glycans specifically has led to the idea that defensins are lectins [44, 45]. The recent study of the human α-defensin 5 (HD5) bound to natural glycoproteins in a self-association and multivalent manner has enhanced the belief that such lectin-like peptides protect humans from viral infection and other invading agents [46]. This antiviral activity appears to be a common trait among the three defensin families. Thus, the rhesus θ-defensins (RTD1-3), α-defensins [47, 48, 49]

and β-defensins (HBD2-3), have also been reported to protect cells from an invasion by viruses such as the human immunodeficiency virus 1 (HIV-1), HSV-1 and HSV-2 viruses. In the θ-defensins family, RTD-2 was the most efficient peptide against HIV-1 and HSV-2 viruses [50]. Concerning the β-defensin family, Quinones-Mateu and coworkers demonstrated that HBD2 and HBD3 peptides could not only inhibit HIV-1 replication, but were also induced by this virus [51]. In contrast, HBD1 expression is highly reduced in alveolar macrophages in patients infected with HIV but not in nasal epithelial cells [52].

1.2.4 Additional Biological Functions

Recent reports have provided new insight into the physiological functions of defensins, in particular the β-subgroup. Seminal studies have identified some relationships between stages of development or types of tumors and the expression patterns of β-defensins [53, 54]. HBD1 was revealed to be a good immunohistochemical marker for the diagnosis of prostate and renal tumors [55].

A remarkable upregulation of HBD1 and HBD3 mRNA was observed in the maturation of keratinocytes indicating a plausible involvement of such peptides in the cell differentiation mechanisms [56]. Moreover, the expression of HBD3 was also observed in osteoarthritic (OA) joints leading Varoga and coworkers to suggest a role for HBD3 in tissue-remodeling processes [57].

Although defensins were originally considered and categorised as merely antimicrobial peptides, which still remains an area of interest for many research programs, it is now clear that this ability constitutes only the “tip of the iceberg”. Many hidden functions were brought to light in the past decade which revealed the extraordinary versatility of such molecules.

Aiming to better understand and clarify the contributions of defensins to different pathways, Lehrer has published a review where he has summarised their role in host defense (Fig. 1.2) [58]. However, the diagram presented in figure 1.2 is non exhaustive as many new defensins implications have been recently described and some remain to be discovered.

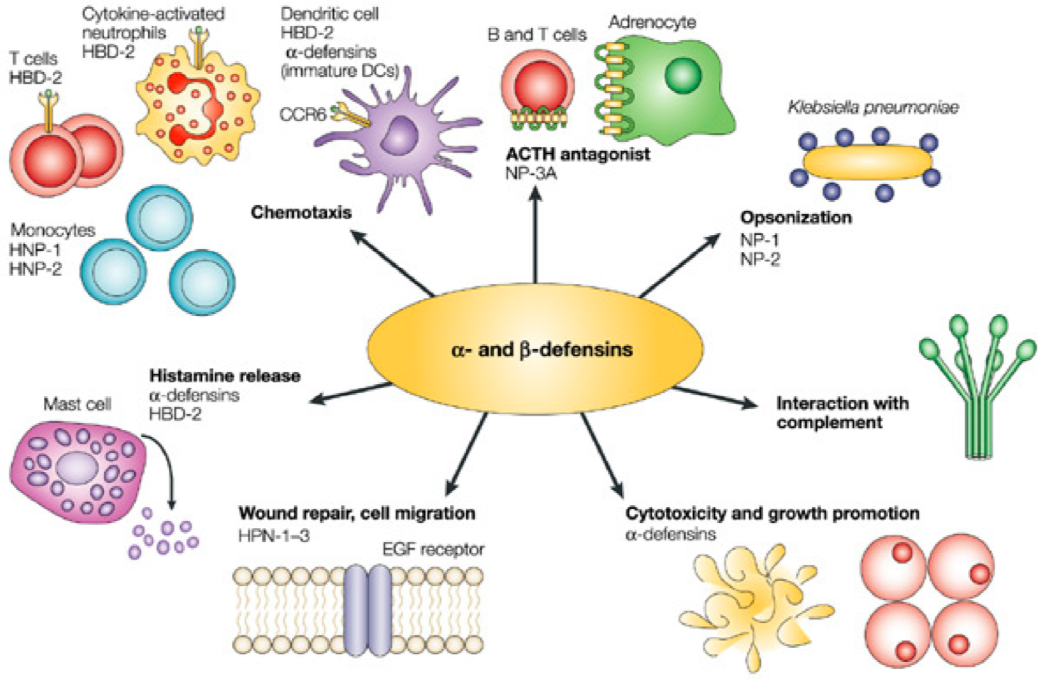

Figure 1.2. The multifaceted role of α- and β-defensins. Figure taken from Lehrer, 2004 [58].

1.3 The Human β-Defensins

1.3.1 Discovery and Isolation

To date only four human beta-defensins have been characterised in detail despite evidence of more defensin genes (*DEFB* genes) in the human genome [59]. The first human defensin (HBD1) was described in 1995 and was isolated from 4800 litres of human hemofiltrate from patients undergoing hemodialysis for renal disease [60]. Purification of HBD1 required a combination of biochemical methods including batch extraction, semi-preparative reverse phase high performance liquid chromatography (RP-HPLC), and cation-exchange chromatography. The mature 36-residue peptide has been shown to be constitutively expressed in various tissues from different tracts. HBD1 is produced from human epithelial cells of mammary gland, parotid gland, small intestine, pancreas, testis, vagina, airways and many more [61-63]. Although HBD1 appears to be constantly produced in various tissues, its expression could also be mediated by inflammation or induced and upregulated by lipopolysaccharides and

interferon gamma (IFN-γ) [64, 65].

HBD2, the second human defensin to be found, was isolated from 50 g of psoriatic scale skin [66]. The observation that patients with psoriasis were not more infected by pathogenic microorganisms despite the deteriorated aspect of the skin led the authors to the discovery and isolation of this 41-residue peptide. Unusually, HBD2 was purified using an "*Escherichia coli* affinity" column where the bacteria were used to extract the defensins from a skin extract. Fractions displaying antimicrobial activity on plate were further purified by HPLC. After amino-acid sequence analysis of the peptide, results revealed a β-defensin consensus sequence with six conserved cysteines homologous to the previously identified HBD1 and the first described mammalian β-defensin, the tracheal antimicrobial peptide (TAP), isolated from cow tongue. HBD2 expression is found in keratinocytes and the gingival mucosa, but generally throughout the entire epithelial system [67, 68].

In 2001, a new β-defensin, the human β-defensin 3 (HBD3), was simultaneously described by three different groups [69-71]. In a similar manner to HBD2, HBD3 was isolated by Harder and coworkers from human lesional psoriatic scales and heel calluses using various chromatographic methods. The tissue extracts were applied to a *Staphylococcus aureus* affinity column and bound material further separated via a RP-HPLC system. Fractions displaying antimicrobial activity towards *S. aureus* were purified with a cation exchange HPLC column. Sequence analysis and mass spectrometry revealed the primary amino acid sequence of this novel peptide. In contrast to this biochemical approach, screening the human genome with the *HBD1* and *HBD2* homologue genes led to the discovery of the *HBD3* gene by two other research teams.

Similar processes were applied for the identification of the human β-defensin 4 gene (*HBD4*) and consequently, HBD4 was synthesised using a chemical approach [72]. The synthetic HBD4 was assembled with protected amino acids from the C- to the N-terminus using a preloaded resin. So far, HBD4 has never been isolated and purified from natural tissues.

1.3.2 Structural Characteristics

The sequence alignment analysis of the most-studied β-defensins, HBD1 through HBD4 (Fig. 1.3 A), revealed that apart from 6 cysteines, only a few other amino acids are conserved within the sequence. However, a common trait shared by the four peptides, and more generally in all defensins, is their overall high content of positive residues, mainly lysine and arginine, leading to a cationicity ranging from +4 to +11. An additional remarkable similarity shared by human β-defensins is their tertiary structure. So far the structures of three human β-defensins have been solved by both NMR and X-ray crystallographic methods [73-77]. The first structure reported concerned HBD2 and was solved by X-ray crystallography (Fig. 1.3 B). Subsequently, structures of HBD1 and HBD3 followed shortly thereafter, and it appears that the core motif shared by the three peptides is a three β-strand motif disposed in an antiparallel sheet. This β-sheet fold is constrained by 3 intramolecular disulfide bridges and constitutes the "defensin-like" fold, which is the 3D "signature" of defensins.

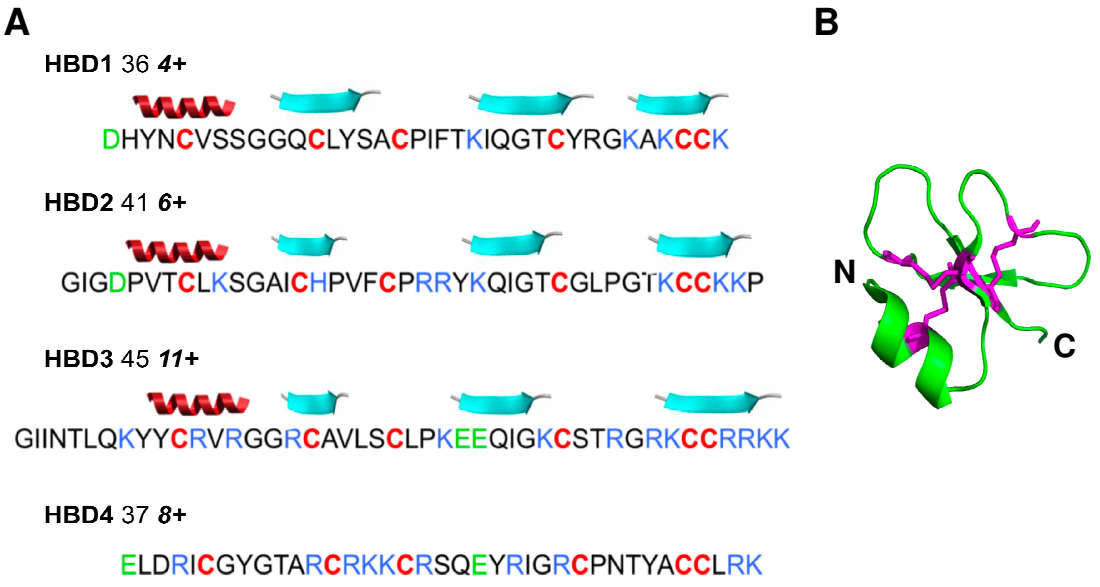

Figure 1.3. A. Amino acid sequence and secondary structures of human β-defensins Number of residues and the formal charges are indicated. Six conserved cysteine residues are coloured in red, basic residues are highlighted in blue and anionic amino acids are shown in green. Adapted from Pazgier et al., 2006 [59]. B. Crystal structure of HBD2.

Similarly to the α-class (which also contain 3 β-sheets), the β-defensins contain an α-helix of variable length at the *N*-terminus of the peptide. Of interest, in 2003, Thouzeau and coworkers isolated two novel β-defensins, named spheniscins, from the stomach contents of the king penguin [78]. Subsequently, the NMR structure of the most abundant spheniscin, Sphe-2, was resolved and confirmed to be very similar to the human β-defensins displaying a β-sheet core and a N-terminal α-helix structural topologies [79].

1.3.3 Expression and Gene Regulation

Human β-defensins are expressed in various tracts and tissues throughout the body. However, their localisation and level of expression is highly variable from a peptide to an other. For example, HBD3 expression was shown to be elevated in tonsil tissue and keratinocytes but low in the epithelia cells of the genitourinary, respiratory, and gastrointestinal tracts. These observations were confirmed by Garcia and colleagues but additionally, they provided evidence of an expression in non-epithelial tissues such as skeletal and heart muscles or leukocytes [69]. High levels of HBD4 expression was found in epididymis, testis and the gastric antrum. In contrast, low expression levels were reported from neutrophils, lung, kidney, thyroid gland and the uterus. The presence and possible role of HBD4 in human skin protection remain unclear as no expression in such tissue was demonstrated. However, and similarly to the other three β-defensins, HBD4 expression was induced in primary keratinocytes [80].

Whilst HBD1 is a constitutively expressed peptide and displays relatively high and constant basal expression, the regulation of the expression of HBD2, HBD3 and HBD4 pathway appears to be distinct from HBD1. Indeed, HBD2-4 expression seems to be upregulated by proinflammatory stimuli or bacterial infection [66, 71, 72]. For each of these three defensins the induced expression was observed in various tissues and tracts including keratinocytes, dendritic cells, peripheral blood, respiratory and gastric epithelium. Moreover, stimulators such as LPS, TNF-α, interleukin-1β (IL-1β), IL-1α, IFN-γ were also reported to induce their expression [81, 82]. Upregulation of HBD3 expression was also observed with induced factors such as insulin-like growth factor 1 (IGF-1) and transforming growth factor α (TGF-α) in human

keratinocytes [83]. Concerning HBD2 expression, its induction in various tissues was stimulated by bacterial components and cytokines *via* transcriptional nuclear factor κB (NF-κB) [84]. Moreover, evidence of upregulation for both HBD2 and HBD3 expression by HIV-1 and Rhinovirus-16 in cultured bronchial epithelial cells was reported by Duits *et al* [85].

In the last decade, a distinct group of receptors have emerged, the toll-like receptors (TLRs), and have been shown to play a critical role in mediating defensins expression through various cells and tissues [86]. It is thought that both TLR-2 and TLR-4 modulate HBD2 expression in airway epithelia cells in response to bacterial components (e.g. LPS) [87, 88]. Despite increased knowledge concerning gene expression and regulation in the defensin field, it is obvious that the overall scheme of such mechanisms is very complex, and consequently far from being fully appreciated. This is due to the diversity of molecular mediators or partners involved, and the complexity of the various "branching" of the signaling pathways.

1.3.4 Genes and Post-Translational Modifications

In humans, defensin genes (*DEFB* genes) are mainly located on chromosome 8. However, four more conserved β-defensin gene clusters have been discovered and detected on chromosomes 6 and 20 [23]. Genes from the β-subgroup appear to have evolved characteristics, and common structures consisting of two exons separated by one intron. The first exon encodes a hydrophobic leucine-rich signal sequence, whereas the second exon encodes a short pro sequence and the peptide in its mature form. Post-translational proteolytic cleavages occur at the signal sequence and the propeptide sequence (Fig. 1.4). It results in the release of defensins in the immediate environment of cells expressing such peptides (e.g. epithelia). The processing enzymes for α-defensins pro-sequences in human and mice are respectively matrilysin and trypsin (human α-defensin 5) [89]. Concerning the β-subfamily, the enzymes responsible for proteolysis remain unknown although it was shown recently that matrilysin MMP-7 did catalyse the removal of six amino acids from the amino terminus of a 47-residue HBD-1 precursor [90].

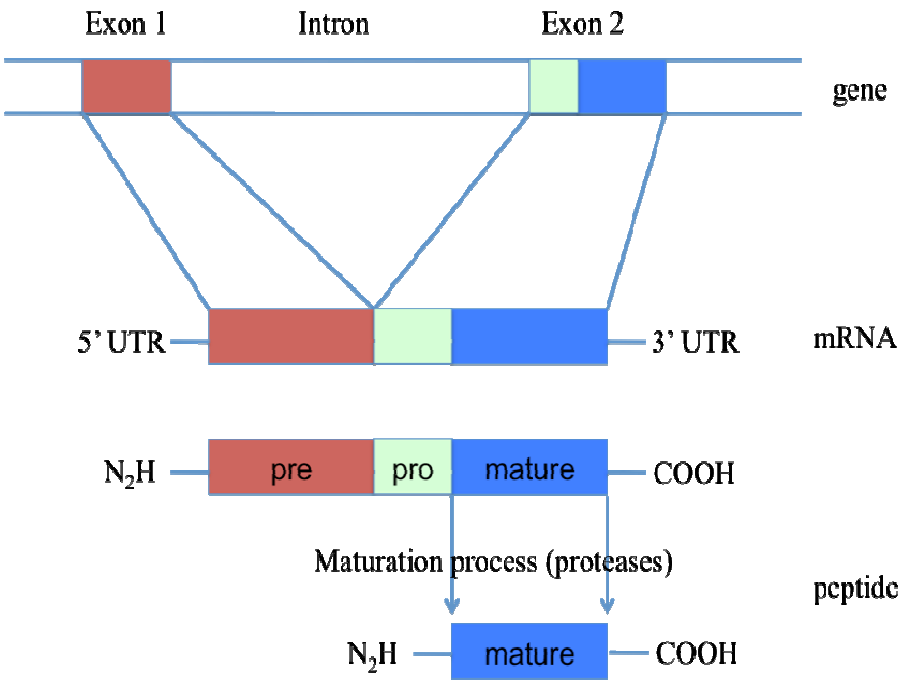

Figure 1.4. Structure of prototypical defensin gene and peptide. The gene product is a prepropeptide where a pre-sequence encodes a peptide signal. The pro-sequence is cleaved by a specific protease to the mature peptide released.

1.3.5 Antimicrobial Activity

In two decades of discovery and characterisation of defensins, the antimicrobial properties of such peptides have been extensively explored. The crisis expected with the lack of new antibiotics has been exacerbated by the growing resistance of bacterial pathogens [91]. Consequently, this need has stimulated interest for such promising molecules. All four β-defensins characterised so far have been reported to inhibit or kill a broad range of microorganisms including fungi and bacteria. However, it appears that the scope of microbicidal activity differs across all of the peptides and their effectiveness is salt-sensitive [92]. In fact high salt concentrations inhibit antimicrobial activity of β-defensins. However, Yu and colleagues have overcome this problem by engineering a new circularised salt-insensitive peptide from an α-defensin template [93]. HBD1 and HBD2 have been shown to be bactericidal against fungi and Gram-negative bacteria at μM concentrations, but were less effective against Gram-positive strains [59, 66, 94]. In contrast, HBD3 was reported to be a potent antibiotic against Gram-positive bacteria but also very effective towards Gram-negative bacteria and yeast. More interestingly, HBD3 displayed its microbicidal

behavior in a salt-independent manner towards *Staphylococcus aureus* and the vancomycin-resistant *Enterococcus faecium* strains [71]. This antimicrobial ability is not true for HBD1, HBD2 and HBD4 as they were all inhibited at physiological concentrations of salt [72, 95]. Goldman *et al.* postulated that the inhibition of HBD1 activity in patients with cystic fibrosis (CF) disease was due to high concentrations of salt in the airways of CF carriers. However, two reports have concluded otherwise stating that no difference in salt concentration was observed between healthy and CF patients [96, 97]. HBD4 was tested against *Burkholderia cepacia*, a pathogenic bacterium known for its ability to invade mucus found in the lung of cystic fibrosis patients, but weak microbicidal activity was observed (MIC>100 μg/ml). In contrast, the peptide displayed a stronger activity towards *Pseudomonas aeruginosa* (MIC 4.1 μg/ml) [72]. In 2005, Chen and coworkers have highlighted the synergistic effect of an antimicrobial "mix" including HBDs (but not HBD4), cathelicidin LL37 and skin lysozyme towards *E. coli* and *S. aureus*. The authors demonstrated that the microbicidal effect of the mixture was enhanced compared to the single activity of an isolated peptide [98].

1.3.6 Structure-Activity Relationships

Crystallographic studies of HBD2 have raised questions about the capacity for such peptides to form oligomers. A number of biophysical experiments revealed that the majority of the peptide was present as a dimer in solution, and this oligomeric form is favoured by the presence of the *N*-terminal α-helix. Moreover, this dimerisation phenomenon would allow the formation of a higher level of oligomerisation. In fact two different crystal forms have provided evidence for an octameric association by four noncovalent dimers [77]. The NMR study of HBD1, 2 and 3 by Schibli and coworkers demonstrated that HBD3 was the best candidate to form symmetric dimers in solution [75]. Therefore the authors concluded that this increased capacity to form dimers could be the reason for the enhanced bactericidal activity of HBD3 towards *S. aureus* in presence of a relatively high concentration of salt. Moreover, the high cationicity of HBD3 would be more advantageous compared to other β-defensins in order to overcome the decreased acidity in *S. aureus* membranes. However, further structural studies on this peptide have not permit to establish an explicit link between

HBD3 oligomerisation and antimicrobial activity. It was suggested that the high positive net charge coupled with a strong hydrophobicity pattern had more impact on the activity of HBD3 [99, 100]. The role of quaternary structure was explored in the case study of the mouse β-defensin-related 1 (Defr1) from our own laboratory, this provided new insights into structure-activity relationships of defensins [101]. Unlike other β-defensins, Defr1 displays 5 conserved cysteines instead of 6. The missing cysteine residue is the first one (from *N*-terminus) and is replaced by a tyrosine at position 5 in Defr1 sequence. Using high resolution mass spectrometry and tandem MS fragmentation techniques the authors showed that Defr1 forms a dimer held together by an intermolecular covalent bond. Thus the dimer contains 5 S-S bonds (4 intramolecular and 1 intermolecular). The synthetic peptide used in the study was oxidised to form these S-S bonds but upon closer inspection it was revealed that Defr1 dimer was a mixture of inseparable S-S bonded isoforms. To study the activity of the dimer, the authors engineered a Defr1 Y5C mutant possessing three disulfide bridges. This Defr1 Y5C oxidised to give a single isoform of β-defensin connectivity that was able to dimerise through noncovalent weak interactions only. Antimicrobial experiments demonstrated that the wild-type Defr1 S-S covalent dimer peptide was more potent than the Defr Y5C against Gram-negative and Gram-positive bacteria but also against the fungi *C. albicans* even under high salt concentrations. Interestingly, the reduced form of Defr1 was less potent against the same microorganisms in comparison to its oxidised form. These results have brought new knowledge with regards to the possibility of new targets for therapeutic purpose.

Originally, it was thought that the conserved cysteines among the defensin family played a crucial role in the antimicrobial activity of those peptides. Although these conserved residues are necessary for the maintenance of the triple stranded β-sheet core and therefore the general folding of defensins, studies have shown that they did not influence their antibiotic ability. In 2003, Wu and colleagues showed that HBD3, unlike HBD1 and HBD2, did not fold to a single isoform under various oxidative conditions *in vitro* [102]. Topological analogues of HBD3, chemically synthesised, displayed the same antimicrobial aptitude towards *E. coli* despite different S-S bond connectivities. Unexpectedly, a mutated linearised HBD3 where all cysteines were replaced by α-aminobutyric acid (Abu-HBD3) exhibited the same killing activity but was also less salt-sensitive than the wild-type peptide. Moreover,

the disulfide-devoid linearised HBD3 mutant did not chemoattract any of the tested cells expressing the GPCR chemokine receptor CCR6. They concluded that antimicrobial activity of HBD3 was S-S independent but chemokine activity required a folded peptide with 3 S-S bonds. This is unsurprising since the chemotactic activity surely relies on a protein/ligand interaction of high specificity. The same conclusions were drawn with the structural and biological studies carried out by Mandal *et al*. on the bovine neutrophil β-defensin 12 (BNBD-12) and the α-defensin HNP1. These authors compared the antimicrobial activity of the peptides with analogues displaying one, two, three or different S-S bond topology. They concluded that the antimicrobial activity was independent of the location and the number of disulfide bridges [103, 104]. A recent study by our laboratory has shed new light on the chemoattractant activity of HBD3 and Defb14 (the mouse ortholog of HBD3). Taylor *et al*. have confirmed that the chemoattractant activity was lost in a Defb14 derivative where all the cys residues had been replaced with alanine. However, activity was restored in peptides containing the cysteine at fifth position (cys^5) [36]. They concluded that for these peptides, the presence of intramolecular disulfide bonds was irrelevant for both chemoattractant and antimicrobial activities and demonstrated that these two properties can be uncoupled. The authors also noticed that the antimicrobial activity was located at the N-terminal region of Defb14. The implication of the N-terminal α-helical section was also linked to the antimicrobial potency of HBD2. In fact the orientation of this α-helix is governed by the aspartate residue at position 4. The lack of this residue in HBD2 resulted in a less structured peptide with less potent activity [105]. However, in a recent study, the peptide-membrane interactions were investigated with HBD2, HBD3 and analogues of these peptides. The authors reported that the β-sheet core appeared to be the primary structural element for membrane disruption while the α-helix would only modulate the antimicrobial activity [106]. This β-sheet core constrained by disulfide bridges, could also protect defensins from proteolytic cleavage by proteases [107].

Despite all the reported evidence and the popularly admitted label of defensins as antimicrobial peptides, the molecular interactions within biological membranes and more generally the mechanisms of action and disruption of membranes are yet to be fully understood. Cationic antimicrobial peptides like defensins, exploit a physiological difference between microbial and eukaryotic membranes. Microbial

membranes tend to be negatively charged due to anionic components embedded within the lipid layer (cardiolipins, phosphatydilglycerol, lipotechoic acid and LPSs). In contrast, eukaryotic membranes possess a little net charge composed mainly with zwitterionic phospholipids such as phosphatidylcholine (PC) and phosphatidylethanolamine (PE).

The first step of membrane-peptide recognition is carried out by electrostatic interaction. This phenomenon was first observed in the early 90's where defensins were shown to be more effective against negatively charged membranes than neutral ones [108, 109]. It is not surprising that amphipathic defensins exploit their overall positive charge to bind bacterial membranes and then use their hydrophobic properties to penetrate deeper into it. However, the molecular mechanism for this phenomenon remains unclear and different models of permeabilisation of cells have been built up and described in an attempt to explain such mechanisms.

The "carpet model" depicts the formation of an extensive layer formed by accumulation of peptides bound to the membrane via electrostatic interactions (Fig. 1.5 A). Peptides would cover the membrane bilayer in a carpet-like manner compromising its fluidity and displacing phospholipids until the membrane disruption [110]. This membrane deterioration mechanism is usually compared as a detergent-like action. In the "carpet model" there is no requirement for the peptides to enter the hydrophobic environment or in forming quaternary structures. An alternative model, the "barrel-stave" model, describes the ability for antimicrobial peptides to form oligomers following the initial electrostatic interaction. This higher order of oligomerisation would allow peptides to form transmembrane pores causing leakage of the cell components (Fig. 1.5 B). The pore formation occurs after a concentration threshold where the peptide self-aggregates and enters deeper in the membrane [110].

A third model was described and despite being another pore-formation model, it differs from the "barrel-stave" mechanism as the peptide is always associated to the lipids head-group so that the lipid monolayer bends continuously through the pore (Fig. 1.5 C). This model is called the "toroidal-pore" model [111].

Concerning β-defensins it is not clear what model is privileged with regards to their antimicrobial action, but it is possible that more than one can be adopted throughout the human defensin family. Although structural studies of HBD2 and human neutrophil peptides (HNPs) have provided evidence of oligomerisation, they

resulted in a distinct approach concerning their antimicrobial action. Crystallographic studies of HBD2 have shown that the octameric oligomers found in some crystals adopted a flat disk shape privileging a mechanical action described in the "carpet" model [77]. In contrast, structural studies of HNP2 and HNP3 revealed that the peptide could form a pore-like oligomeric structure [109, 112].

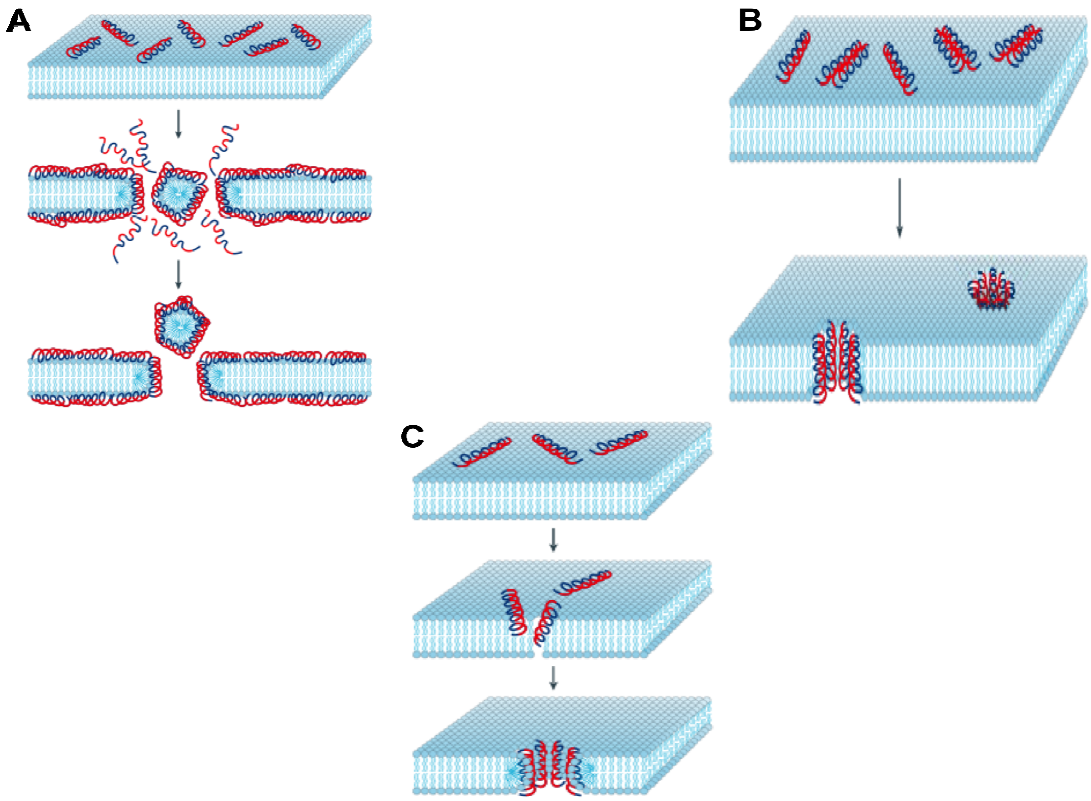

Figure 1.5. The proposed models of membrane disruption by defensins. A. The "carpet" model. B. The "barrel-stave" model. C. The "toroidal-pore" model. Figure adapted from Brogden, 2005 [110].

The models mentioned above depict the disruption of membrane cell walls and the lysis of cells, but there is increasing evidence that antimicrobial peptides can also target the intracellular components of cells. These secondary targets could include nucleic acids, glycoproteins, but also the inner membrane [45, 113]. This action towards inner membranes was observed in the late 80's by Lehrer and colleagues.

1.3.7 Mode of Production of Defensins

The first human defensins to be discovered were extracted from their host environment e.g. blood or skin. Despite being a natural method of isolation there are many obvious problems related to such methods; the difficult availability of the tissues carrying the peptide but also the convoluted extraction steps followed by extensive purification and activity tests. Last, but not least, the product recovery is poor. HBD1 isolation from 4800 litres of human hemofiltrates led to 3 mg of peptide while only 200-400 μg of HBD2 were recovered from 50 g of psoriatic scales [60, 66]. Moreover, the interesting discovery of the first β-defensin from king penguins has highlighted the laboriousness of such isolation. Spheniscins were extracted from 60 ml of stomach contents from wild penguins [78].

Fortunately, different techniques allow the production of such peptides in a more convenient and efficient manner. Solid phase peptide synthesis is an efficient method which was developed in the 60's by Robert Bruce Merrifield to produce small proteins and peptides [114]. This chemical approach has been developed for the production of several α- and β-defensins including HBD1 to HBD4. However, this method is limited by the amphiphilic nature of defensins and the cysteine-protection strategies lowering the overall yield of production [72, 102, 115, 116].

The recombinant expression for defensins *via* a host organism has also been extensively used. Concerning defensins, an extra challenge has to be overcome due to the inherent antimicrobial activity of such molecules. Excess of mature soluble peptide within bacteria would impact severely on their viability. In order to avoid the toxicity of the peptide towards the host organism, a carrier protein is fused to the *N*-terminal part of the target peptide. Usually this method uses an optimized easy-to-use *Escherichia coli* host strain for protein expression and purification but recently a different strategy using yeast as host organism was also developed [117, 118]. Over the past 10 years, various fusion partners including thioredoxin (trxA), green fluorescent protein (GFP) or light meromyosin (LMM) have been used to overcome the toxicity of defensins [119-121]. However, the cleavage of such fusion partners from the target peptide involves expensive proteases leading to substantial increasing cost. In 2006, Pazgier and colleagues succeeded in the preparation and analysis of 26 site-specific, single-change HBD1 mutants [122]. This *tour de force* led to the

determination of X-ray crystal structures of 14 of the mutants. The authors used a tryptophan operon sequence as a fusion-tag and the proteins were produced within *E. coli* as inclusion bodies. A recent emerging method using a cell-free system (cell-free extracts) was used for the production of HBD2 [123]. This method allows an *in vitro* protein expression and purification using the bacterial machinery from cell extracts and a DNA plasmid. Tomas Ganz and coworkers produced HBD1, HBD2 and various defensins with a recombinant baculovirus-infected insect cell system [124-127].

The isolation and different mode of productions of human beta-defensins are summarised in the following Table 1.2.

In this thesis, a method for the recombinant production of a mature, bioactive, single isoform of HBD2 and isotopically labelled ^{15}N-HBD2 in *E. coli* is presented. The method described is straight-forward, low-cost and leads to the production of pure oxidised and folded HBD2 in milligram quantities [128, 129] (see papers attached in Appendix). The peptide was characterised by various structural techniques and displayed excellent structural properties suitable for further investigation of HBD2 in complex with biological partners.

	First isolation (form) and discovery	Purification methods	References	Structures	PDB files
HBD1	4800 litres of human hemofiltrates	Recombinant SPPS Baculovirus-inf. cell	[122] [102] [125]		NMR: **1E4S, 1KJ5** X-ray: **1IJU, 1IJV**
HBD2	50g of psoriatic scales	Recombinant SPPS Baculovirus-inf. cell Cell-free system	[120,121,128] [102] [127] [123]		NMR **1E4Q, 1FQQ** X-ray: **1FD3, 1FD4**
HBD3	Psoriatic scales (7-50 g) and heel calluses (80-120 g)	SPPS	[102]		NMR: **1KJ6**
HBD4	Genomic-base screenin method	SPPS Recombinant	[72] [130]		

Table 1.2. Discovery and tissue isolation of the human beta-defensins. The three known structures of HBDs are also presented.

Chapter 2: Expression, Purification and Characterisation of the Mature Recombinant Human β-Defensin 2 (HBD2)

2.1 Cloning of HBD2

The *HBD2* gene was synthesised using six overlapping primers with codons optimised for expression in *E. coli*. The PCR product containing the codon-optimised gene preceded by a methionine was then ligated into the expression plasmid pET-31b (Novagen) and named pET-31b/HBD2. This plasmid was then used to express an insoluble ketosteroid isomerase (KSI) tag upstream *HBD2* gene. The idea behind the insoluble-fused tag cloning was to knock-out the antimicrobial activity of such a peptide which would considerably affect the expression process. Therefore, KSI-HBD2 species was expressed as inclusion bodies. The pET-31b plasmid contained a tandem repeat unit of the *HBD2* gene which renders any future preparation of HBD2 mutants difficult. Therefore to prepare an expression construct with a single *HBD2* gene the KSI/HBD2-fusion fragment from pET-31b/HBD2 was isolated and ligated into a pET-28a(+) (Novagen) in order to introduce a *N*-terminal His(6)-tag sequence. Furthermore, to avoid multiple cleavage sites with CNBr, two methionine residues were replaced by two alanine using site-directed mutagenesis in the KSI sequence to give the pET-28a/HBD2 plasmid (Fig. 2.1). This process was carried out in collaboration with Gareth Morrison, PhD student at the University of Edinburgh.

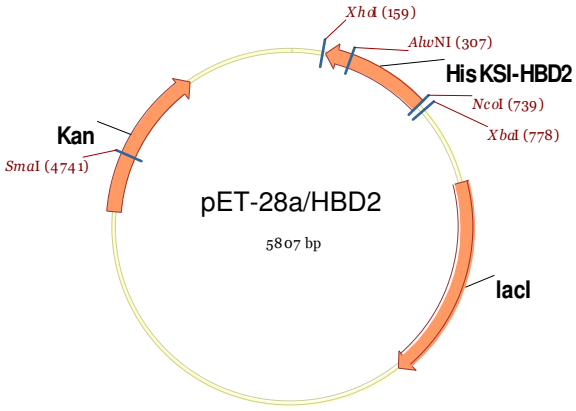

Figure 2.1. The pET-28a/HBD2 plasmid used for the production of HBD2.

Both vector constructs (pET-31b/HBD2 and pET-28a/HBD2) were used in this study to express and purify HBD2.

2.2 Overexpression and Purification of KSI-HBD2 Fusion Protein

The aim of this project was to develop a suitable method for the production of a single isoform of biologically active, oxidised β-HBD2 in a reproducible and efficient procedure of high analytical purity.

The first plasmid used for the expression and purification was pET-31b/HBD2. *E. coli* BL21(DE3) competent cells were transformed with the plasmid and a growth of 3 L culture was routinely used. The cells were induced with IPTG for several hours which allowed them to reach a high level of expression of inclusion bodies. The expression was monitored by SDS-PAGE gel (Fig. 2.2). A strong band corresponding to KSI-HBD2 at around 17.5 kDa was observed in both non-induced and induced sample (Fig. 2.2.A). Since expression was observed in the non-induced sample we concluded that the control of expression was "leaky", but this did not influence the growth of the cells and subsequent yield of the fused-HBD2 expression.

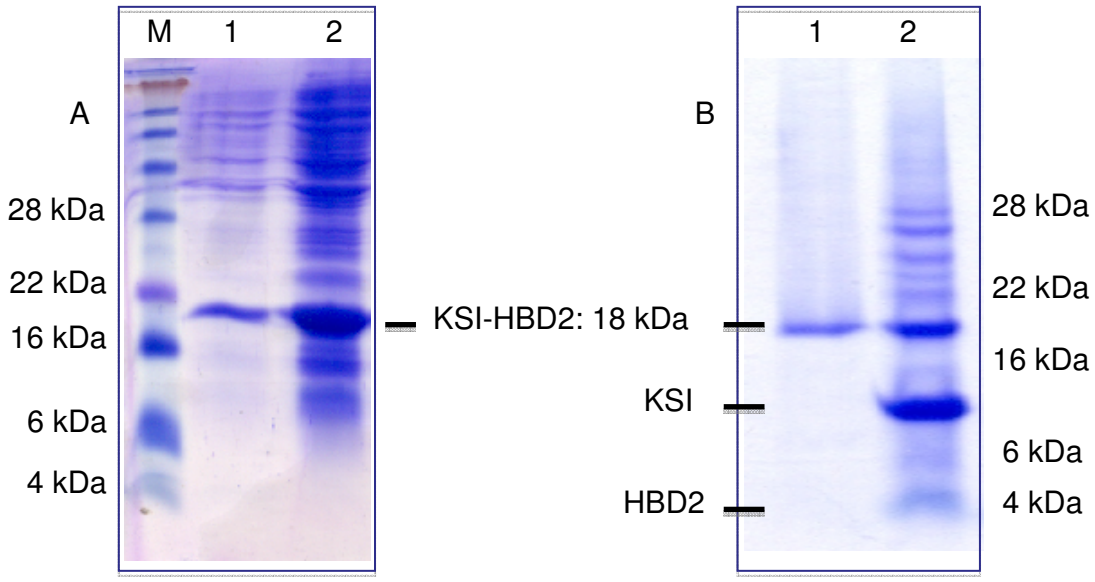

Figure 2.2. Expression of KSI-HBD2. A. before and after induction with IPTG (lanes 1 and 2). B. Purification (lane 1) and CNBr cleveage (lane 2) of KSI-HBD2.

Cells harvested by centrifugation were lysed by treatment with lysozyme and freeze-thawing. The inclusion bodies were furthermore purified with a series of washes and sonications as described in *Materials and Methods* (Chapter 6, section 6.1.3.4).

2.3 CNBr Cleavage of KSI-HBD2 Fusion Protein and Purification of HBD2 Using a Fast Protein Chromatography Liquid (FPLC) System

The solubilisation step of inclusion bodies with guanidine was followed by cleavage with CNBr. The last wash and subsequent cleavage of the inclusion bodies in their soluble form by CNBr cleavage was visualised on the SDS-PAGE gel (Fig. 2.3, lane 1 and 2). A remaining band at around 18 kDa corresponding to uncleaved KSI-HBD2 can be observed in addition to the cleaved products KSI (13.5 kDa) and HBD2 (4.5 kDa). Due to the highly insoluble properties of the KSI amino acid sequence, the unwanted products KSI-HBD2 and KSI were removed after precipitation in a single step dialysis resulting in a crude soluble HBD2 sample, which remained in the supernatant (see SDS-PAGE analysis in figure 2.3, lane 3).

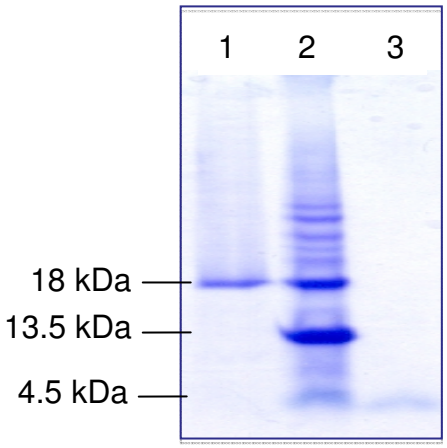

Figure 2.3. SDS-PAGE of the crude HBD2 (lane 3) soluble fraction after CNBr cleavage (lane 2).

Initial attempts to purify the peptide from the crude soluble extract after cleavage and separation of the insoluble fraction were realised by the use of a strong cationic exchange column attached to an AKTA Fast Purification Liquid Chromatography system (FPLC). After purification, the sample was concentrated and injected onto Mono S 5/50 GL (Amersham Bioscience) a strong cationic exchange column. Ten mls of the sample was injected at 1 mg/ml and eluted with a linear gradient from 0% to 100% NaCl 1 M (Fig. 2.4). Fraction 16 which corresponds to the last peak eluted was analysed by LC-ESI-MS. The experimental mass observed from

fraction 16 is 4327.9 ± 0.07 Da which is in agreement with the predicted mass of 4328.02 Da for the oxidised HBD2 (Fig. 2.5). Analysis of fractions 14 and 15 by LC-ESI-MS revealed a mixture of partially oxidised peptide with adducts (data not shown). The final peptide concentration calculated with the BCA assay was ~300 µg of pure peptide.

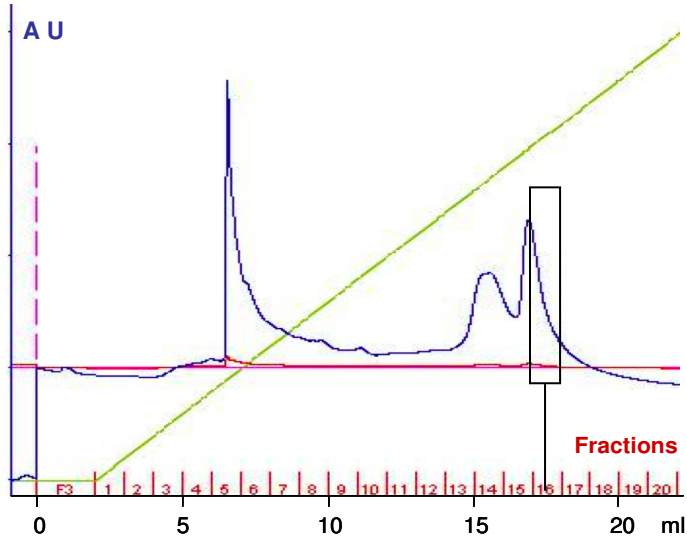

Figure 2.4. Elution profile of crude HBD2 by FPLC. Fraction 16 (outlined) was collected and analysed by LC-ESI-MS.

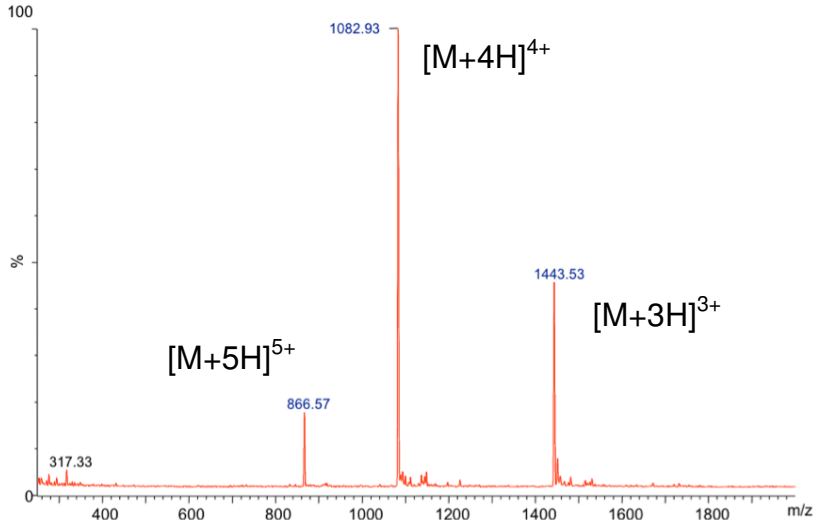

Figure 2.5. ESI mass spectrum of HBD2 from fraction 16 (Fig. 2.4). The ion envelope of the peptide shows the +5 (m/z 866.57), +4 (m/z 1082.93) and +3 (m/z 1443.53) charge states.

Despite positive results obtained with this protocol, the method proved to be problematic. The reproducibility was poor and the yield of the purified sample

remained low. Actually, the FPLC profile of the eluted sample with a clean peak corresponding to a pure oxidised peptide was difficult to reproduce. Many attempts resulted in a mixture of peptides with adducts leading to a heterogeneous sample. At this stage of the project it was necessary to adopt a new strategy using an optimised plasmid and another purification system. We decided to replace the FPLC system with an HPLC system with a reverse-phase column which would give a better product separation. Moreover, the optimised plasmid pET28a/HBD2 was thereafter the expression plasmid used.

2.4 Expression and Purification of HBD2 Using the pET-28a/HBD2 Plasmid and an HPLC System

The expression and purification protocol until the last wash and solubilisation of the inclusion bodies remained the same as previously described (see chapter 3.3). After the solubilised solution was mixed with nickel resin, the HisKSI-HBD2 fusion protein was eluted and monitored by SDS-PAGE (Fig. 2.6). A band at around 20 kDa was observed corresponding to the predicted molecular weight of the HisKSI-HBD2 fusion protein of 189aa. The eluted protein was then cleaved by CNBr and the unwanted KSI fragments precipitated by dialysis. After a centrifugation step, the supernatant containing the soluble fraction was extracted and analysed by SDS-PAGE (Fig. 2.6 lane 3).

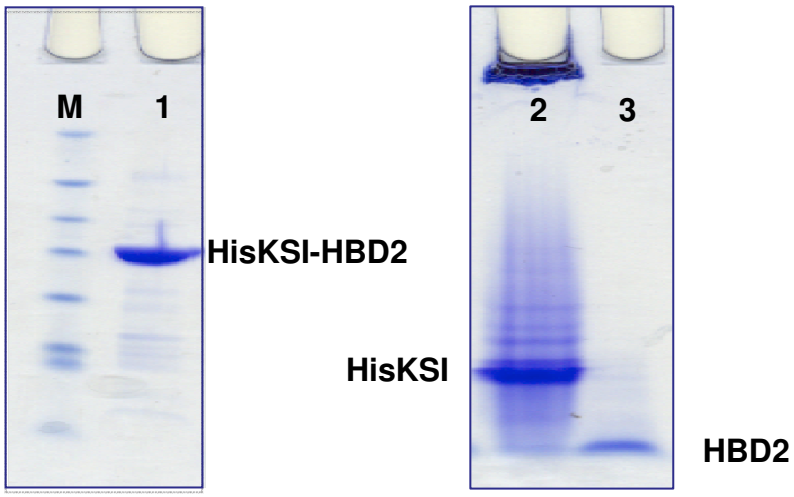

Figure 2.6. Elution profile of HisKSI-HBD2 monitored by SDS-PAGE (lane 1). The sample was cleaved by CNBr (lane 2). Lane 3 shows the crude soluble fraction of HBD2 after dialysis and precipitation of the insoluble fragments.

An HPLC system with a reverse-phase semi-preparative C18 column was used to purify the crude extract from the supernatant. The sample was reduced with an excess of TCEP (tris(2-carboxyethyl)phosphine), concentrated and loaded onto the column. The HPLC chromatograph profile of the eluted crude sample is represented in figure 2.7. The gradient used was 5-55 % acetonitrile over 50 minutes. Although this chromatograph profile could change from one preparation to another, peaks eluted between 32-34 minutes were always present at this stage of the purification (Fig. 2.7 outlined in red).

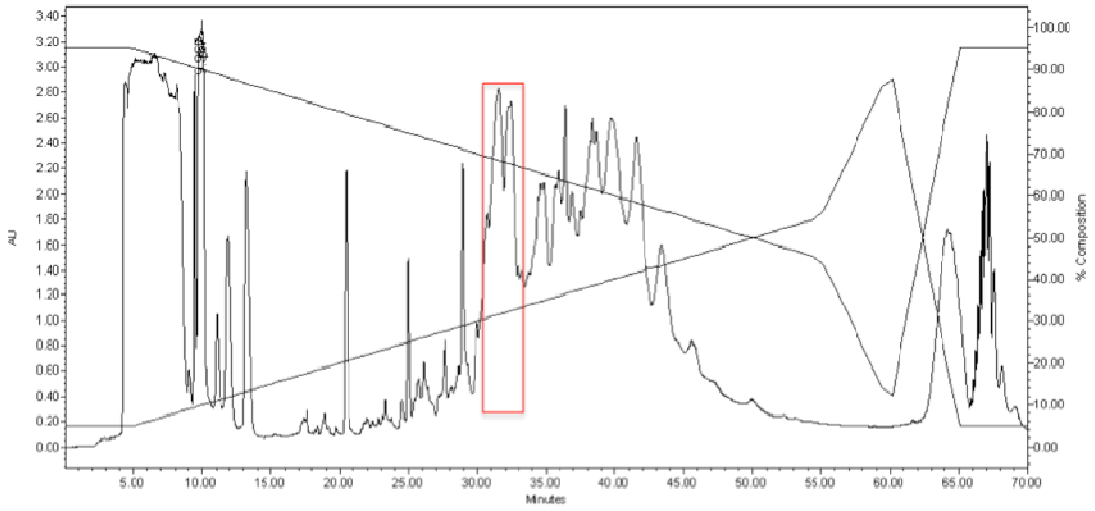

Figure 2.7. Reverse-phase HPLC chromatogram of the crude sample reduced with TCEP. Peaks outlined in red were extracted and further analysed by ESI-MS.

These peaks were collected manually and analysed by direct injection ESI-MS. This analysis gave the molecular weight of the peptide as 4334.1 ± 0.12 Da which is in good agreement with the predicted value of the reduced HBD2 defensin: 4334.0 Da (data not shown). A second run of HPLC was used when a higher purity of the reduced peptide was needed.

2.5 Refolding of the Recombinant Defensin

Once the peptide was purified in its fully reduced form, a freeze-drying step was required in order to obtain the peptide in a lyophilised form. Reduced HBD2 was then resuspended in a cysteine/cystine (10:1) redox buffer for 2-3 hours. The refolding reaction was terminated with an excess of TFA and the sample was reinjected into the

semi-preparative C18 column. The peptide was eluted with the same gradient described for the crude sample (Fig. 2.8).

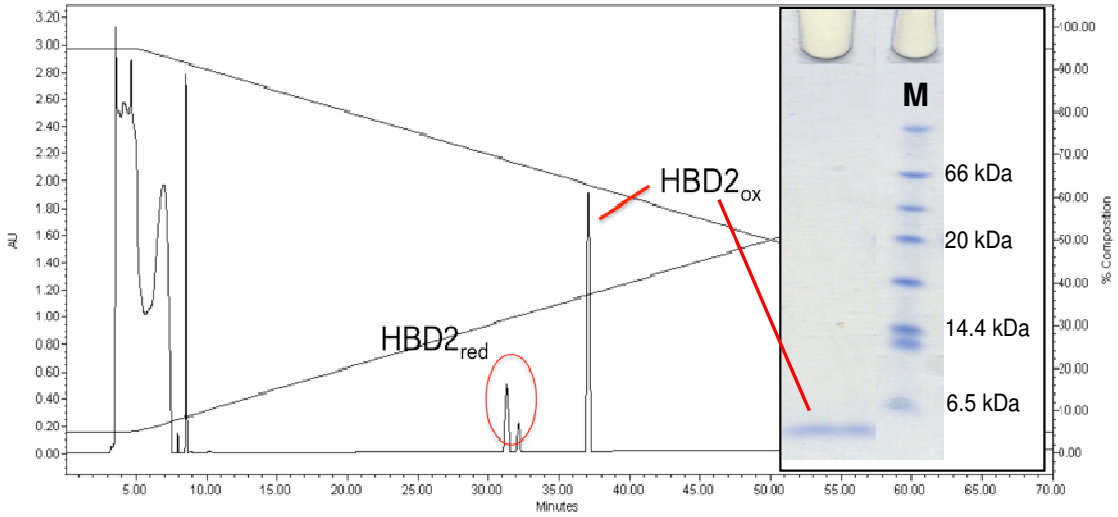

Figure 2.8. Reverse-phase HPLC chromatogram of HBD2 after the refolding reaction. The peak eluted at 34 min. was extracted, monitored by SDS-PAGE (inset) and analysed by direct injection ESI-MS.

After the refolding step, the HPLC elution profile showed a sharp clean peak at a retention time of 37 minutes. This species was eluted 5 minutes after the reduced peptide (32 minute). The 37 minute peak was collected and was analysed by ESI-MS which showed a convoluted mass of 4328.1 ± 0.7 Da which is in agreement with the predicted mass of 4328.0 Da which corresponds to the oxidised peptide form (Fig. 2.9). The average recovery of oxidised peptide over the fully reduced starting material lies between 50% and 80%. The yield of pure oxidised peptide, calculated with the BCA assay for at least 10 preparations, was between 3 to 6 mg from 3 litres of bacterial culture.

Despite the fact that the observed mass (4328.1 ± 0.7 Da) matched the theoretical mass (4328.0 Da) of oxidised HBD2 it was necessary to check if the sample was fully oxidised (no cysteine in the reduced form). To analyse the oxidation state of the peptide, HBD2 was incubated with iodoacetamide, a compound which reacts with free thiol groups of cysteines. The iodoacetamide-modified peptide yields a 57 Da mass increase per reduced cysteine.

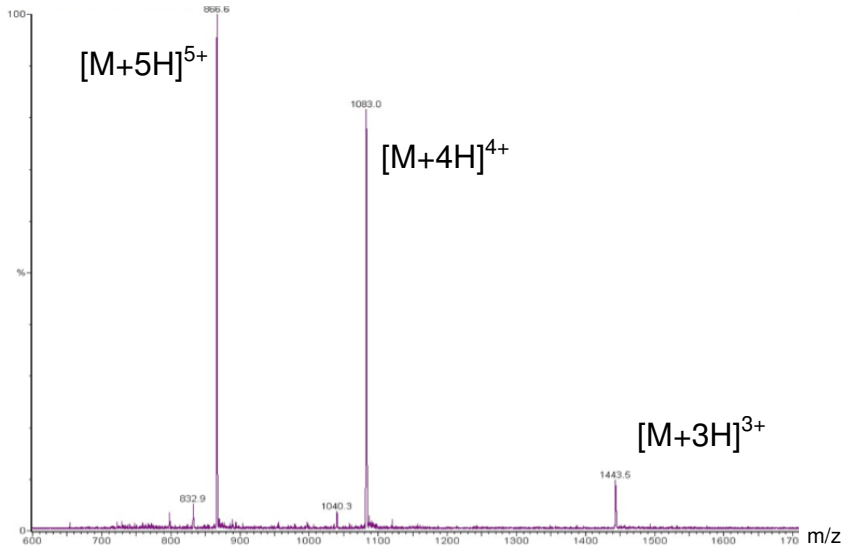

Figure 2.9. ESI mass spectrum of HBD2 from fraction eluted at 37 minutes (Fig. 2.8). The ion envelope of the peptide shows the +5 (m/z 866.6), +4 (m/z 1083.0) and +3 (m/z 1443.5) charge states.

After the reaction, the sample was analysed by LC-ESI MS and the deconvoluted major peak at 4328 Da corresponding to the oxidised form was observed (Fig. 2.10). In addition, peaks at 4385 and 4442 Da were also present. These peaks correspond to an increased mass of 57 Da and 114 Da (2 X 57 Da) compared to the unmodified peptide. Obviously only a very small amount of the peptide is partially modified as the major peak still remains at 4328 Da. The increased mass of 57 Da could be due to iodoacetamide adducts at the *N*-terminal of the peptide. This assay confirmed that HBD2 at this stage was fully oxidised.

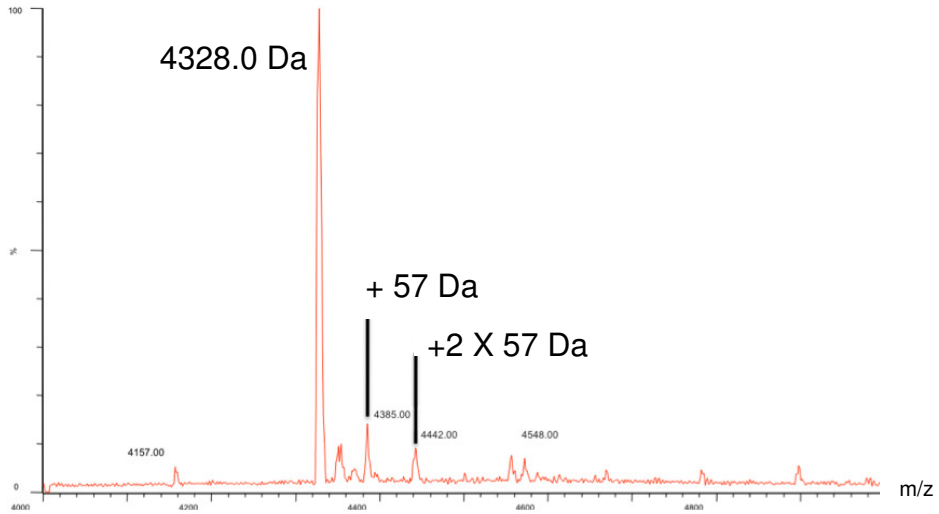

Figure 2.10. ESI mass spectrum of HBD2 incubated with iodoacetamide. Deconvoluted masses indicate that HBD2 is in its complete oxidised form as the major peak is observed at 4328.0 Da.

2.6 Determination of Disulfide Connectivity for HBD2

The level of oxidation does not explain the S-S connectivities between cysteine residues in HBD2, which are Cys^1-Cys^5, Cys^2-Cys^4 and Cys^3-Cys^6 in a folded β-isoform of the peptide. To verify whether HBD2 is folded correctly a digestion with trypsin and chymotrypsin was performed and analysed by ESI-MS. Fragments cleaved by both proteases were initially predicted with PAWS software (The Protein Analysis Worksheet). The different steps of proteolysis and the final reaction with Edman's reagent are shown in figure 2.11. The predicted mass of each fragment is also indicated.

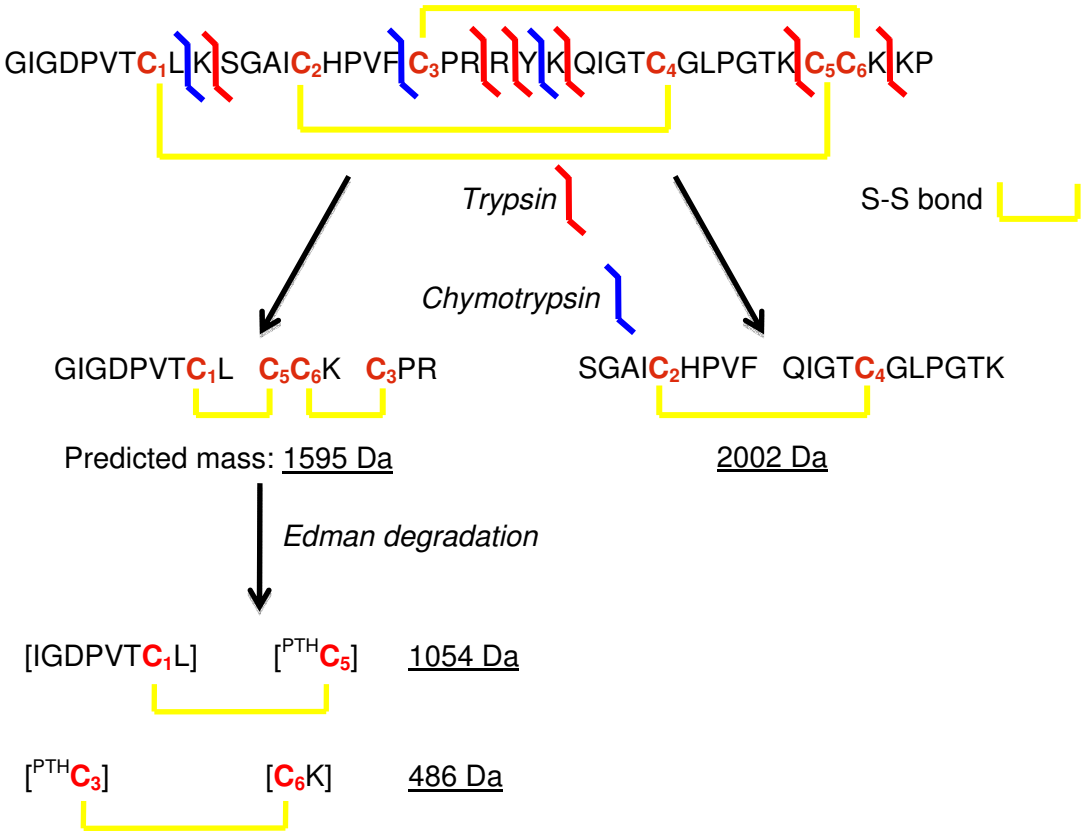

Figure 2.11. Proteolysis and Edman degradation of HBD2. The peptide was first digested by trypsin and chymotrypsin. Edman's reagent was then used to verify the S-S bond connectivities between cysteine residues Cys1, Cys3, Cys5 and Cys6.

After digestion with trypsin and chymotrypsin the sample was analysed by LC-ESI MS. Two peaks showing masses at 1002 Da and 799 Da were detected (Fig.

2.12 A, 1 and 2) which upon deconvolution represent masses respectively at 2002 Da and 1596.0 Da (Fig. 2.12 in red numbers). These observed masses were in agreement (± 1 Da) with the predicted ones according to PAWS software. However, an extra step was needed to segregate what S-S connectivities were contained in the fragment with cysteine residues Cys1, Cys3, Cys5 and Cys6. At this stage only the Cys^2-Cys^4 connection was confirmed, but it was impossible to assign the other disulfide bonds as two possibilities remain; Cys^1-Cys^5 and Cys^3-Cys^6 or Cys^1-Cys^6 and Cys^3-Cys^5. After the first digestion with trypsin and chymotrypsin the fragment of mass = 1596 Da was extracted and submitted to an Edman degradation. With this method, the amino-terminal residue is chemically modified to generate a phenylthiohydantoin (PTH) adduct and then cleaved from the peptide. After the reaction, the derivatised fragments were reinjected and analysed by LC-ESI-MS. The mass spectrum analysis revealed a deconvoluted peak at 1055 Da (Fig. 2.12 B). This mass corresponds to the fragment containing cysteines 1 and 5 with a predicted mass of 1054 Da.

The proteolysis of the oxidised peptide plus an additional step of Edman degradation led us to believe that HBD2 was folded in the typical β-defensin disulfide bond connectivity: Cys^2-Cys^4, Cys^1-Cys^5 and Cys^3-Cys^6.

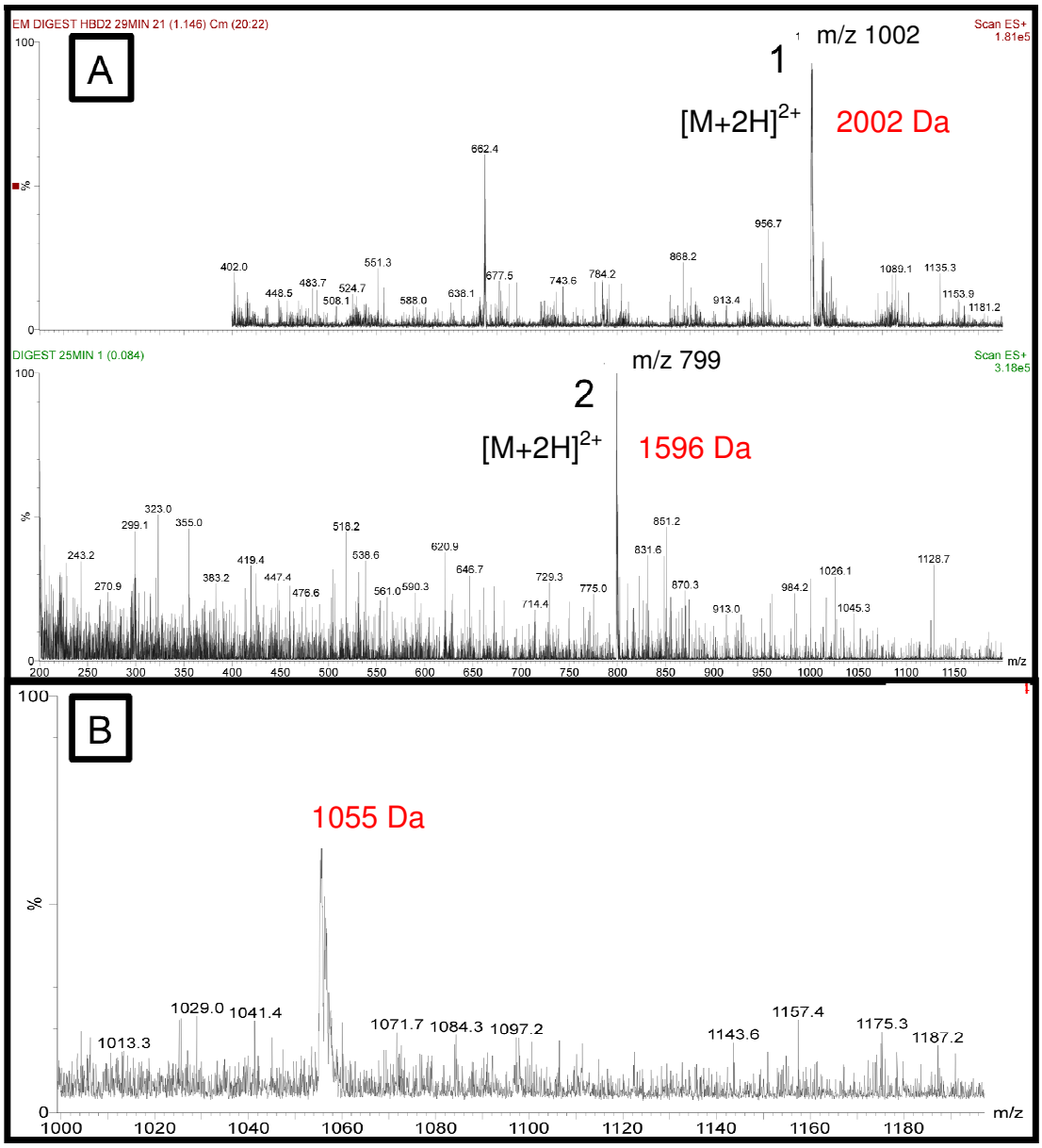

Figure 2.12. Analysis of the S-S bond connectivities in HBD2 by ESI-MS. Fragments generated by proteolysis and Edman degradation are shown respectively in section A and B. Deconvoluted masses are represented with red numbers.

2.7 Structural Characterisation of Mature β-Defensins

The structure of synthetic HBD2 has been determined using NMR and X-ray crystallography and both methods gave essentially the same results [74, 77]. To investigate our own structural studies of HBD2 complexes we began by analysing if the purified oxidised recombinant material was suitable for NMR studies. NMR data collection was carried out at pH 3.7 at a peptide concentration of 0.6 mM. A 2D-

TOCSY spectrum was obtained after scanning for 2 h 30 min. (Fig. 2.13). The outlined region (in red) between 7 and 10 ppm contains the amide protons which are exposed to solvent exchange faster than those which are buried or form stable hydrogen bonds. This method exploits the constant exchange of peptide backbone amide protons with solvent protons to evaluate protein structure, stability and dynamics. By looking in the 6-10 ppm region, we can get information about whether the peptide is folded or not. The 1D ^{1}H NMR spectrum shows sharp and distinctive peaks in the amide region while the 2D ^{1}H NMR spectrum details well-dispersed signals. Both spectra are indicative of a folded structure.

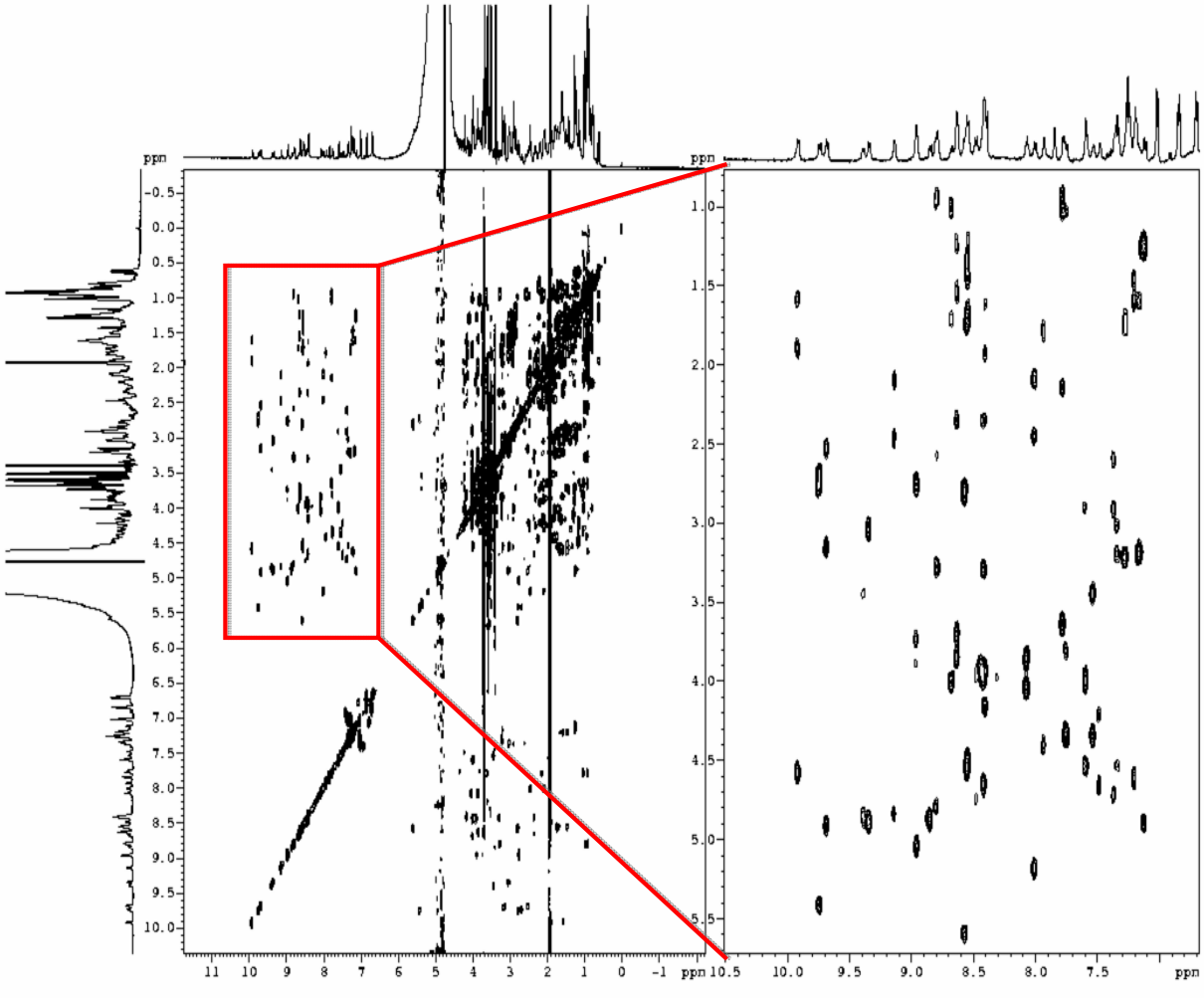

Figure 2.13. 1D ^{1}H NMR and 2D ^{1}H NMR spectra of oxidised HBD2. The amide region outlined in red is indicative of a folded structure.

2.8 Expression, Purification and Characterisation of the ^{15}N Labelled-HBD2.

Once a valid method was obtained for the isolation of the mature HBD2 peptide, we thought it would be interesting and very valuable to purify an enriched version of HBD2 by incorporation of a nitrogen-15 (^{15}N) label into the peptide. This isotope is frequently used in nuclear magnetic resonance spectroscopy (NMR). Unlike the abundant isotope nitrogen-14 (99.634%), ^{15}N has a nuclear spin of ½, which can be observed by NMR. So far all NMR-defensins structural studies involved the use of natural isotope ^{1}H NMR which can be problematic for binding studies due to overlapping signals. The interaction of such peptides is facilitated if all the amino acid can be assigned distinctively.

The main changes concerning the production of the ^{15}N HBD2 concern the expression step. Briefly optimised growth conditions involving a defined mixture of trace metals and ^{15}N-ISOGRO™ (available from Sigma) in a M9 minimal medium was used (Chapter 6, section 6.1.1.3). The isolation, purification and folding steps used were similar to those described previously in this chapter.

The protein expression system used the *E. coli* strain BL21(DE3)plysS freshly transformed with pET-28a/HBD2 plasmid. After induction with IPTG the inclusion bodies were washed, further purified and chemically cleaved as mentioned before for the unlabelled HBD2 (Fig. 2.14 lane 2 to 4). After precipitation of undesired insoluble fragments, the reduced crude soluble preparation was monitored on SDS-PAGE gel (Fig. 2.14 lane 5) and injected onto a semi-preparative C18 column attached to a HPLC system. The different crude fractions were collected, analysed by direct injection ESI-MS (Fig. 2.15) and selected for the reduced enriched peptide. Analysis of the sample by ESI-MS revealed, after deconvolution, that a major species was present with a 4389.0 ± 0.1 Da mass which is in agreement with the theoretical mass of fully reduced peptide based on the mature ^{15}N-incorporated HBD2 sequence (GIGDPVTCLKSGAICHPVFCPRRYKQIGTCGLPGTKCCKKP) lacking all disulfide bonds (calculated mass 4388.5 Da).

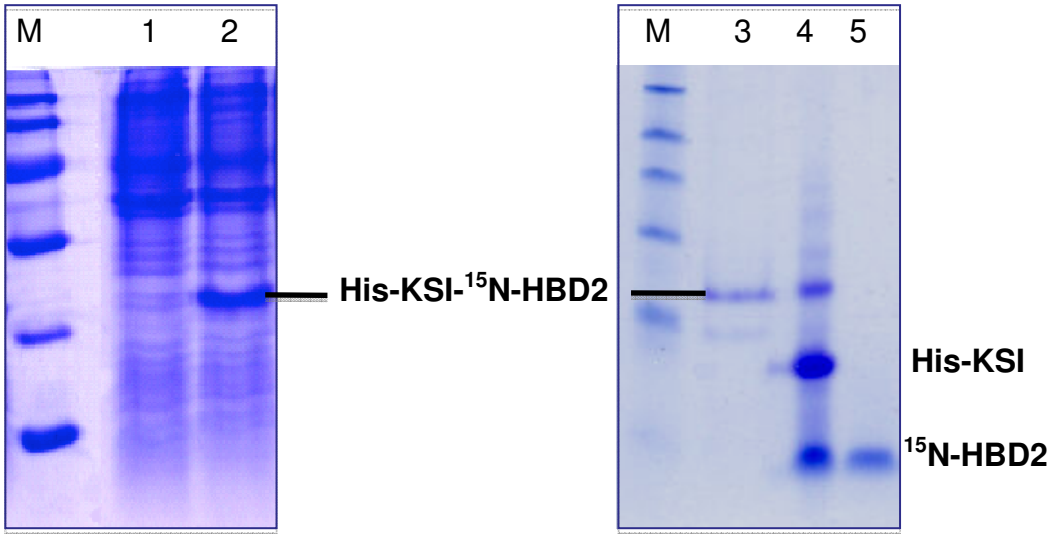

Figure 2.14. The different step of expression and purification of ^{15}N HBD2 monitored by SDS-PAGE. Lane 1 and 2 represent respectively the cell extracts before and after induction with IPTG. Inclusion bodies were solubilised (lane 3) and the KSI tag cleaved by CNBr (lane 4). The insoluble fraction was removed and soluble crude sample (lane 5) further purified.

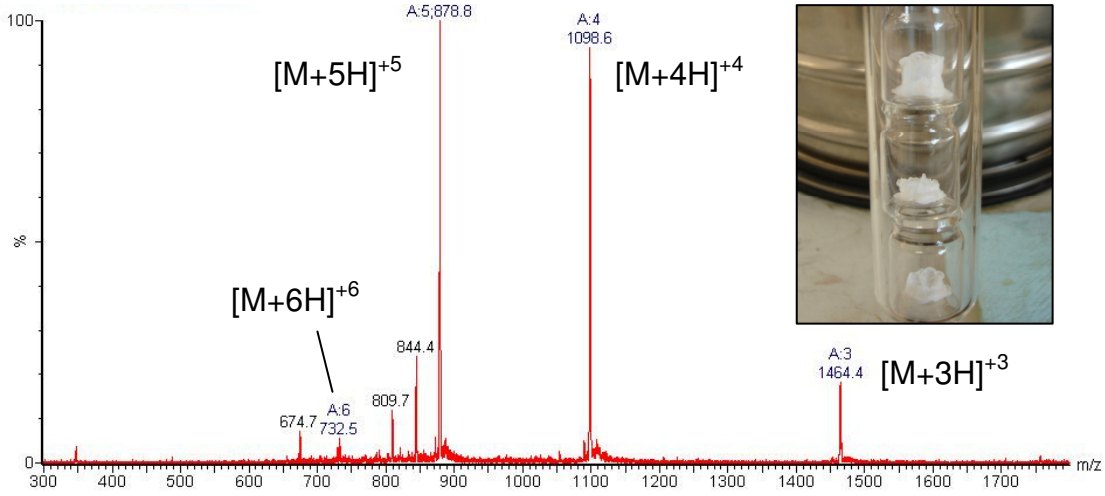

Figure 2.15. Analysis by ESI-MS of the reduced labelled-HBD2 shows an ion envelope with four charge states; +6 (m/z 732.5), +5 (m/z 878.8), +4 (m/z 1098.6), and +3 (m/z 1464.4). Picture of reduced lyophilised sample is shown in insert.

A lyophilised sample was resuspended in the cysteine/cystine redox (10:1) buffer for few hours. Both reduced and oxidised labelled-HBD2 were monitored by reverse phase-HPLC (Fig. 2.16) and analysed by high resolution nanoelectrospray FT-ICR (Fig. 2.17).

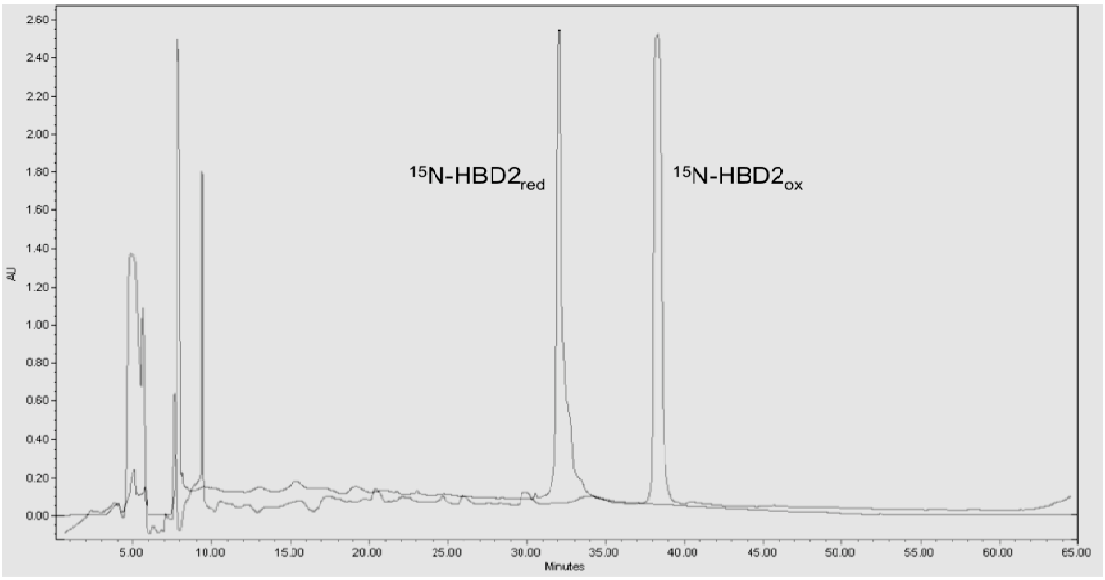

Figure 2.16. HPLC chromatogram of the oxidised and reduced form of ^{15}N HBD2. Analysis was performed on a C18 reverse phase HPLC column using a 5-55% acetonitrile gradient over 50 minutes. The oxidised form is eluted 4 to 6 minutes after the reduced species.

The FT-ICR MS analysis of ^{15}N labelled HBD2 shows an ion envelope containing three charge states ($[M+5H]^{5+}$, $[M+4H]^{4+}$, $[M+3H]^{3+}$). After deconvolution, the average mass of the oxidised ^{15}N HBD2 was 4382.5 Da (Fig. 2.17 red) which is in good agreement with the theoretical mass of the fully oxidised peptide based on the amino acid sequence with three S-S bonds. The oxidised form of the isotopically labelled HBD2 has a molecular formula of $^{12}C_{188}$ $^{1}H_{310}$ $^{16}O_{50}$ S_6 $^{15}N_{55}$ whereas the reduced peptide has a molecular formula of $^{12}C_{188}$ $^{1}H_{316}$ $^{16}O_{50}$ S_6 $^{15}N_{55}$. Figure 2.17 displays the mass spectra of labelled (red) *versus* the unlabelled (black) peptide. Upon deconvolution the masses of the two species differ by 55 Da validating the 100% incorporation of the ^{15}N isotope corresponding to the 55 nitrogen atoms of HBD2.

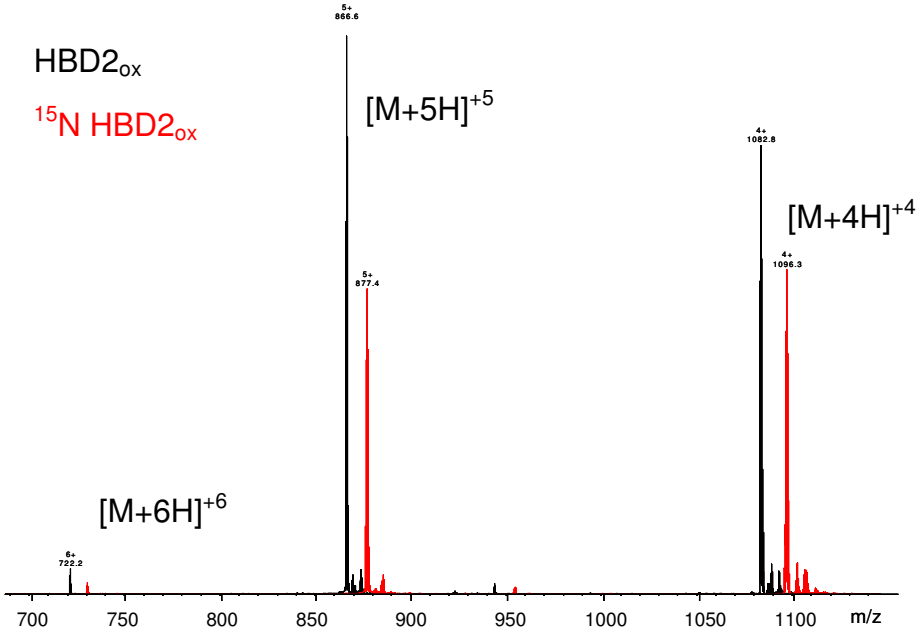

Figure 2.17. FT-ICR high resolution mass spectrum of oxidised ^{15}N HBD2 (red) versus oxidised ^{14}N HBD2 (black) showing the +6 (m/z 722.2/730.8), +5 (m/z 866.6/877.4), and +4 (m/z 1082.8/1096.3) charge states. The deconvoluted mass of ^{15}N HBD2 was calculated at 4382.5 Da.

In order to evaluate the full potential of Nitrogen-15 incorporation, it was necessary to obtain the NMR spectra of the peptide. Previous work on NMR structure of unlabelled HBD2 reported the use of phosphate buffer at pH 3.7 and 6.4 [74]. Data collected at pH 3.7 gave spectra with better resolution despite working outside the range of the buffer (pH 6-13). In this study, an acetate buffer was used in order to apply the desired acidic pH in accordance with its buffer range (pH 3.8-5.8). The solution was adjusted to pH 4.7 and the NMR spectrum obtained has a much improved spectral resolution. Figure 2.18 shows the 1D ^{1}H NMR spectra of unlabelled HBD2 versus its ^{15}N labelled version in the amide region.

Similarly to ^{14}N HBD2, the ^{15}N HBD2 amide region shows well-dispersed, sharp peaks corresponding to a defined folded structure. However, as notified on figure 2.18, if the chemical shifts within the amide region remain the same, each resonance peak is split into a doublet in the labelled sample. This phenomenon is due to the ^{1}J (^{15}NH) coupling. While the data used to solve the NMR structure of HBD2 (biological Magnetic Resonance Data Bank, PDB file 1fqq) [74] contained several overlapping amide proton chemical shifts, the 2D ^{1}H-^{15}N HSQC spectrum in figure 2.19 shows distinctive chemical shifts and unambiguous identified amino acids (the

assignments have been solved by E.S. Seo and published Seo *et al*., 2009 [129] – see Appendix).

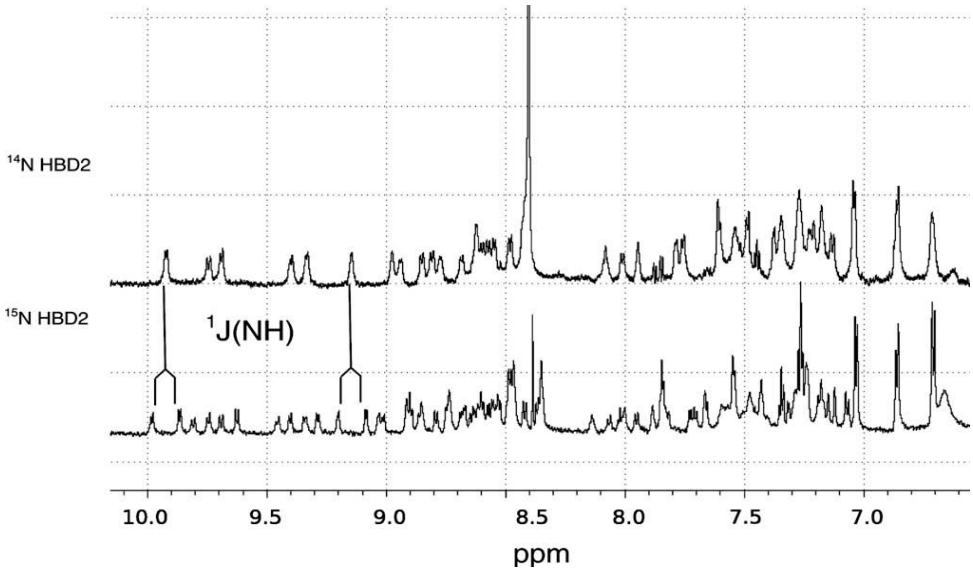

Figure 2.18. The amide region of the 600 MHz 1D ^{1}H NMR spectra of ^{14}N and ^{15}N HBD2 in 20 mM acetate buffer at pH 4.7 and 25 ^{o}C.

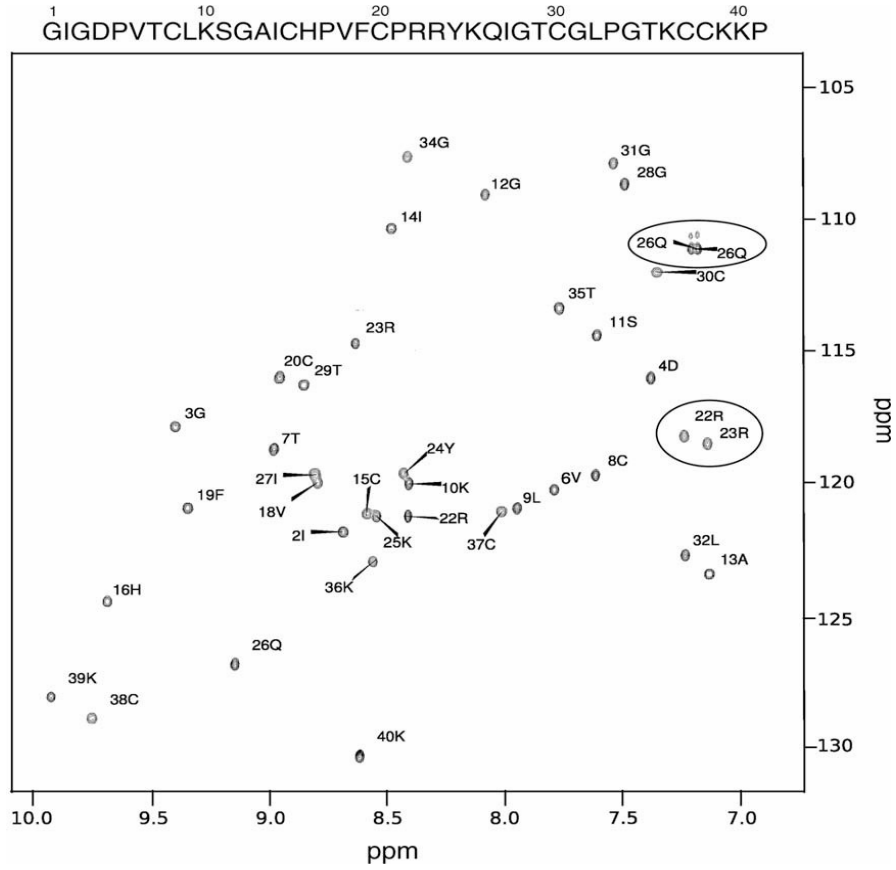

Figure 2.19. 2D ^{1}H–^{15}N HSQC spectrum (600 MHz) of 0.23 mM ^{15}N labelled HBD2 in 20 mM sodium acetate buffer at pH 4.7 and 25 ^{o}C. The sequence is given above the spectrum. The side chain amide cross peaks of residues 22R, 23R and 26Q are circled.

2.9 Antimicrobial Properties of HBD2

In order to evaluate the antimicrobial activity of the mature peptide it was necessary to test its antibiotic properties towards diverse microorganisms. We selected four strains including two Gram-negative bacteria, *Escherichia Coli* (K-12, MG1655), *Pseudomonas Aeruginosa* (PAO1) and one Gram-positive bacteria *Staphylococcus aureus* (ATCC 25923). We also tested the peptide against a fungus, *Candida albicans* (J2922). The antimicrobial assay consisted of incubating different concentration of peptide against a fixed concentration of the microorganism in a method used previously in the lab [101]. Two sets of plates were used; one was spreaded with the undiluted sample and the other was spreaded a 100-fold diluted sample. Each plate was counted and the results were processed in order to calculate values for the minimum bactericidal concentration at 99.99% ($MBC_{99.99}$). Briefly, we have determined the concentration of peptide where we observed >99.99% killing of the initial inoculum. The same principle was applied to determine the LD_{90} and LD_{50} values (Lethal Dose: amount of peptide required to kill 50% and 90% of the initial inoculum).

As a positive control we tested a well-studied cAMP antibiotic, Polymyxin B, towards the same organisms. The results are summarised in the Table 3 1. All experiments were performed at least 3 times for each strain and the mean of each was calculated.

Organism	Type	$MBC_{99.99}$	LD_{90}	LD_{50}
E. coli K12-MG1655	Gram-negative	**<20** (<1.5, PMB)	**3-6**	**<1.5**
P. aeruginosa PAO1	Gram-negative	**<25** (<1.5, PMB)	**<3**	**<1.5**
S. aureus ATCC 25923	Gram-positive	**>50** (6, PMB)	**>12**	**>3**
C. albicans J2922	Fungus	**>50** (<3, PMB)	**>6**	**>1.5**

Table 3 1. Antimicrobial Activity of HBD2 against different organisms (Values are in µg/mL, PMB: Polymyxin B as Control AMP).

Killing assay results showed that HBD2 exhibited broad spectrum antimicrobial activity, with MBCs lower than 25 μM against the Gram-negative bacteria (*Escherichia coli* and *Pseudomonas aeruginosa*). Moreover HBD2 also displayed antifungal activity against *Candida albicans* in the μM range. All LD90 values were observed below 10 μM with the exception of Gram-positive *Staphylococcus aureus* where HBD2 had a lower bactericidal effect as previously observed by Harder and colleagues [66]. They observed that natural HBD2 isolated from psoriasis scales achieved only bacteriostatic effect on *S. aureus* at concentration as high as 100 μg/mL.

Concerning the antimicrobial activity of Polymyxin B, MBCs values did not exceed 6 μM for any of the strains used.

2.10 Surface Plasmon Resonance (SPR) Binding Studies of HBD2 with Biological Membrane Models.

In this study we investigated the binding properties of HBD2 with different vesicles using the technique of surface plasmon resonance (SPR). Briefly, SPR is a phenomenon that occurs at an interface between media of different refractive index. SPR-based instruments use an optical method to measure this refractive index near a sensor surface. In the BIAcore system (the most widely used SPR-based instrument), the sensor surface (a chip) forms the floor of a small flow cell, through which an aqueous solution passes under a continuous flow (Fig. 2.20 A). To detect an interaction, a molecule (ligand) is immobilised onto the chip and its binding partner (the analyte) is injected in aqueous solution through the flow cell. When the analyte, also injected through a continuous flow, binds to the ligand, a response is observed resulting in an increase in the refractive index. This difference in refractive index is measured and monitored in real time on a sensorgram (Fig. 2.20 B). The results are plotted as time versus response which is measured in response units (RU) and is directly proportional to the concentration of biomolecules on the surface.

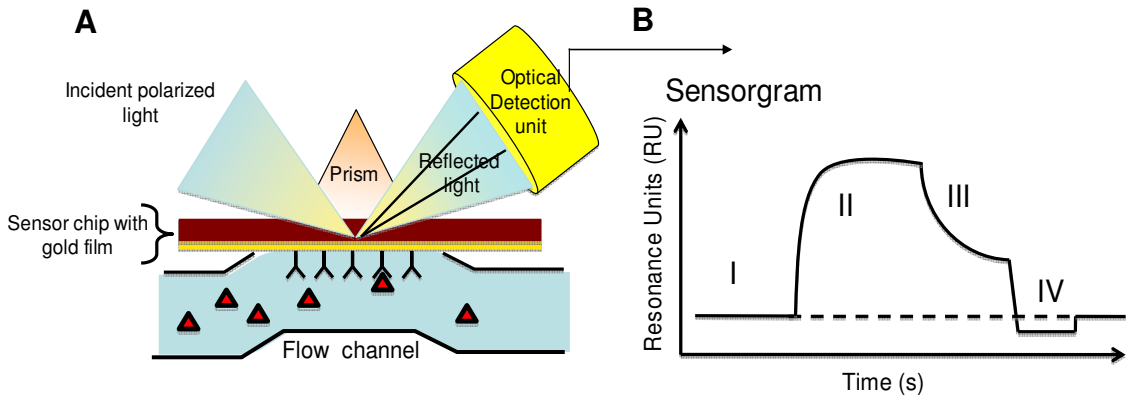

Figure 2.20. The BIAcore biosensor technology (A). Interaction between analytes and ligands are monitored on a sensorgram (B). On the sensorgram are indicated the different phases of a binding curve (I. baseline, II. association, III. dissociation, IV. regeneration).

BIAcore studies were performed with purified recombinant HBD2 in its oxidised form. Three different types of large unilamellar vesicles were formed by lipid extrusion through a 100 nm extruder. The first type of vesicles coated on the L1 chip was the pure POPC (1-palmitoyl-2-oleoyl-*sn*-glycero-3-phosphocholine) vesicles. A second cell was coated with the POPC/POPG (POPG: 1-palmitoyl-2-oleoyl-*sn*-glycero-3-phospho-(1'-*sn*-glycerol) (7:3) vesicles and finally the third cell was coated with the POPE/Kdo_2-lipid A (10:1) vesicles. The choice to mix POPE with Kdo_2-lipid A instead of POPC was motivated by a recent paper where the use of POPC with the deep-rough LPS led to heterogeneous quarternary structures undesirable for vesicle preparation [131]. Those aggregates were not observed for POPE/Kdo2-Lipid A mixture. The vesicle capture sensor chip L1 has dextran modified (liphophilic anchors) matrix molecules on the surface that allow binding of liposomes to mimic a fluid bilayer membrane. SPR sensorgrams monitor the strength of association and dissociation on the chip surface with AMPs.

The aim of this study was to investigate the interaction of HBD2 with different type of membranes. The pure POPC vesicles generate zwitterionic membranes whereas POPC/POPG (7:3) and POPE/Kdo_2-lipid A (10:1) vesicles share both negatively charged membranes. Moreover, the introduction of the deep-rough LPS (Kdo_2-lipid A) from *E. coli* into the phospholipidic membranes presented a model with increased biological relevance. The coating process for the 3 type of vesicles

onto the L1 chip gave a response higher than 10000 RUs (data not shown). This response, once normalised, constitutes the starting baseline for the binding experiments (Fig. 2.20. B, I).

Peptides were injected to the three lipid systems at concentrations of 1.25, 2.5, 5, and 10 μM. The sensorgrams representing the binding curves of HBD2 to each lipid system are shown in figure 2.21. It is interesting to note that the same binding kinetics is observed for the three different types of membranes. In addition, the peptide concentration was proportional to the response monitored on the sensorgram. For each lipid composition, HBD2 demonstrated an increase in the initial binding with a saturation level observed from 25 seconds to less than 5 seconds.

Concerning the mixed POPC/POPG membrane model, the response for each of the different concentrations of peptide injected was higher compared to the binding with zwitterionic vesicles (Fig. 2.21, A and B). The differences between the values from sensorgram B to A are ranged from 50 RUs (1.25 μM) to 100 RUs (10 μM). This difference in the affinity was expected as positively charged peptides are attracted to negatively charged membranes. When compared to the mixed POPE/Kdo_2-lipid A vesicles, these differences are even more pronounced ranging from 200 RUs (1.25 μM) to 400 RUs (10 μM). Despite the identical overall negative charges shared by the two membranes it is interesting to notice the threshold in the binding response between these two models. The incorporation of the deep-rough LPS into the membrane confers a stronger affinity towards HBD2 than the POPG-incorporated phospholipids suggesting a possible role for Kdo2-Lipid A in the membrane disruption process when Gram-negative bacteria are challenged by cAMPs.

After the peptide injection (time ~ 200s) the dissociation curves show a slower rate compared to the association curves. The time observed for dissociation is between 150 and 300 seconds with the slower rate observed for the POPE/Kdo_2-lipid A vesicles. The contrast between the two phases could be explained by the fact that the peptides penetrate deeper into the membrane bilayer. It is postulated that the initial interactions between cationic antimicrobial peptides and anionic bacterial membranes are electrostatic in nature. Thereafter the hydrophobic properties of defensins force the peptides to penetrate deeper into the membrane and interact with the fatty acid chains of the lipids. Thus the time required for the removal of peptides is higher than the time required for their electrostatic binding.

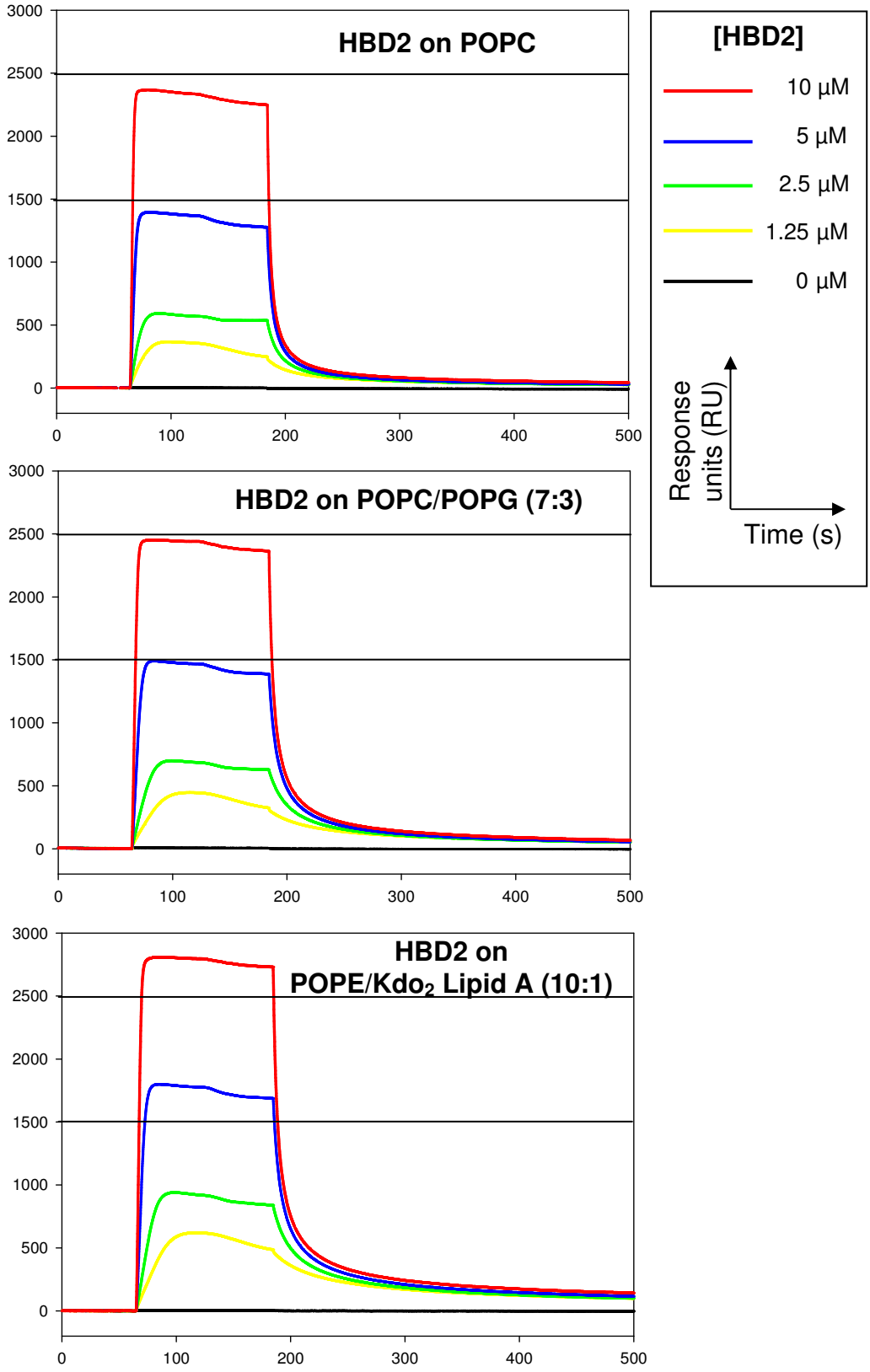

Figure 2.21. SPR sensorgrams of HBD2 interactions with POPC, POPC/POPG (7:3) and POPE/Kdo_2-Lipid A (top to bottom) membrane systems. Concentrations of HBD2 and axis units are indicated in the inset.

Chapter 3: Comparison of Synthetic and Recombinant Production of Defensins

In this study, two different methods were used to produce HBD1. A chemical approach was employed via the solid-phase peptide synthesis (SPPS) method in collaboration with Dr. Derek Macmillan (UCL, London). Then a second approach using the recombinant method as previously described (Chapter 2) was tested.

3.1 Solid-Phase Peptide Synthesis (Attempt) of HBD1.

Solid-phase peptide synthesis (SPPS) is highly convenient for natural peptides which are difficult to express in bacteria. Therefore its use for the synthesis of antimicrobial peptides such as defensins was tested as an alternative method of peptide production.

The general principle of SPPS is the construction of a peptide chain from the *C*-terminus to the *N*-terminus. The *C*-terminal amino acid residue is attached to an insoluble solid support via its carboxyl group while its *N*-terminus is protected by a group (Boc or F-moc). The targeted peptide is built-up by repeated cycles of coupling-deprotection of a free amino acid itself protected at its *N*-termini.

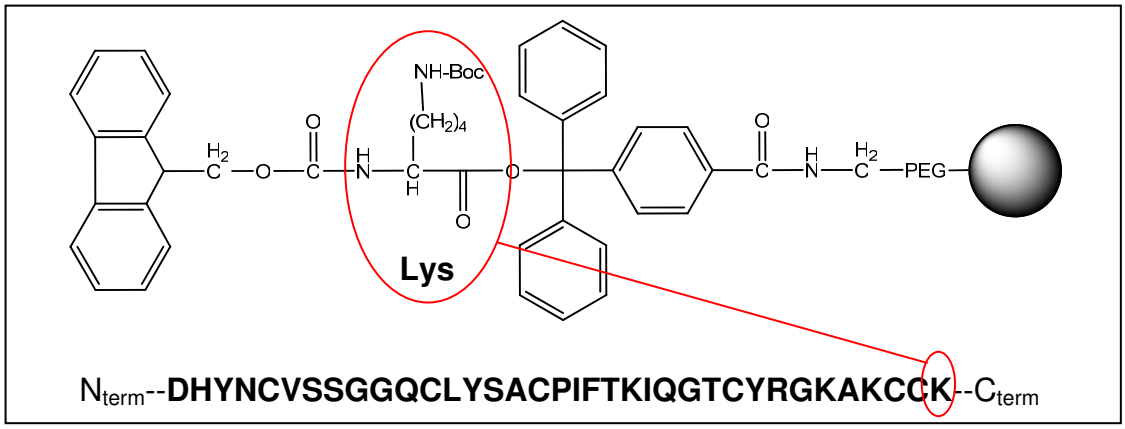

Figure 3.1. Chemical structure of the resin used for the synthesis of HBD1. The location of the starting lysine residue on the resin and within the HBD1 sequence is indicated in red circles.

The mature HBD1 is a 36 amino acid peptide with a lysine residue at the *C*-terminus (Fig. 3.1). The theoretical mass of the reduced peptide (6 free thiols) is 3934.1 Da. In order for the reaction to proceed from C-terminus to *N*-terminus the starting material used was a Fmoc-Lys(Boc)-NovaSyn® TGT resin (Fig. 3.1) where the first *C*-terminal amino acid is a lysine protected with a F-moc group.

The synthesis of HBD1 was performed in two steps; the first half was synthesised (36th to 19th amino acids) and the process analysed by ESI-MS. After the

first half synthesis, four major species were observed including the correct fragment of HBD1 of 2049.6 Da (2048.4 Da for calculated mass) which at this stage remains the major species (data not shown). However, after the second half synthesis, an RP-HPLC column was used to analyse the crude product (Fig. 3.2). The chromatograph profile of the crude product shows several overlapping peaks. Analysis by LC-ESI-MS confirmed the complexity of the crude sample and the full length HBD1 was difficult to detect. Therefore the isolation of the peptide from other truncated or larger fragments remained improbable.

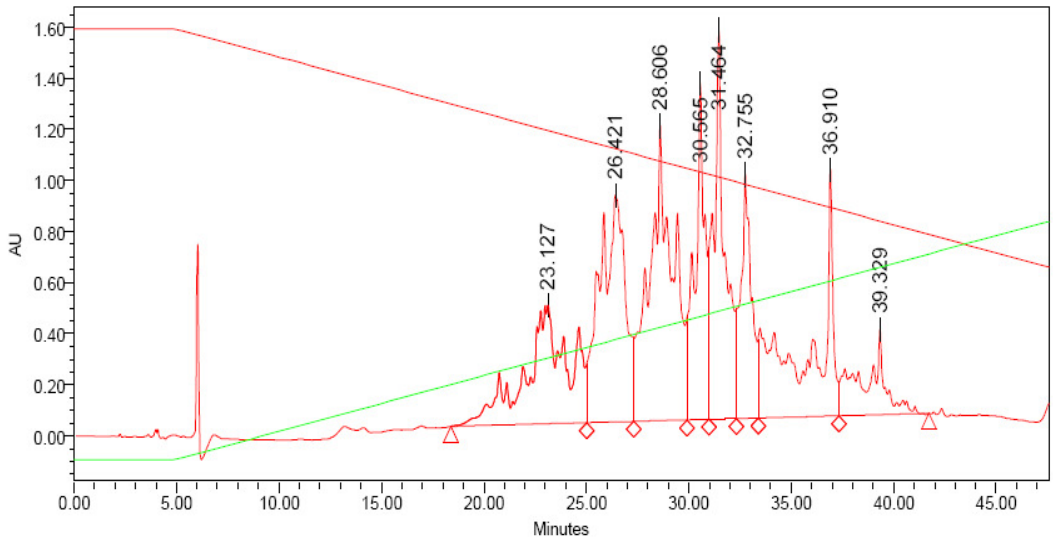

Figure 3.2. Chromatogram of crude HBD1 after the attempt of the full peptide synthesis.

A second chemical synthesis of HBD1 was attempted. We decided to fractionate the synthesis in 3 equal parts of 12 mers each. The fragment containing the first twelve amino acids from the C-terminus was synthesised without any technical difficulty leading to one main species. However, synthesis of the subsequent twelve amino acid segment proved unsuccessful. The errors in the synthesis could be caused by a sequence of hydrophobic amino acids. This hydrophobic patch is located in the middle of the amino acid sequence and could involve the following sequence: ACPIFTKI (Fig. 3.1). This hydrophobic sequence tends to make the accessibility harder for the coupling of other amino acids.

There are reports in the literature of the preparation of HBD1 using SPPS [102, 132], but in these reports no mention is made of any technical difficulties encountered, or indeed in any problems with obtaining full length product. As a result,

and since our recombinant method has shown success in generating HBD2, we decided to abandon the synthesis of HBD1 in favour of a recombinant method.

3.2 Recombinant Expression and Purification of HBD1

A codon-optimised, synthetic *HBD1* gene was purchased from CLONTECH and cloned alongside with the HisKSI sequence in the pUC19 vector. The HisKSI-HBD1 fragment was cloned into the pET28a vector using NcoI and XhoI restriction sites. We used the pET-28a/HBD2 plasmid as template and replaced the HisKSI-HBD2 sequence with KSI-HBD1 to finally generate the pET28a/HBD1 plasmid (not shown). The method of expression and purification used was similar to the method described in Chapter 2. HBD1 was expressed as inclusion bodies due to the highly insoluble fused-tag KSI.

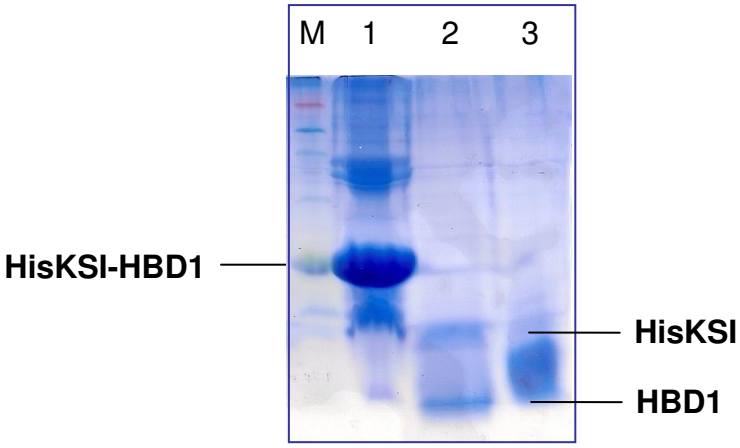

Figure 3.3. Purification steps of HBD1. HisKSI-HBD1 fused peptide was solubilised (lane 1) before being cleaved (lane 2). The crude fraction containing HBD1 after precipitation is shown on lane 3.

The last steps of purification and cleavage of the inclusion bodies leading to a crude HBD1 solution were monitored by SDS-PAGE (Fig. 3.3). The crude HBD1 solution was then injected onto a reverse-HPLC system fitted with a semi-preparative C18 column. The different eluted fractions were collected and analysed by ESI-MS. The fractions including the reduced HBD1 were collected, lyophilized, and reinjected onto the C18 semi-preparative column (Fig. 3.4). The main peak at a retention time of 35-36 min. was analysed by ESI-MS (Fig. 3.4, inset) and a deconvoluted mass of

3934.0 ± 2.8 Da was obtained, which is in agreement with the predicted mass of 3934.6 Da corresponding to the reduced form of the peptide. However, another species was present in the sample with a calculated mass of 3982.4 ± 1.55 Da which correspond to an increase of 48 Da compared to reduced HBD1. This adducted species was difficult to separate from the genuine peptide. Therefore the folding step was carried out in the presence of this unknown species.

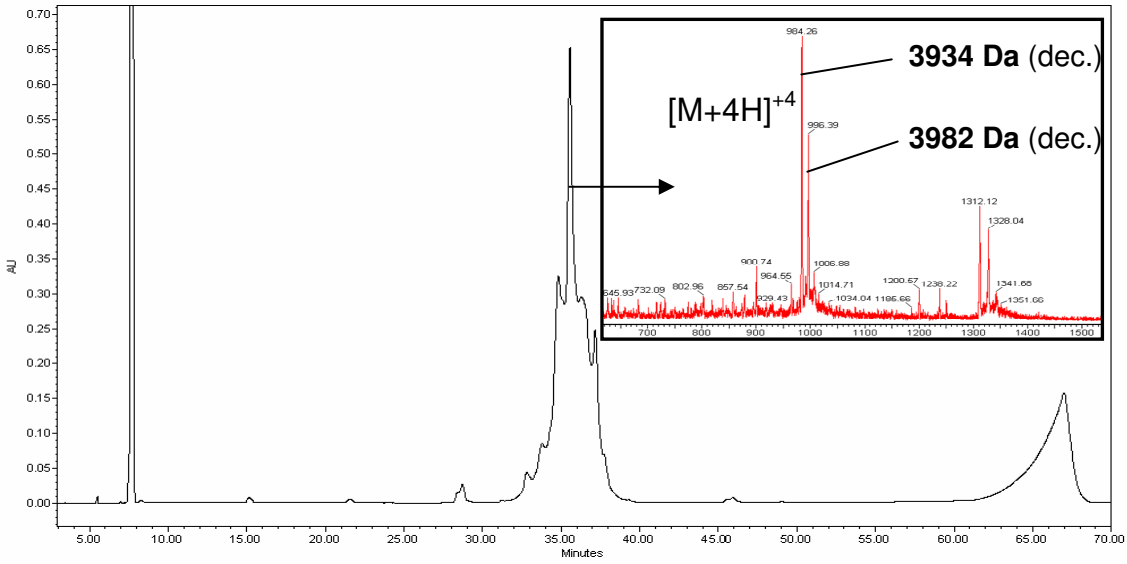

Figure 3.4. Reverse-phase chromatogram of reduced HBD1. Peak at elution time of 35-36 minutes was extracted and analysed by ESI-MS. Deconvolution of the +4 charge state generated masses of 3934 Da and 3982 Da corresponding respectively to reduced HBD1 and a 48 Da HBD1 adduct (inset).

After being subjected to a cysteine/cystine redox buffer for 4 hours, the sample was injected onto the semi-preparative C18 column. The main peak eluted at 33 min. (Fig. 3.5) was manually extracted and analysed by ESI-MS.

ESI-MS analysis showed that the main species had a molecular mass of 3927.5 ± 1.6 Da after deconvolution. This mass approximated the theoretical mass of oxidised HBD1 of 3928.6 Da. Unfortunately, the 48 Da adduct previously described in the reduced sample was still present with a calculated molecular mass of 3977.2 ± 0.5 Da corresponding to approximately 5 Da loss compared to the reduced peptide mass. This result strongly suggests that the second species is an HBD2 peptide with a 48 Da adduct.

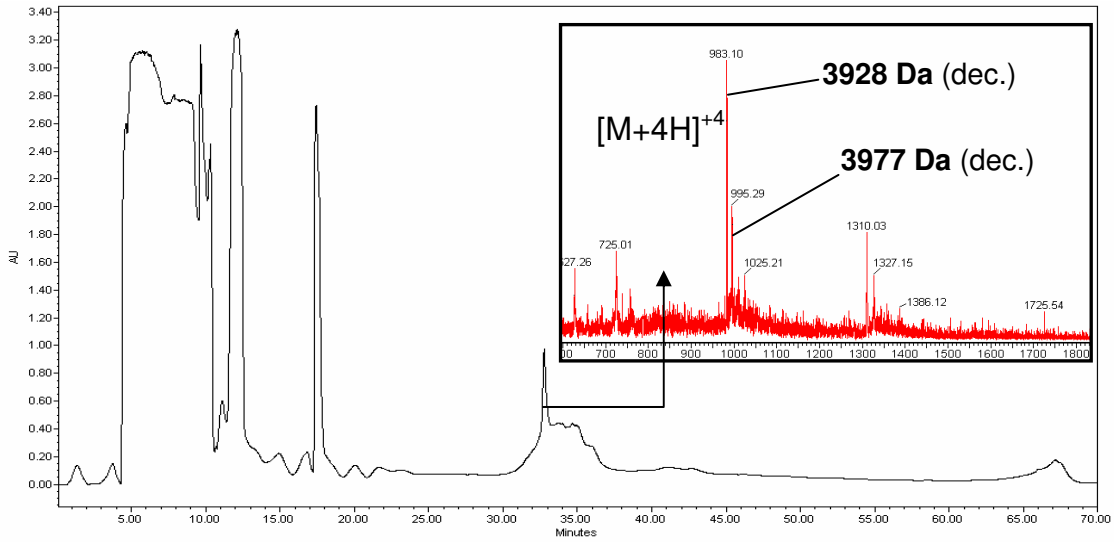

Figure 3.5. Reverse-phase HPLC chromatogram of HBD2 after a folding step. ESI-MS analysis of the peak eluted at 33 minutes confirmed the presence of a ~48 Da adduct (inset).

We suggest that the presence of a 48 Da adduct on HBD1 could be due to a cysteine oxidation leading to the presence of a cysteic acid. This modification thus prohibits disulfide bridge formation between two cysteines. Therefore the peptide remains in an incomplete folded state with only the possibility to form two disulfide bridges.

NMR studies confirmed the lack of folding for HBD1 as the ^{1}D ^{1}H NMR spectrum showed a poor dispersion profile noticeable in the amide region at around 8 ppm (Fig. 3.6). The NMR spectrum profile indicates the presence of a random coil conformation.

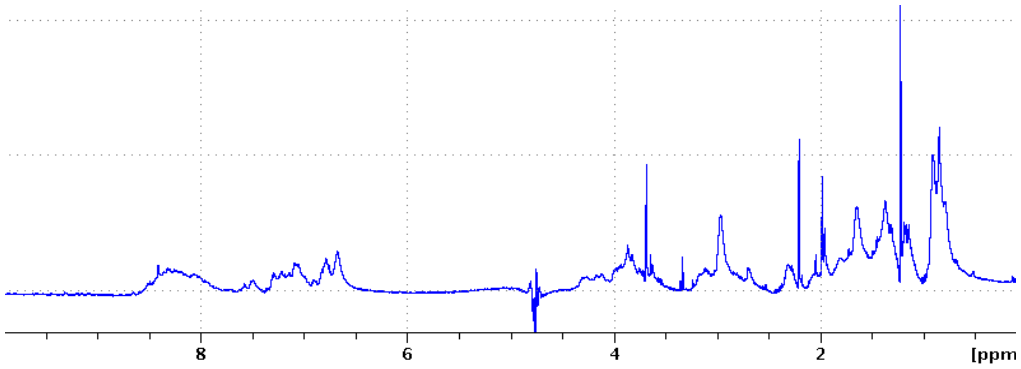

Figure 3.6. 1D ^{1}H NMR spectra of HBD1. A poor dispersion profile can be observed in the amide region (~8 ppm) suggesting a lack of folding for HBD1.

Since we encountered technical difficulties with the preparation of HBD1 it was decided to focus more on the successful HBD2 studies. Our decision was further vindicated by the publication of a *tour-de-force* study in early 2007 [122]. In this report the authors developed a fusion strategy to prepare wild-type HBD1 and 26 mutants. The authors used a novel trytpophan operon fusion, CNBr cleavage and the expensive GSSG/GSG system to oxidise the peptides. The wild type and mutants were tested for antimicrobial and chemotactic activity and incredibly, 19 of the 26 were crystallized. This confirms that a recombinant method is a powerful tool to study defensins.

3.3 Conclusions (Chapters 2 & 3)

The isolation and characterisation of various defensins has been a challenge over the past 20 years. The process of isolation of such peptides from their natural environment yields only a few micrograms of chemically homogeneous product. The necessity to develop tools for the production of peptides is required before structural and biological analyses can be carried out. In this study we investigated methods for production of HBD2 and HBD1.

The first method describes the recombinant expression and purification of HBD2 in *E. coli*. The *HBD2* gene, codon-optimised for bacterial expression, was cloned with a KSI sequence in order to overcome the inherent antimicrobial activity of the defensin. KSI acts as an insoluble carrier that inactivates the antimicrobial activity of HBD2 during the expression process. The purification process involves isolating the inclusion bodies with a series of washes and sonications leading to a relatively pure KSI-HBD2 species. These inclusion bodies are solubilised and chemically cleaved at a single Met residue using an inexpensive reagent to separate the target peptide from the unwanted KSI. Moreover, our method does not use expensive proteases which require a specific target cleavage sites which are present in the amino acid sequence of the final product. The folding process within the defensin field has always been challenging. The disulfide bridge connections are a typical signature where defensins fall into 3 sub-families. Six cysteines are always present in defensins but their connection varies. The β-defensins display disulfide bonds between Cys^1-Cys^5, Cys^2-Cys^4 and Cys^3-Cys^6 whereas the α-defensins display Cys^1-Cys^6, Cys^2-Cys^4 and Cys^3-Cys^5 connectivities. After the folding step, HBD2 was

purified as a single isoform and proteolysis and MS analysis revealed it to have beta-defensin connectivity. This peptide was characterised by different biophysical techniques (NMR, mass-spectrometry) and its antimicrobial activity tested and validated against four strains including Gram-negative strains *E. coli* and *P. aeruginosa*, Gram-positive *S. aureus* bacteria and a fungus, *C albicans*. The HBD2 was also tested by our collaborator Dr. Julia Dorin against HEK293 cells expressing the GPCR receptor CCR6 and was found to be an active chemoattractant peptide (see Vargues *et al*., [128] – Appendix).

Furthermore, using surface plasmon resonance, binding studies of HBD2 with different membrane models indicated that HBD2 had a higher affinity for negatively-charged vesicles. However, the higher binding effect was observed when the deep-rough LPS Kdo_2-lipid A was embedded within the membrane. Thus we concluded that our method generated HBD2 which was suitable for structural and functional studies.

In order to carry out defensin/ligand binding studies we investigated the expression and purification of the labelled version of HBD2 incorporating the ^{15}N isotope. Using the same strategy as previously described, ^{15}N HBD2 was purified with an equivalent quality and quantity as observed for the non-labelled HBD2. Mass spectrometry and multi-dimensional NMR spectroscopy experiments showed that not only the peptide had 100% incorporation of ^{15}N, but the assignment of resonances revealed no ambiguous or overlapping peaks. This characteristic was not observed for the non-labelled peptide. Therefore the isotopically labelled peptide is a very potent tool for studying its interaction with diverse biologically relevant targets from bacteria to mammalian immune systems. Our success with HBD2 led us to attempt the production of HBD1 by this method, but problems during the purification process led to the formation of HBD1 adducts. The HBD1 purification was attempted only once and further attempts and optimizations are needed to reach the same standard of analytical purity as that found for HBD2.

The second method investigated used a chemical approach with solid phase peptide synthesis and Fmoc-protected amino acids. This method, allowing the chemical synthesis of peptides and small proteins, is very convenient and suitable for defensins or antimicrobial peptides as it avoids the fusion-tag strategy to counteract their toxicity towards bacteria. Solid-phase peptide synthesis was used to produce HBD1. The targeted peptide was 36 amino acids in length and taking into

consideration previous published synthetic methods, several attempts to synthesise the full length HBD1 remained unsuccessful. A hydrophobic patch of amino acids situated in the middle of the sequence made the coupling process difficult leading to a mixture of peptide with truncated peptide segments. The recovery and the purity of the full length HBD1 were very poor so that the synthesis could not be progressed.

The chemical synthesis of HBD2 was also attempted by a colleague with the same solid-phase method (E. Seo, data not shown). However, identical problems were encountered during the synthesis process and manual coupling was necessary to obtain the fully synthesised peptide.

3.4 References: Chapter 1, 2 & 3

1 Izadpanah, A., and Gallo, R. L. (2005) *J. Am. Acad. Dermatol*. **52**, 381-390

2 Wang, Z., and Wang, G. (2004) *Nucleic. Acids. Research.* **32**, 590-592

3 Wang, G., Li, X., and Wang, Z. (2009) *Nucleic. Acids. Research*. **37**, 933-937

4 Brogden, K. A., Ackermann, M., and Huttner, K. M. (1997) are *Antimicrob. Agents Chemother*. **41**, 1615-1617

5 Steiner, H., Hultmark, D., Engstrom, A., Bennich, H., and Boman, H. G. (1981) *Nature* **292**, 246-248

6 Ganz, T., Selsted, M. E., Szklarek, D., Harwig, S. S., Daher, K., Bainton, D. F., and Lehrer, R. I. (1985) *J. Clin. Invest*. **76**, 1427-1435

7 Oyston, P. C., Fox, M. A., Richards, S. J., and Clark. G. C. (2009) *J. Med. Microbiol.* **58**, 977-987

8 Hancock, R. E., and Patrzykat, A. (2002) *Curr. Drug. Targets. Infect. Disord.* **2**, 79-83

9 Hancock, E., and Lehrer, R. (1998) *Trends. Biotechnol.* **16**, 82-88.

10 Zasloff, M., (2002) *Nature* **415** 389-395

11 Perron, G.G., Zasloff, M., and Bell. G. (2006) *Proc. Biol. Sci.* **273**, 251-256

12 Tang, Y. Q., Yuan, J., Osapay, G., Osapay, K., Tran, D., Miller, C. J., Ouellette, A. J., and Selsted, M. E. (1999) *Science* **286**, 498-502

13 Tang, Y. Q., Yuan, J., Osapay, G., Osapay, K., Tran, D., and Miller, C. J. (1999) *Science* **286**, 498–502

14 Janeway, C. A. Jr., and Medzhitov, R. (2001) *Annu. Rev. Immunol*. **20**, 197-216

15 Hoffmann, J. A., Kafatos, F. C., Janeway, C. A. Jr., and Ezekowitz, R. A. B. (1999) *Science* **284**, 1313–1318

16 Zanetti, M. (2004) *J. Leukoc. Biol.* **75**, 39-48

17 Bals, R., Wang, X., Zasloff, M., Wilson, J. M. (1998) *Proc. Natl. Acad. Sci. U S A* **95**, 9541-9546

18 Rice, W. G., Ganz, T., Kinkade, J. M. Jr., Selsted, M. E., Lehrer, R. I., Parmley, R. T. (1987) *Blood* **70**, 757-765

19 Faurschou, M., Sørensen, O. E., Johnsen, A. H., Askaa, J., and Borregaard, N. (2002) *Biochim. Biophys. Acta*. **1591**, 29-35

20 Wehkamp, J., Chu, H., Shen, B., Feathers, R. W., Kays, R. J., Lee, S. K., and Bevins, C. L. (2006) *FEBS. Lett.* **580**, 5344-5350

21 Ayabe, T., Satchell, D. P., Wilson, C. L., Parks, W. C., Selsted, M. E., and Ouellette, A. J. (2000) *Nature. Immunol*. **1**, 113-118

22 Salzman, N. H., Ghosh, D., Huttner, K. M., Paterson, Y., Bevins, C. L. (2003) *Nature* **422**, 522-526

23 Schutte, B. C., Mitros, J. P., Bartlett, J. A., Walters, J. D., Jia, H. P., Welsh, M. J., Casavant, T. L., and McCray, P.B. Jr. (2002) *Proc. Natl. Acad. Sci. U S A* **99**, 2129-2133

24 Zhao, C., Wang, I., and Lehrer. R. I. (1996) *FEBS Lett.* **396** 319-322

25 Fulton, C., Anderson, G. M., Zasloff, M., Bull, R., and Quinn. A. G. (1997) *Lancet* **350**, 1750-1751

26 McCray, P. B. Jr., and Bentley. L. (1997) *Cell. Mol. Biol.* **16**, 343-349

27 Valore, E. V., Park, C. H., Quayle, A. J., Wiles. K. R., McCray. P. B. Jr., and Ganz, T. (1998) *J. Clin. Invest.* **101**, 1633-1642

28 Bals, R., Weiner, D., Meegalla, R., Accurso, F., and Wilson, J. (2001) *Am. J. Respir. Cell. Mol. Biol*. **25**, 21-25

29 Morrison, G., Kilanowski, F., Davidson, D., Dorin, J. (2002) *Infect Immun*.

70, 3053-3060

30 Kanda, N., and Watanabe, S. (2007) *Am. J. Physiol. Cell. Physiol.* **293**, 1916-1923

31 Moser, C., Weiner, D. J., Lysenko, E., Bals, R, Weiser, J. N., and Wilson, J. M. (2002) *Infect. Immun*. **70**, 3068-3072

32 Lehrer, R. I. (2004) *Nat. Rev. Microbiol*. **2**, 727-738

33 Borghesi, L., and Milcarek. C. (2007) *Cancer. Research.* **67**, 3989-3993

34 Territo, M. C., Ganz, T., Selsted, M. E., and Lehrer, R. (1989) *J. Clin. Invest.* **84**, 2017-2020

35 Yang, D., Chen, Q., Chertov, O., and Oppenheim, J. J. (2000) *J. Leukoc. Biol.* **68**, 9-14

36 Taylor, K., Clarke, D. J., McCullough, B., Chin, W., Seo, E., Yang, D., Oppenheim, J., Uhrin, D., Govan, J. R., Campopiano, D. J., MacMillan, D., Barran, P., and Dorin, J. R. (2008) *J. Biol. Chem.* **283**, 6631-6639

37 Yang, D., Chertov, O., Bykovskaia, S. N., Chen, Q., Buffo, M. J., Shogan, J., Anderson, M., Schröder, J. M., Wang, J. M., Howard, O. M., and Oppenheim, J. J. (1999) *Science* **286**, 525-528

38 Niyonsaba, F., Ogawa, H., and Nagaoka, I. (2004) *Immunology* **111**, 273-281

39 Hoover, D. M., Boulegue, C., Yang, D., Oppenheim, J. J., Tucker, K., Lu, W., and Lubkowski. J. (2002) *J. Biol. Chem*. **277**, 37647-37654

40 Yang, D., Chen, Q., Hoover, D. M., Staley, P., Tucker, K. D, Lubkowski, J., and Oppenheim, J. J. (2003) *J. Leukoc. Biol*. **74**, 448-455

41 Daher, K. A., Selsted, M. E., and Lehrer, R, I. (1986) *J. Virol.* **60**, 1068-1074

42 Lehrer, R. I., Daher, K., Ganz, T., and Selsted, M. E. (1985) *J. Virol.* **54**, 467-472

43 Sinha, S., Cheshenko, N., Lehrer, R. I., and Herold, B. C. (2003) *Antimicrob. Agents. Chemother*. **47**, 494-500

44 Leikina, E., Delanoe-Ayari, H., Melikov, K., Cho, M. S., Chen, A., Waring, A. J., Wang, W., Xie, Y., Loo, J. A., Lehrer, R. I., and Chernomordik, L. V. (2005) *Nat. Immunol*. **6**, 995-1001

45 Wang, W., Cole, A. M., Hong, T., Waring, A. J., and Lehrer, R. I. (2003) *J. Immunol.* **170**, 4708-16

46 Lehrer, R. I., Jung, G., Ruchala, P., Andre, S., Gabius, H. J., and Lu, W. (2009) *J. Immunol.* **183**, 480-490

47 Münk, C., Wei, G., Yang, O. O., Waring, A. J., Wang, W., Hong, T., Lehrer, R. I., Landau, N. R., and Cole, A. M. (2003) *AIDS. Res. Hum. Retroviruses.* **19**, 875-881

48 Cole, A. M., Hong, T., Boo, L. M., Nguyen, T., Zhao, C., Bristol, G., Zack, J. A., Waring, A. J., Yang, O. O., Lehrer, R. I. (2002) *Proc. Natl. Acad. Sci. U S A* **99**, 1813-1818

49 Wang, W., Owen, S. M., Rudolph, D. L., Cole, A. M., Hong, T., Waring, A. J., Lal, R. B., and Lehrer, R. I. (2004) *J. Immunol*. **173**, 515-520

50 Yasin, B., Wang, W., Pang, M., Cheshenko, N., Hong, T., Waring, A. J., Herold, B. C., Wagar, E. A., and Lehrer, R. I. (2004) *J. Virol.* **78**, 5147-5156

51 Quiñones-Mateu, M. E., Lederman, M. M., Feng, Z., Chakraborty, B., Weber, J., Rangel, H. R., Marotta, M. L., Mirza, M., Jiang, B., Kiser, P., Medvik, K., Sieg, S. F., and Weinberg, A. (2003) *AIDS* **17**, 39-48

52 Alp, S., Skrygan. M., Schlottmann, R., Kreuter, A., Otte, J. M., Schmidt, W. E., Brockmeyer, N. H., and Bastian, A. (2005) *Eur. J. Med. Res*. **10**, 1-6

53 Markeeva, N., Lisovskiy, I., Lyzogubov, V., Usenko, V., Soldatkina, M.,

Merentsev, S., Zaitsev, S., Kondratskii, Y., Tofan, A., Osinskiy, S., and Pogrebnoy, P. (2005) *Exp. Oncol*. **27**, 130-135

54 Donald, C. D., Sun, C. Q., Lim, S. D., Macoska, J., Cohen, C., Amin, M. B., Young, A. N., Ganz, T. A., Marshall, F. F., and Petros, J. A. (2003) *Lab. Invest.* **83**, 501-505

55 Young, A. N, de Oliveira Salles, P. G., Lim, S. D., Cohen, C., Petros, J. A., Marshall, F. F., Neish, A. S., and Amin, M. B. (2003) *Am. J. Surg. Pathol.* **27**, 199-205

56 Abiko, Y., Nishimura, M., Kusano, K., Yamazaki, M., Arakawa, T., Takuma, T., and Kaku, T. (2003) *J. Dermatol. Sci.* **31**, 225-228

57 Varoga, D., Pufe, T., Harder, J., Schröder, J. M., Mentlein, R., Meyer-Hoffert, U., Goldring, M. B., Tillmann, B., Hassenpflug, J., Paulsen, F. (2005) *Arthritis. Rheum.* **52**, 1736-1745

58 Lehrer, R. I. (2004) *Nat. Rev. Microbiol*. **2**, 727-738

59 Pazgier, M., Hoover, D. M., Yang, D., Lu, W., and Lubkowski, J. (2006) *Cell. Mol. Life. Sci*. **63**, 1294-1313

60 Bensch, K. W., Raida, M., Mägert, H. J., Schulz-Knappe, P., and Forssmann, W. G. (1995) *FEBS. Lett.* **368**, 331-335.

61 Zhao, C., Wang, I., and Lehrer, R. I. (1996) *FEBS. Lett*. **396**, 319-322

62 McCray, P. B. Jr., and Bentley, L. (1997) *Am. J. Respir. Cell. Mol. Biol***. 16**, 343-349

63 Valore, E.V., Park, C. H., Quayle, A. J, Wiles, K. R, McCray, P. B. Jr., and Ganz, T. (1998) *J. Clin. Invest*. **101**, 1633-1642

64 Feng, Z., Jiang, B., Chandra, J., Ghannoum, M., Nelson, S., and Weinberg. A. (2005) *J. Dent. Res.* **84**, 445-450

65 Joly, S., Organ, C. C., Johnson, G. K., McCray, P. B. Jr., and Guthmiller, J. M. (2005) *Mol. Immunol.* **42**, 1073-1084

66 Harder, J., Bartels, J., Christophers, E., and Schröder, J. M. (1997) *Nature.* **387**, 861

67 Bals, R., Wang, X., Wu, Z., Freeman, T., Bafna, V., Zasloff, M., and Wilson, J. M (1998) *J. Clin. Invest.* **102**, 874-880.

68 Singh, P. K., Jia, H. P., Wiles, K., Hesselberth, J., Liu, L., Conway, B. A. D., Greenberg, E. P., Valore, E. V., Welsh, M. J., Ganz, T., Tack, B. F., and McCray, P. B. Jr. (1998) *Proc. Natl. Acad. Sci. U S A* **95**, 14961-14966

69 Garcia, J. R., Jaumann, F., Schulz, S., Krause, A., Rodriguez-Jimenez, J., Forssmann, U., Adermann, K., Klüver, E., Vogelmeier, C., Becker, D., Hedrich, R., Forssmann, W. G., and Bals, R. (2001) *Cell. Tissue. Res.* **306**, 257-264

70 Jia, H. P., Schutte, B. C., Schudy, A., Linzmeier, R., Guthmiller, J. M., Johnson, G. K., Tack, B. F., Mitros, J. P., Rosenthal, A., Ganz, T., and McCray, P. B. Jr. (2001) *Gene* **263,** 211-218

71 Harder. J., Bartels, J., Christophers, E., and Schröder, J. M. (2001) *J. Biol. Chem.* **276**, 5707-5713

72 García, J. R., Krause, A., Schulz, S., Rodríguez-Jiménez, F.J., Klüver, E., Adermann, K., Forssmann, U., Frimpong-Boateng, A., Bals, R., and Forssmann, W. G. (2001) *FASEB. J.* **15**, 1819-1821

73 Hoover, D. M., Chertov, O., and Lubkowski. J. (2001) *J. Biol. Chem.* **276**, 39021-39026

74 Sawai, M. V., Jia, H. P., Liu. L., Aseyev, V., Wiencek, J. M., McCray, P. B. Jr., Ganz, T., Kearney, W. R., and Tack, B. F. (2001) *Biochemistry* **40**, 3810-

3816

75 Schibli, D. J., Hunter, H. N., Aseyev, V., Starner, T. D., Wiencek, J. M., McCray, P. B. Jr. Tack, B. F., and Vogel, H. J. (2002). *J. Biol. Chem.* **277**, 8279-8289

76 Bauer, F., Schweimer, K., Kluver, E., Conejo-Garcia, J. R., Forssmann, W. G., Rosch, P., Adermann, K., and Sticht, H. (2001). *Protein. Sci.* **10**, 2470-2479

77 Hoover, D. M., Rajashankar, K. R., Blumenthal, R., Puri, A., Oppenheim, J. J., Chertov, O., and Lubkowski, J. (2000) *J. Biol. Chem.* **275**, 32911-32918

78 Thouzeau, C., Le Maho. Y., Froget. G., Sabatier, L., Le Bohec, C., Hoffmann, J. A., and Bulet, P. (2003) *J. Biol. Chem*. **278**, 51053-51058

79 Landon, C., Thouzeau, C., Labbé, H., Bulet, P., and Vovelle, F. (2004) *J. Biol. Chem*. **279**, 30433-30439

80 Harder, J., Meyer-Hoffert, U., Wehkamp, K., Schwichtenberg, L., Schröder, J. M. (2004) *J. Invest. Dermatol.* **123**, 522-529

81 Chadebech, P., Goidin, D., Jacquet, C., Viac, J., Schmitt, D., and Staquet, M. J. (2003) *Cell. Biol. Toxicol*. **19**, 313-324

82 King, A. E., Fleming, D. C., Critchley, H. O., and Kelly, R. W. (2002) *Mol. Hum. Reprod*. **8**, 341-349

83 Sørensen, O. E., Cowland, J. B., Theilgaard-Mönch, K., Liu, L., Ganz, T., and Borregaard, N. (2003) *J. Immunol.* **170,** 5583-5589

84 Tsutsumi-Ishii, Y., and Nagaoka, I. (2002) *J. Leukoc. Biol.* **71,** 154-162

85 Duits, L. A., Nibbering, P. H., van Strijen, E., Vos, J. B., Mannesse-Lazeroms, S. P., van Sterkenburg, M.A., and Hiemstra, P. S. (2003) *FEMS. Immunol. Med. Microbiol.* **38**, 59-64

86 Froy, O. (2005) *Cell. Microbiol.* **7**, 1387-1397

87 Wang, X., Zhang, Z., Louboutin, J. P., Moser, C., Weiner, D. J., and Wilson, J. M. (2003) *FASEB. J.* **17**, 1727-1729

88 MacRedmond, R., Greene, C., Taggart, C. C., McElvaney, N., O'Neill, S. (2005) *Respir. Res.* **6**, 116

89 Ghosh, D., Porter, E., Shen, B., Lee, S. K., Wilk, D., Drazba, J., Yadav, S. P., Crabb, J. W., Ganz, T., and Bevins, C. L. (2002) *Nat. Immunol.* **3**, 583-590

90 Wilson, C. L., Schmidt, A. P., Pirilä, E., Valore, E. V., Ferri, N., Sorsa, T., Ganz, T., and Parks, W. C. (2009) *J. Biol. Chem*. **284**, 8301-8311

91 Croft, A. C., D'Antoni, A. V., and Terzulli, S. L. (2007) *Med. Sci. Monit*. **13**, 103-118

92 Lehrer, R. I., Ganz, T. (2002) *Curr. Opin. Immunol.* **14**, 96-102

93 Yu, Q., Lehrer, R. I., and Tam, J. P. (2000) *J. Biol. Chem.* **275**, 3943-3949

94 Bals, R., Wang, X., Wu, Z., Freeman, T., Bafna, V., Zasloff, M., and Wilson, J. M. (1998) *J. Clin. Invest.* **102**, 874-880

95 Goldman, M. J., Anderson, G. M., Stolzenberg, E.D., Kari, U.P., Zasloff, M., and Wilson, J. M. (1997) *Cell.* **88**, 553-560

96 Knowles, M. R., Robinson, J. M., Wood, R. E., Pue, C. A., Mentz, W. M., Wager, G. C., Gatzy, J. T., and Boucher, R. C. (1997) *J. Clin. Invest*. **100**, 2588-2595

97 Matsui, H., Grubb , B.R., Tarran, R., Randell, S. H., Gatzy, J. T., Davis, C. W., and Boucher, R. C. (1998) *Cell* **95**, 1005-1015

98 Chen. X., Niyonsaba, F., Ushio, H., Okuda, D., Nagaoka, I., Ikeda, S., Okumura, K., and Ogawa, H. (2005) *J. Dermatol. Sci.* **40**, 123-132

99 Boniotto, M., Antcheva, N., Zelezetsky, I., Tossi, A., Palumbo, V., Verga, Falzacappa, M. V., Sgubin, S., Braida, L., Amoroso, A., and Crovella, S.

(2003) *Biochem. J.* **374,** 707-714

100 Klüver, E., Schulz-Maronde, S., Scheid, S., Meyer, B., Forssmann, W. G., and Adermann, K. (2005) *Biochemistry.* **44**, 9804-9816

101 Campopiano, D.J., Clarke, D.J., Polfer, N.C., Barran, P. E., Langley, R. J., Govan, J. R., Maxwell, A., and Dorin, J. R. (2004) *J. Biol. Chem.* **279**, 48671-48679

102 Wu, Z., Hoover, D. M., Yang, D., Boulègue, C., Santamaria, F., Oppenheim, J. J., Lubkowski, J., and Lu, W. (2003) *Proc. Natl. Acad. Sci. U S A* **100**, 8880-8885

103 Mandal, M., Jagannadham, M. V., and Nagaraj, R. (2002) *Peptides* **23**, 413-418

104 Mandal, M., and Nagaraj, R. (2002) *J. Pept. Res.* **59,** 95-104

105 Antcheva, N., Boniotto, M., Zelezetsky, I., Pacor, S., Verga, Falzacappa, M. V., Crovella, S., Tossi, A. (2004) *Antimicrob. Agents. Chemother*. **48**, 685-688

106 Morgera, F., Antcheva, N., Pacor, S., Quaroni, L., Berti, F., Vaccari, L., and Tossi, A. (2008) *J. Pept. Sci.* **14**, 518-523

107 Maemoto, A., Qu, X., Rosengren, K. J., Tanabe, H., Henschen-Edman, A., Craik, D. J., and Ouellette, A. J. (2004) *J. Biol. Chem.* **279**, 44188-44196

108 Fujii, G., Selsted, M. E., and Eisenberg, D. (1993) *Protein. Sci.* **2**, 1301-1312

109 Wimley, W. C., Selsted, M.E., and White, S. H. (1994) *Protein. Sci.* **3**, 1362-1373

110 Brogden, K. A. *Nature. Reviews. Microbiology.* **3**, 238-250

111 Yang, L., Harroun, T. A., Weiss, T. M., Ding, L., and Huang, H. W. (2001) *Biophys. J*. **81**, 1475-1485

112 Hill, C. P., Yee, J., Selsted, M. E., Eisenberg, D. (1991) *Science* **251**, 1481-

1485

113 Lehrer, R. I., Barton, A., Daher, K. A., Harwig, S. S., Ganz, T., and Selsted, M. E. (1989) *J. Clin. Invest*. **84**, 553-561

114 Merrifield, R. B. (1963) *J. Am. Chem. Soc*. **85**, 2149-2154

115 Raj, P. A., Antonyraj, K. J., and Karunakaran, T. (2000) *Biochem. J.* **347**, 633-641

116 Klüver, E., Adermann, K., and Schulz, A. (2006) *J. Pept. Sci*. **12**, 243-257

117 Cipáková, I., and Hostinová, E. (2005) *Protein. Pept. Lett*. **12**, 551-554

118 Wang, A., Wang, S., Shen, M., Chen, F., Zou, Z., Ran, X., Cheng, T., Su, Y., Wang, J. (2009) *Appl. Microbiol. Biotechnol*.

119 Fang, X., Peng, L., Xu, Z., Wu, J., and Cen, P. (2002) *Protein. Pept. Lett*. **9**, 31-37

120 Huang, L., Wang, J., Zhong, Z., Peng, L., Chen, H., Xu, Z., and Cen, P. (2006) *Biotechnol. Lett.* **28,** 627-632

121 Xu, Z., Peng, L., Zhong, Z., Fang, X., and Cen, P. (2006) *Biotechnol. Prog*. **22**, 382-386

122 Pazgier, M., Prahl, A., Hoover, D. M., and Lubkowski, J. (2007) *J. Biol. Chem*. **282**, 1819-1829

123 Chen, H., Xu, Z., and Cen, P. (2006) *Protein. Pept. Lett*. **13**, 155-162

124 Valore, E. V., Martin, E., Harwig, S. S., and Ganz, T. (1996) *J. Clin. Invest*. **97**, 1624-1629

125 Valore, E. V., Park, C. H., Quayle, A. J., Wiles, K. R., McCray, P. B. Jr., and Ganz, T. (1998) *J. Clin. Invest*. **101,** 1633-1642

126 Porter, E. M., van Dam, E., Valore, E. V., and Ganz, T. (1997) *Infect. Immun*. **65**, 2396-2401

127 Liu, A. Y., Destoumieux, D., Wong, A. V., Park, C. H., Valore, E. V., Liu, L., and Ganz, T. (2002) *J. Invest. Dermatol*. **118,** 275-281

128 Vargues, T., Morrison, G. J., Seo, E. S., Clarke, D. J., Fielder, H. L., Bennani, J., Pathania, U., Kilanowski, F., Dorin, J. R., Govan, J. R., Mackay, C. L., Uhrín, D., and Campopiano, D. J. (2009) *Protein. Pept. Lett*. **16**, 668-676

129 Seo, E. S., Vargues, T., Clarke, D. J., Uhrín, D., and Campopiano, D. J. (2009) *Protein. Expr. Purif*. **65**, 179-184

130 Xu, Z., Zhong, Z., Huang, L., Peng, L., Wang, F., and Cen, P. (2006) *Appl. Microbiol. Biotechnol*. **72**, 471-479

131 Nomura, K., Inaba, T., Morigaki, K., Brandenburg, K., Seydel, U., and Kusumoto, S. (2008) *Biophys. J*. **95**, 1226-1238

132 Morrison, G. M., Davidson, D. J., Kilanowski, F. M., Borthwick, D., W., Crook, K., Maxwell. A. I., Govan, J. R., and Dorin, J. R. (1998) *Mamm. Genome* **9**, 453-457

Chapter 4: Into the Resistance

4.1 Bacteria Fight Back

Over the last 25 years the discovery of hundreds of natural antimicrobial peptides found among all classes of life triggered hope that they could be developed into new sources of antibiotics and therapeutic agents. Despite the fact that members of the "antimicrobial peptide" family display a range of favourable properties with novel features, only a select few have proceeded into clinical trials and no published data of commercial success have been reported to date [1, 2].

The challenges faced by such compounds in a clinical setting are tightly linked to the ingenuous adaptability of pathogenic bacteria presenting multifaceted countermeasures to annihilate antibiotic actions. A majority of these countermeasures are membrane-related features. In 2003, Yeaman and Yount have published a review that summarises the different known mechanisms of bacteria resistance [3]. Within the review, the authors present two distinct strategies for resistance, a constitutive (or passive) and an inducible (or adaptive) mechanism. Examples of passive resistance include electrostatic shielding where bacteria encapsulate in anionic matrices acting as a "lure" for cAMPs and also bacteria that constitutively express a membrane pattern with more neutral or positively charged components despite the lack of cAMPs in their close environment.

Some Gram-positive bacteria such as *Staphylococcus* or *Enterococcus* species "naturally" display structural features within their membrane which render the accessibility or interactions of antimicrobial peptides difficult [4]. Membranes of Gram-positive bacteria are composed of teichoic acid polymers and peptidoglycans and no outer membrane is present in such bacteria. *S. aureus* display a lipid composition enriched in phosphatidyl glycerol (PG) derivatives (modification of PG with l-lysine) or teichoic acids (incorporation of d-alanine) substituted with d-alanine resulting in a significantly less electronegative membrane composition [5-7]. These techoic acids may play a key role in adherence, colonisation, bio-film formation and nosocomial infections by *Staphylococcus aureus* [8, 9]. Moreover, membrane fluidity appears to play a key role in *S. aureus* resistance to platelet microbicidal protein (PMP), a small cationic antimicrobial peptide. Bayer and coworkers found a higher degree of fluidity in membranes from resistant strains in comparison to PMP-sensitive strains [10].

With regard to the adaptive resistance mechanism, different strategies adopted by various microorganisms have been reported. One of the resistance mechanisms developed by some bacteria is an efflux-dependent process whereby pathogens are able to expel AMPs through energy dependent pumps. Shafer *et al*. reported this mechanism for *Neisseria gonorrheoea* in 1998 after observing that the susceptibility of gonococci towards defensins and various cAMPs was modulated by an energy-dependent efflux pump termed multiple transferrable resistance (tmr) [11]. Resistance involving such efflux systems has also been observed in *Yersinia* sp., the Gram-positive bacteria *S. aureus* and some fungi [12-14].

Another inducible resistance mechanism found in many bacteria is the ability to produce proteases or peptidases in response to an antimicrobial stress. In *Salmonella*, an outer membrane endopeptidase (PgtE) was identified and was related to the same proteases family found in *E. coli* and *Yersinia* [15]. Such proteases are able to specifically cleave peptides between two successive basic residues targeting various antimicrobial peptides. However, the PgtE protease in *Salmonella* is unable to provide resistance towards antimicrobial peptides with a β-sheet core structure constrained by disulfide bridges such as protegrins or defensins.

In 2001, a new concept of cAMPs resistance was observed in *Shigella* species, a pathogen able to reduce or turn off the expression of HBD1 and LL37 in infected epithelial cells. Despite the lack of molecular evidence, the authors indicated that this downregulation could be due to a *Shigella* plasmid DNA [16]. Various other resistance mechanisms which have been reported are either linked to an adaptive or innate response. The remarkable adaptability of bacteria generates unlimited opportunities to allow them to occupy any kind of niche even under hostile environments. In fact many mechanisms, if not ill defined, remain unknown. However, it is interesting to draw parallels between antimicrobial peptides and resistance mechanism in bacteria as both have evolved side by side in an adaptive or innate manner trough a multifaceted creative adversity.

Nonetheless, in Gram-negative bacteria, a common and well-studied mechanism of resistance is the alteration of their cell envelope by the structural modification of a major component of the outer membrane, the lipopolysaccharides (LPSs).

4.2 LPS and Lipid A Biosynthesis in Gram-Negative Bacteria

LPS is one of the major components of the outer membrane in Gram-negative bacteria and belongs to the phosphorylated lipoglycans family. The LPS molecule consists of three parts, the O-antigen repeat units, the core polysaccharide and the lipid A (Fig. 4.1). In a single cell of *E. coli*, there are approximately 10^6 lipid A molecules, 10^7 glycerophospholipids and 10^5 undecaprenyl phosphate–sugar residues [17]. Lipid A is the hydrophilic anchor of LPS and is also defined as "endotoxin" since it shares the structural motif necessary for the activation of the innate immune response via the TLR4/CD14/MD2 receptor complex [18-20]. The immune response mechanism triggered by LPS is illustrated in an excellent recent review written by Raetz and Whitfield [21]. It appears that the lipid A and Kdo (3-deoxy-D-*manno*-oct-2-ulosonic acid) motifs constitute the minimum domain required for Gram-negative bacterial growth [17]. However the reasons for such structural domains to be essential for bacterial viability and multiplication remain uncertain.

In *E. coli* the core Kdo_2-lipid A unit is expressed via a constitutive biosynthetic pathway involving nine enzymes each encoded by a single structural gene (Fig. 4.2) [22]. These genes are conserved among Gram-negative bacteria with the exception of the *Sphingomonas* species where LPSs are replaced by glycosphingolipids [23]. The biosynthetic pathway of Kdo_2-lipid A is constitutive in all Gram-negative bacteria, and is not dependent on a regulation mechanism, supporting the theory that the Kdo_2-lipid A core is critical for bacteria growth and viability. The early steps of the pathway use water-soluble substrates and LpxA, C and D enzymes are cytoplasmic proteins while LpxK, LpxL, KdtA and LpxM are inner membrane proteins. Concerning LpxB and LpxH, studies have shown that both enzymes were peripheral membrane proteins [22]. Interestingly, due to the central position of such enzymes in the bacteria viability and growth, they appear to be ideal drug targets. Recently, McClerren and colleagues have reported a LpxC inhibitor termed CHIR-090 that was tested against diverse strains including *E. coli* and *P. aeruginosa* and potent at nanomolar concentrations [24-26].

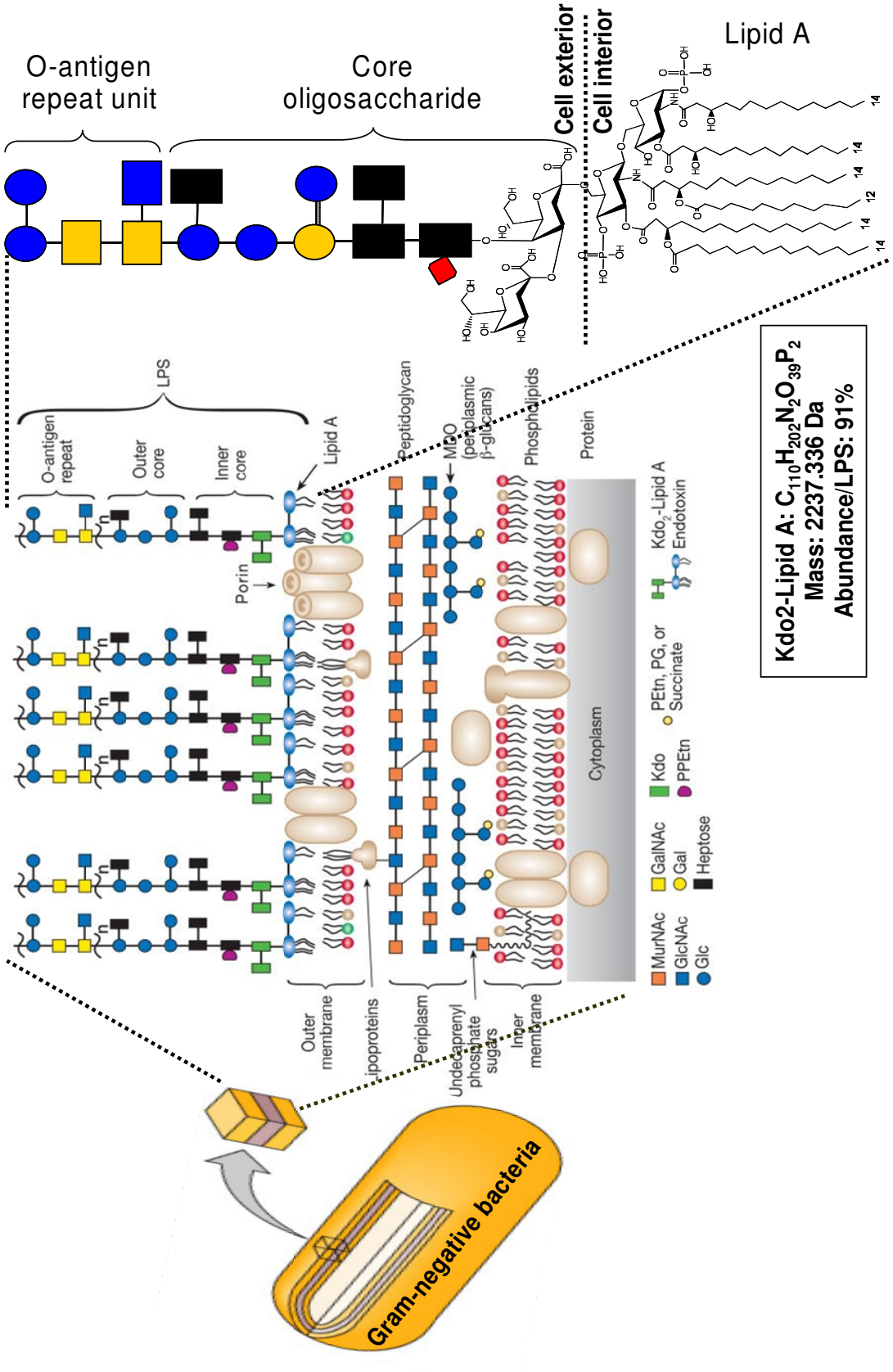

Figure 4.1. From Gram-negative bacteria cell wall to LPS. Model of the outer and inner membrane in *E. coli* K12 strain with the structure of Kdo_2-lipid A. Adapted from Raetz and Whitfield, 2002 [21].

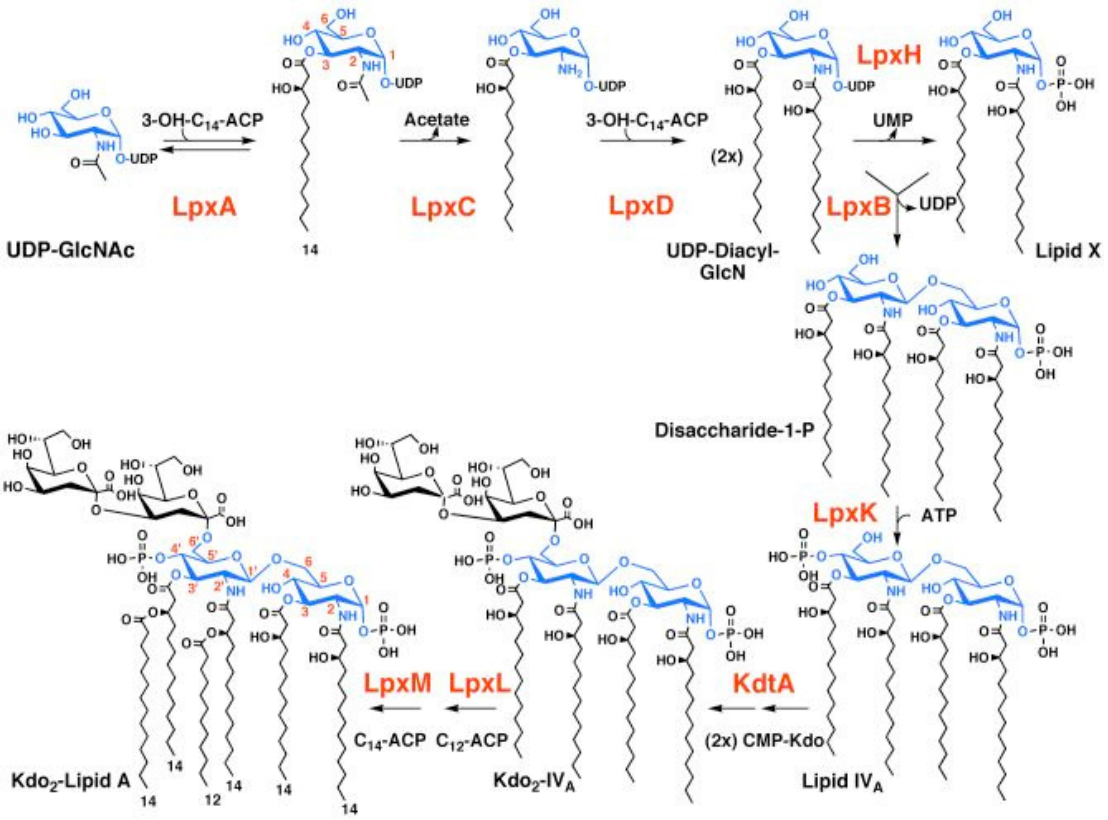

Figure 4.2. Structure and biosynthesis of Kdo_2-lipid A in *E. coli* K-12 strain. The figure was taken from Raetz *et al*., 2007 [22].

The newly synthesised Kdo_2-lipid A is flipped from the inner side to the outer surface of the inner membrane by an ABC transporter MsbA. The *msbA* gene was first reported as essential for *E. coli* viability in 1993 by Karow and Georgopoulos [27]. A few years later it was proposed that the MsbA protein could be the inner membrane flippase for the core lipid A and could be the quality filter element for the LPS transport system [28]. The full mechanism of export of LPS from the inner membrane to the exterior of the outer membrane still remains unclear. The transport process of a hydrophobic molecule through an hydrophilic milieu, the periplasm, is thermodynamically unfavorable and until recently, little was known about such physiological mechanisms. However in a recent review, and in light of new studies, Sperandeo and colleagues have proposed new insights concerning such a puzzling matter [29]. A cluster of three genes essential for *E. coli* viability was identified and the genes termed *lptA*, *lptB* and *lptC* [30, 31]. The authors demonstrated that the lipopolysaccharide transport (Lpt) machinery including proteins LptA, B, C, D, E, F and G was operating downstream of MsbA, which resulted in the formation of a large complex that could span the periplasmic region (Fig. 4.3). LptA was shown to bind

lipid A and shield its hydrophobic region facilitating its passage trough a soluble milieu. Moreover LptA binds indiscriminately hexa or tetraacylated lipid A, which suggests that the LPS filter selection might occur upstream the Lpt machinery and could be carried out by MsbA [32]. Very recently the structure of ligan-free *E. coli* LptA revealed a highly-unusual fold and the protein displayed oligomeric properties [33]. The exact nature of the LptA/LPS interaction requires further study.

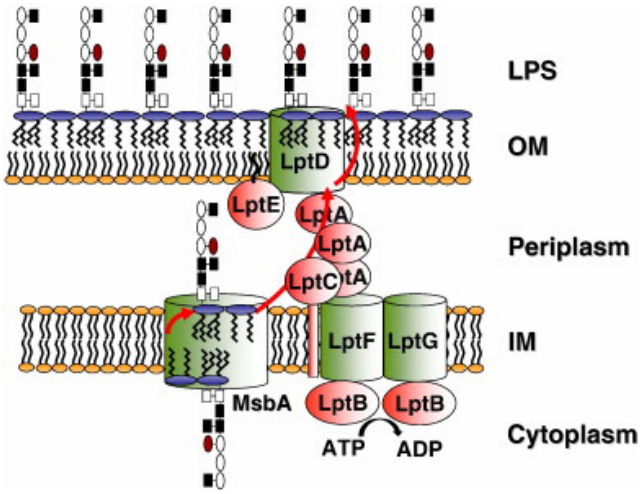

Figure 4.3. Model for the LPS transport through the periplasm in Gram-negative bacteria according to Sperandeo and coworkers, 2009 [29].

4.3 Lipid A Modifications in Gram-Negative Bacteria

The ability of Gram-negative bacteria to resist and adapt to environmental stress partly resides in their aptitude to induce covalent modifications on the lipid A core moiety of LPS. In contrast to the biosynthetic pathway of lipid A, which is constitutively expressed, the lipid A modification mechanism is an induced phenomenon mediated by various conditions such as the presence of divalent cation concentrations, AMPs or changes in pH. For instance, low concentration of Mg^{2+}, high concentrations of Fe^{3+} or acidic pH have been reported to trigger bacterial resistance via lipid A modifications, but millimolar concentrations of magnesium or calcium downregulate the effect [34, 35]. In *E. coli*, *S. typhimurium* and the majority of Gram-negative bacteria, these modifications are under the regulation of the two-component systems (TCSs) PhoP-PhoQ and PmrA-PmrB [36-38].

PhoQ protein was reported to be activated directly by AMPs [39]. When AMPs bind to the phosphate group of lipid A, they displace divalent cations and

therefore activate PhoQ which according to Bader *et al*. acts as an antimicrobial sensor. The PmrA/B TCS was first described in 1993 and named after the study of a mutated strain resistant to Polymyxin B (PMB), a small cationic antimicrobial peptide, and other AMPs [40, 41]. PMB is a natural compound produced by *Bacillus polymyxa* [42]. Both PMB and its synthetic derivative colistin have been extensively used and tested towards various bacteria however, it appears that they have little effect towards Gram-positive microorganisms. The PMB peptide is used as a reference for clinical and in-vitro killing tests for Gram-negative bacteria. PMB has been used as an antibiotic reference and *S. typhimurium* as the bacterial model for the study of the two-component systems in relation with bacteria virulence. So far, thirty eight TCSs have been identified in this species [43].

PmrA/B can be initiated by PhoP/Q TCS but it can also independently induce modifications [38]. Such modifications appear to be one of the primary roles of PmrA/B and include the covalent addition of groups on both LPS and lipid A core. For example, two modifications consist with the attachment of phosphoetanolamine (pEtN) and aminoarabinose (4-amino-4deoxy-L-arabinose, L-Ara4N, discussed later *c. f.* part 4.5) by respectively EptA and ArnT enzymes on the different phosphate group of the lipid A moiety [44, 45].

These modifications not only mask the negative charges of the phosphate groups but also add a positive moiety to the lipid A core as both pEtN and L-Ara4N are cationic at neutral pH.

In *Salmonella* and *E. coli* bacteria, the transfer of phosphoethanolamine by EptA occurs on the outer side of the inner membrane and essentially at position 1 of phosphate group (Fig. 4.4) [46]. However with the absence of L-Ara4N modifications and under specific growth conditions, a second pEtN can be attached to the 4' position of the lipid A [47]. Additionally, pEtN can be incorporated to the first heptose of the LPS core by the product of the *cptA* gene [48]. In *E. coli*-K12 strain, the transfer of phosphoethanolamine only occurs under mild acidic condition whereas it is constitutively expressed in the pathogenic *E. coli* O157:H7 suggesting a relation between virulence and pEtN modifications [49]. Phosphoethanolamine moiety can be also incorporated by EptB, a homologous protein to EptA in *S. typhimurium* and *E. coli*. In contrast to EptA, EptB is not under the control of PmrA but is regulated by the σ^E transcription factor and the transfer of pEtN by EptB is carried out on the outer Kdo sugar of lipid A (Fig. 4.4) [50].

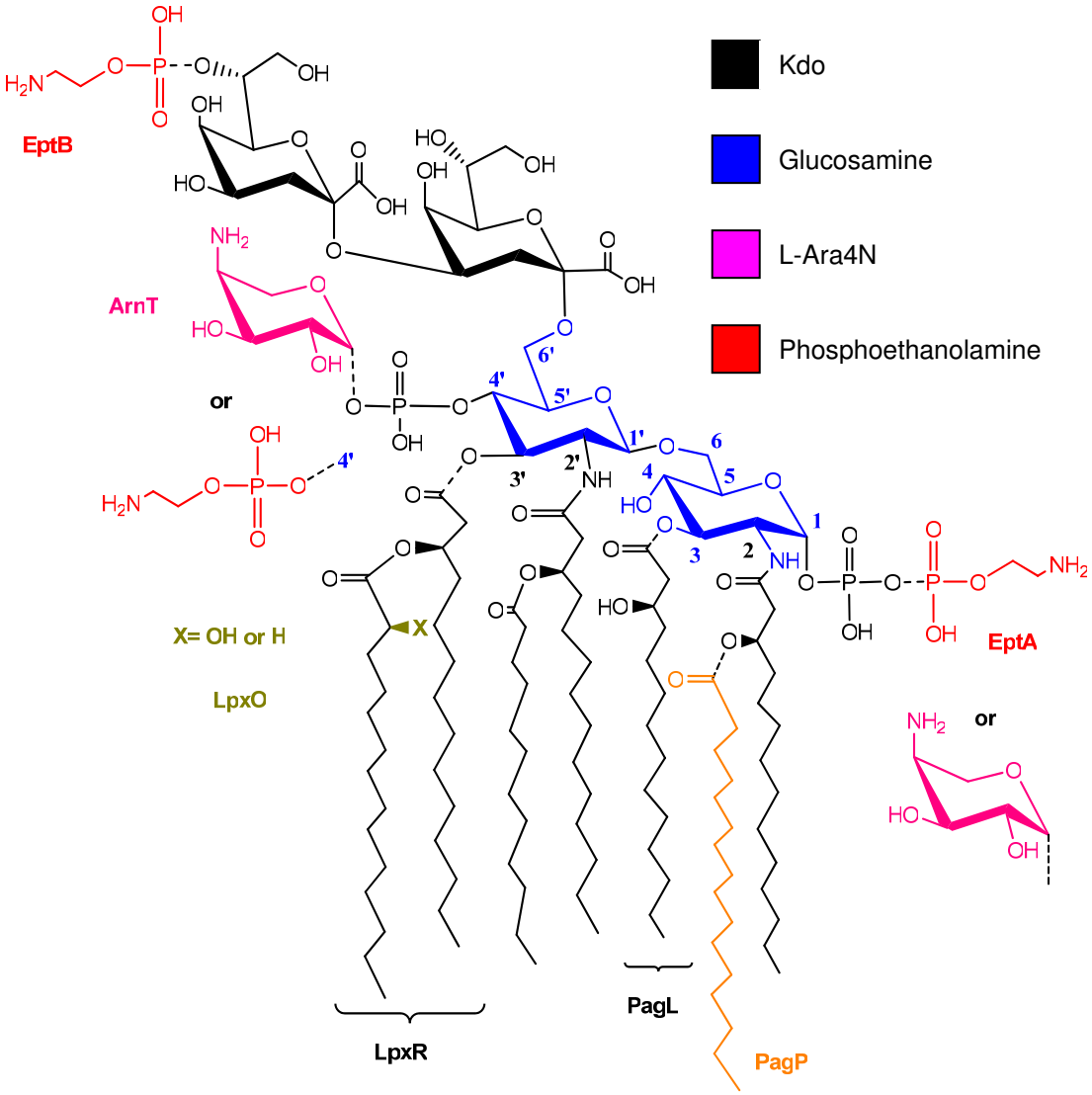

Figure 4.4. Covalent modifications of Kdo_2-lipid A in *E. coli* K-12 and *Salmonella*. The blue numbers represent the glucosamine ring positions. Adapted from Raetz *et al*., 2007 [22].

In *Neisseria meningitidis*, a bacterium unable to incorporate L-Ara4N, it was found that pEtN modifications are present and directly-related to the PMB resistance for this human pathogen [51]. But contrary to L-Ara4N modifications, which are decisive for PMB resistance [52, 53], the functions of pEtN modifications remain unclear. Other modifications of lipid A have been reported and involve the fatty acyl chain moiety. The incorporation of the fatty acid palmitate in *E. coli* and *S. typhimurium* is carried out by the PagP protein (Fig. 4.4) and controlled by the PhoP/PhoQ system itself activated by cAMPs or low Mg^{2+} concentration [47, 54]. PagP is an outer membrane enzyme which uses phospholipids as palmitoyl donors

[55]. The reaction of palmitoylation occurs in the outer side of the outer membrane and this process could be modulated by the accessibility of phosphate sporadically present on this side of the membrane [56]. *S. typhimurium* mutants lacking the palmitate moiety on the lipid A were shown to be sensitive to cationic AMPs. Membrane permeabilisation was shown to be faster than wild type strains when exposed to different structural classes of cAMPs such as C18G and protegrin peptides [57]. Moreover, the *pagP* gene seems to be highly related to the virulence of bacteria and regulated in close relation to their pathogenic ability. Hence PagP expression appears to be the privilege of only a certain class of pathogenic bacteria [58].

Additional enzymes found in *Salmonella* but not in the *E. coli* K-12 wild-type strain have been reported to modify lipid A. LpxR, an outer membrane lipase can remove the 3'-O-acyloxyacyl residue of lipid A under high concentration of Ca^{2+} and the presence of Kdo moiety [59]. PagL is also an outer membrane esterase that catalyses the 3-O-deacylation of lipid A at position 3 [60]. If both outer membrane enzymes are regulated by PhoP/PhoQ system it is not the case for LpxO, an inner membrane protein which uses α-ketoglutarate, Fe^{3+} and oxygen cofactors to hydroxylate the secondary acyl chain at 3' position of lipid A [61, 62]. The roles of these three enzymes are unclear but it seems that LpxR and PagL could reduce the cytokine activation effect of LPS [63, 64]. All modifications mentioned above are represented on figure 4.4.

It appears that lipid A modifications are "mandatory" for pathogenic bacteria. In fact, LPSs constitute not only a "shield" acting as a defense barrier but its flexible architecture elaborated by various modifications can also dictate a level of bacterial virulence. Therefore, it is interesting to note that the capacity of resistance and adaptation of a microorganism often, if not always, correlates somehow with its degree of pathogenicity.

Aminoarabinose modifications on lipid A have been directly related with a resistance mechanism towards all sort of antibiotics. Such modifications are induced by diverse stimuli in most Gram-negative bacteria and are under the control of regulators such as PhoP/Q and PmrA/B systems. However some bacteria have evolved to protect themselves and therefore have enhanced their virulence. This is the case of bacterial species found in the *Burkholderia cepacia* complex (Bcc) where bacteria are able to constitutively express aminoarabinose modifications on the lipid A core [65]. This characteristic is crucial for antibiotic resistance towards PMB. In

2003, Shimomura *et al*. have observed an unusual interaction between LPS from *B. cepacia* and PMB. LPSs not only bound to PMB with high affinity, in spite of containing Ara4N, but also increased its IL-1ß-inducing activity [66]. The authors have concluded that LPS from *B. cepacia* has unique characteristics in both structure and activity. Interestingly, highly pathogenic and resistant bacteria from Bcc can be found in the lung environment of cystic fibrosis (CF) sufferers and immunocompromised patients [67[a]]. Constitutive modifications of Lipid A by the aminoarabinose moiety in such bacteria may play a crucial role in the invasion and deterioration of cystic fibrosis patients' lung tracts [67[b]].

4.4 Cystic Fibrosis (CF) and The *Burkholderia Cepacia* Complex

Cystic fibrosis is a monogenic autosomal recessive disease and is also the most common life-threatening disease among people of European heritage. In UK, 8000 individuals are diagnosed with CF (www.cftrust.org.uk) and 1 out of 25 people carries the defective gene. The average life expectancy for CF patients lays netween 30 to 40 years. This genetic disorder, when expressed, affects various organs such as the liver, the pancreas but also tissues in the respiratory, gastrointestinal and reproductive tracts. CF is caused by mutations located on the cystic fibrosis transmembrane conductance regulator gene (*CFTR*). The gene encodes a member of the ATP-binding cassette (ABC) transporter family; the CFTR protein with a molecular weight of 168 kDa [68, 69]. This protein is located in the epithelia cells of skin and all tracts mentioned above. The protein acts as an anion channel regulator that mediates anion conductance, a crucial function for the maintenance of ion equilibrium and fluid homeostasis in epithelia cells [70]. First reported as a chloride channel, CFTR can also inhibit sodium absorption in lung epithelial cells and play an important role in HCO_3^- secretion [68, 71].

Over 1600 mutations have been identified on the CFTR gene (www.genet.sickkids.on.ca/cftr/StatisticsPage.html). These mutations have been classified into 6 classes (I to VI) according to the protein domain affected and their nature; frame shift, nonsense or splice site mutations [72, 73]. Not all mutation lead systematically to CF but the most common mutation, a 3-bp deletion termed ΔF508, accounts for 70% of worldwide cystic fibrosis cases (www.ornl.gov/sci/techresources/Human_Genome/posters/chromosome/cftr.shtml).

This class II deletion results in the loss of only a phenylalanine at position 508 of the CFTR protein but has dramatic effects for the ΔF508 homozygous individuals [74]. ΔF508 mutation creates an abnormal fold which prevents the protein to be matured properly leading to its degradation by the cell [75].

Consequently, loss of CFTR-associated functions leads to impaired pancreatic HCO_3^- and chloride secretion, enhanced Na^+ absorption, dehydration of the airway surface which impairs mucociliarity clearance [76]. Such physiological alterations contribute to immunodeficiency in lung environment and are propitious for chronic airway invasion by opportunistic pathogens. Lung disease represents the major cause of morbidity and mortality in CF community. Examples of pathogenic bacteria species found in airways of CF patients include *S. aureus*, *P. aeruginosa* and *B. cepacia*. The latter was reported to be the most contagious and problematic among pathogens leading to drastic changes in clinical and social habits for CF patients [77].

Half a century ago, a plant pathogen that causes onion bulb rot was identified by Walker H. Burkholder [78]. Despite being an emerging concern among cystic fibrosis and immunocompromised patients over the past two decades [79 Goldmann, 80], Bcc species are ecologically versatile Gram-negative bacteria found in water, soil and rhizosphere of plants [81]. They are able to protect plants from disease and degrade environmental pollutants. Such abilities have been attributed to their remarkable genomic complexity [82]. In fact, Bcc bacteria possess some of the largest genomes ever observed within Gram-negative species (6 to 9 Mb) and are usually shared by two or three chromosomes. Previously reported as *Pseudomonas cepacia* due to their phenotypic resemblance with the *Pseudomonas* genus, Bcc bacteria were transferred to the *Burkholderia* genus in 1992 [83]. This differentiation was followed in 1997 by a new classification within the *B. cepacia* genus where five sub groups were organised into genomovars [84]. With the recent addition of 6 new species [85], a total of fifteen genomovars (I to XV) have been identified to date [86].

Among the *Burkholderia cepacia* complex, two species have been highly related to CF disease; *B. multivorans* and *B. cenocepacia* (Genomovar II and III). If both strains are responsible for epidemic outbreaks and are transmissible between patients, *B. cenocepacia* represent the major issue for CF infection with 70% rate of Bcc infection [87, 88]. Moreover, *B. cenocepacia* has the remarkable ability to overtake *B. multivorans* during CF infection [89]. Over the past two decades, increasing concern and effort have been focused on three epidemic strains in *B.*

cenocepacia; the Midwest, PHDC and ET-12 lineages. These strains are responsible for the main morbidity and mortality in the cystic fibrosis community with the latter being the cause of the largest CF epidemic in the late 80's to mid 90's spreading through Canada, United Kingdom and Europe [90, 91].

B. cenocepacia J2315 strain is a member of the epidemic ET-12 lineage. It was isolated by Prof. Govan and colleagues in 1989 during an epidemic outbreak amongst Scottish CF sufferers. It is a highly resistant microorganism against all class of antibiotics and was recently sequenced [92]. The genome of the J2315 strain is organised in three large chromosomal replicons and a small plasmid for a total size of approximately 8 Mb. The gene cluster responsible for aminoarabinose modification on lipid A is located on chromosome 1. The sequence of J2315 genome is available at www.sanger.ac.uk/Projects/B_cenocepacia/.

4.5 The Biosynthetic Pathway of Aminoarabinose (L-Ara4N) Modification of Lipid A: The *Burkholderia Cenocepacia* Case

The mechanism of L-Ara4N modification of lipid A was first described and mainly studied in *E. coli* and *S. typhimurium* (Fig. 4.5). All genes involved in this pathway with the exception of *ugd* (the gene encoding for the first enzyme) are located in the arn operon which is divided in two transcription units; *arnBCAD* and *arnTFE* (Fig. 4.5 B) [52, 93]. Originally termed the *pmr* operon due to its relation to PMB resistance, the nomenclature was changed to the *arn* locus for its fundamental role in L-Ara4N biosynthesis.

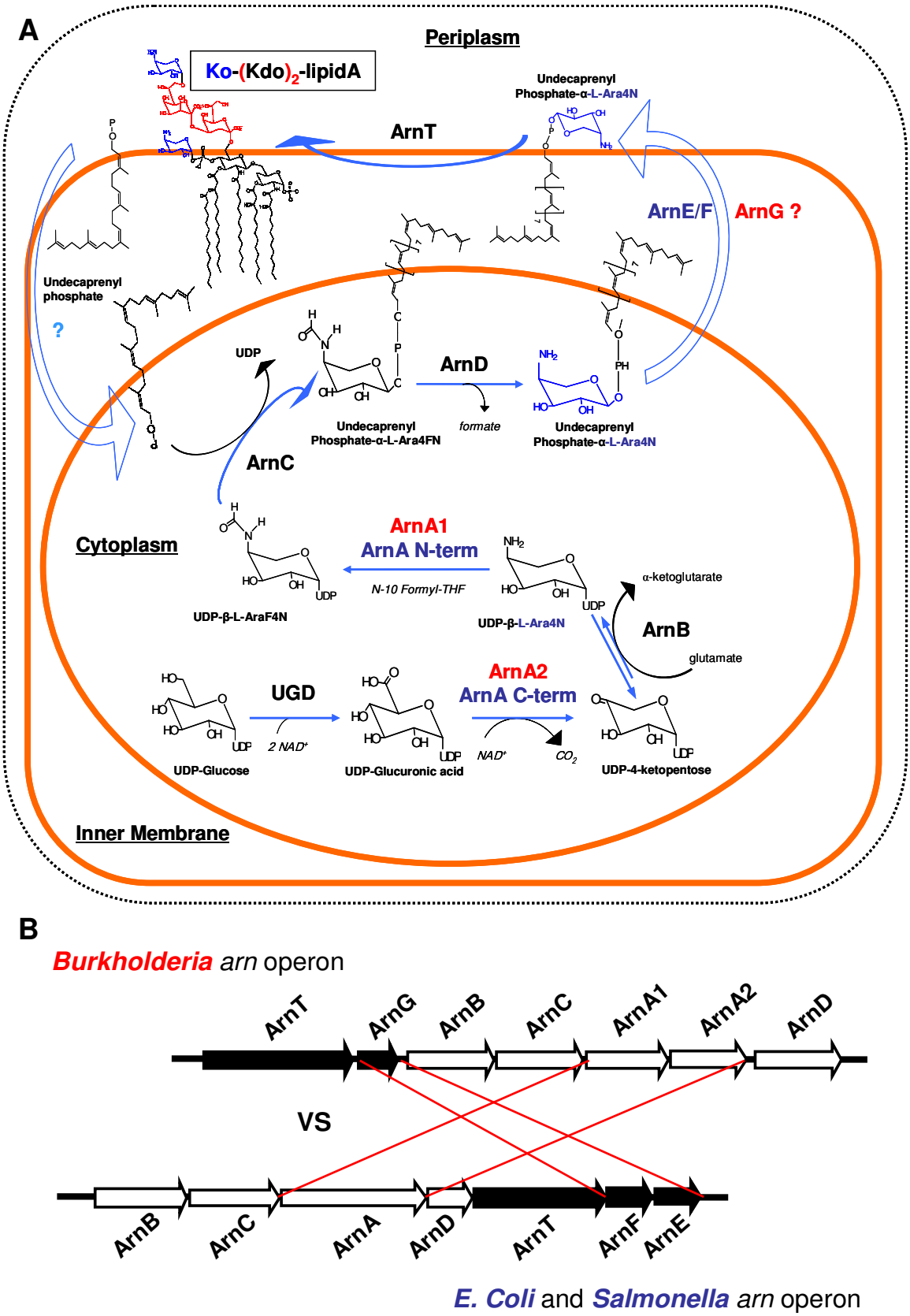

Figure 4.5. A. Biosynthetic pathway of aminoarabinose (L-Ara4N, blue) and its attachement to Lipid A moiety (A). B. Organisation of the arn operon from *B. cenocepacia* J2315 (red) is compared with the arn operon from *E. coli* and *Salmonella* (blue).

Eight proteins are involved in the biosynthetic pathway of L-Ara4N modification in *E. coli* and *S. typhimurium* (Fig. 4.5 A, in blue characters) [22]. The first step is carried out by an UDP-glucose dehydrogenase (UgD) that converts UDP-glucose to UDP-glucuronic acid [52]. The second step is the oxidative decarboxylation of UgD product to release UDP-4''-ketopentose (UDP-Ara4O). This reaction is carried out by the C-terminal domain of ArnA [94]. Newly synthesised ketosugar is then transaminated by a PLP-dependent enzyme, ArnB, which uses glutamate as cofactor [95]. In vitro studies of the transamination reaction for the production of aminoarabinose is unfavorable. It suggests that the following enzyme, ArnA, shifts the equilibrium to the formation of L-Ara4N. Indeed, the biosynthesis of UDP-L-Ara4-formyl-N by the N-terminal domain of ArnA would compensate for the unfavorable formation of UDP-L-Ara4-FN. However, despite the fact that X-ray structures of both ArnA and ArnB have been solved, the interaction and transfer of product and substrates between their active site is unknown [94-97]. ArnC, the third enzyme of the pathway, is extremely specific and accepts only the N-formyl substrate and then transfers L-Ara4-FN onto an undecaprenyl phosphate moiety [94]. Deformylation by ArnD to undecaprenyl phosphate Ara4N is necessary for its transport trough the inner membrane protein [94]. Recently Yan and coworkers have reported that an undecaprenyl phosphate L-Ara4N flippase was necessary for the PMB resistance in *E. coli* [98]. ArnE and ArnF, two inner membrane proteins, would likely form an homodimer to flip out the ArnD product to the periplasmic side of the inner membrane. Finally, an additional inner membrane protein, ArnT, incorporate L-Ara4N to the 4'-phosphate group of lipid A moiety [44].

Recently, homologues of the *arn* genes were found in *B. cenocepacia* J2315 [99]. The authors demonstrated that this operon was essential for *B. cenocepacia* K56-2 viability (K56-2 strain is clonally related to J2315 strain and was used since it is amenable to genetic manipulation). However it shares a different genetic organisation than its homologues previously described in *E. coli* and *Salmonella*. The *arn* operon in *B. cenocepacia* is transcribed as follows: *arnTG/arnBCA$_1$A$_2$D* (Fig. 4.5 B). Ortega *et al*. have used conditional mutants where a rhamnose-inducible promoter was inserted upstream of *arnB* (XAO12) and *arnT* (XAO11) genes. When the promoter was "switched-off" by the addition of glucose, it highly affected the viability of the cells and deformation of the cell envelope was observed (Fig. 4.6, XOA11 and XOA12) [99]. Although the authors did not determine if the membraneous material

was modified by Ara4N it still provided a link between the arn operon and some essential process for the viability of *B. cenocepacia*. However, the exact reason for the requirement of this locus by such bacteria is still not clear.

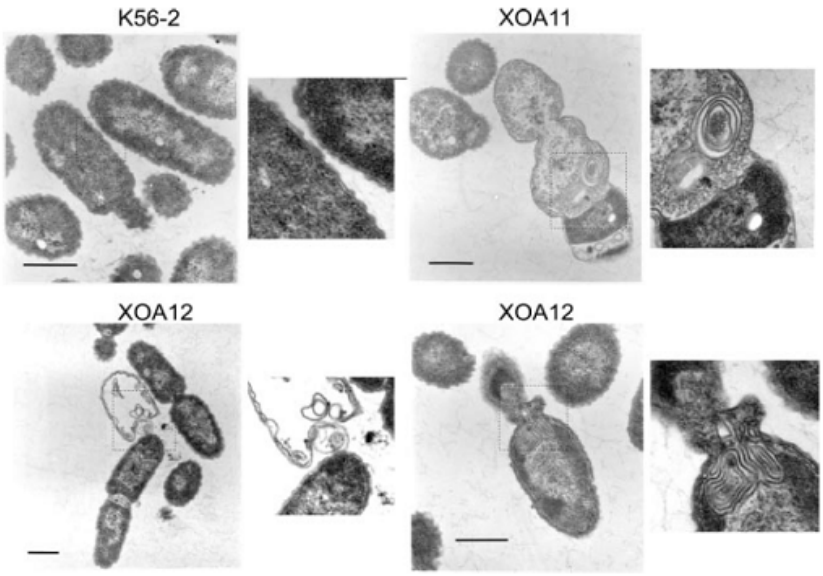

Figure 4.6. Ultrastructural analysis of bacterial cells of K56-2, XOA11 and XOA12 strains by transmission electron microscopy. This figure was taken from Ortega *et al*., 2007 [99].

Concerning *B. cenocepacia* and more generally *Burkholderia* species, the biosynthetic pathway of L-Ara4N modifications on lipid A is constitutively expressed. This is in contrast to other microbes where this process appears to be an adaptive "option". This exceptional ability allows this species to be highly advanced in terms of resistance and virulence.

Although *in silico* analysis suggest similar characteristics in the L-Ara4N modification pathway, the genomic organisation of *arn* operon from *B. cenocepacia* possesses two obvious differences from non Bcc specie and it concerns *arnA* and *arnG* genes (Fig. 4.5 B). In *E. coli* and *S. typhimurium*, one gene encodes for ArnA protein that contains two catalytic domains (N- and C-termini), which are able to proceed two enzymatic reactions. In contrast, *B. cenocepacia* shares two genes, *arnA1* and *arnA2*, encoding for two distinct proteins: ArnA1 and ArnA2 [99]. Both enzymes carry out the same reactions that ArnA does in *E.* coli and *Salmonella*. Concerning the *arnG* gene, an opposite phenomenom takes place, ArnE and ArnF proteins have been reported to associate as an heterodimer for the flippase activity in *E. coli* while one

protein acting hypothetically as an homodimer (ArnG) could complete the same reaction in *B. cenocepacia*.

So far only few biochemical studies have been carried out on the different enzymes responsible of L-Ara4N modification in *B. cenocepacia*. Recently, the Ugd homologs that encode UDP-glucose dehydrogenase, the first enzyme of the pathway were characterized by our groups in collaboration with Miguel Valvano. The authors identified 3 *ugd* genes in the genome, but only two were essential for *B. cenocepacia* viability and one was required for PMB resistance [100].

4.6 Structure of *B. Cenocepacia* Lipopolysaccharide

In Bcc, many virulence factors are thought to be responsible for the clinical outcomes. Examples of such factors include zinc metalloproteases [101], siderophores [102], haemolysins [103], flagella [104], exopolysaccharides (EPSs) [105] or adhesins [106]. However, one of the major virulence factors of *B. cenocepacia* and most Gram-negative bacteria, is the LPS molecule which is a potent inflammatory agent [107]. LPSs from the Bcc group, have been shown to be more endotoxic and ninefold more efficient to release cytokines from leukocytes than LPSs found in *Pseudomonas aeruginosa* [108 Shaw]. Until recently, little was known about the LPS structure in *Burkholderia cenocepacia*.

In 2007, a structure of rough LPS (lipooligosaccharide, LOS) from *B. cenocepacia* J2315 strain was published by Silipo *et al.* [109]. The Ara4N-Ko(D-*glycero*-D-*talo*-octulosonic acid)-Kdo(3-*deoxy*-D-*manno*-octulosonic acid) unique feature shared by *Burkholderia* species reported by others was confirmed by structural methods such as NMR and mass spectrometry (Fig. 4.7 A) [110, 65]. This trisaccharide moiety is distinct from *E. coli* and *Salmonella* (Kdo_2) and the presence of Ko monosaccharide is shared by only few bacteria specie such as *Serratia*, *Acinetobacter* and *Yersinia* [111-113]. In addition to the Ara4N-Ko-Kdo moiety, the core oligosaccharide (OS) is constituted of 3 heptoses in the inner core region and two glucose sugars are attached to heptose I and heptose II which carries also a terminal heptose (Fig. 4.7 B). Recently, it was demonstrated that the core level truncations of LOS derived from smooth LPS K56-2 strains was proportionally linked to the level of PMB resistance [114]. Moreover, the heptose-less mutant was not able to survive in macrophages contrary to the wild-type strain.

LPSs extracted from *Burkholderia* J2315 strain consisted of a mixture of tetra- and pentaacylated lipid A species [109]. The main species, a tetraacylated lipid A, carried two 14:0 chains and two 16:0 chains with a secondary fatty acid attached to one of the 16:0 chain (Fig. 4.7 A). The presence of this secondary acylation in lipid A could be crucial for the induction of inflammatory responses and the integrity of the outer membrane in many bacteria [115, 116].

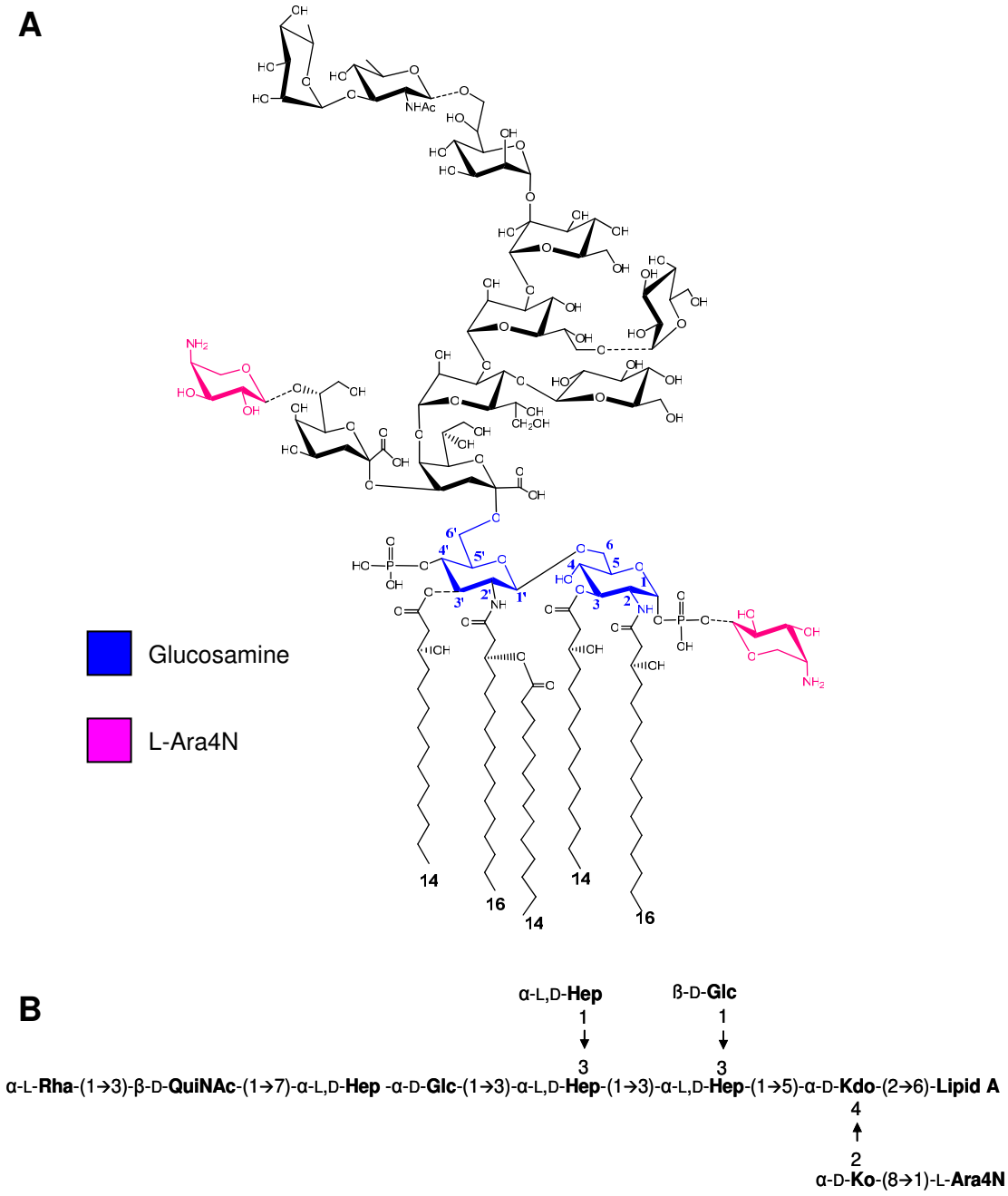

Figure 4.7. Structure (A) and sugar organisation (B) of the lipooligosaccharide from *Burkholderia cenocepacia* (J2315 strain). The dotted line indicates non-stoichiometric substitution. The figure was adapted from Silipo *et al*. 2007 [109].

4.7 Aims

Due to the essential role of the L-Ara4N biosynthetic pathway for *B. cenocepacia* viability (Ortega *et al.*, 2007 [99]), it was felt that we should explore the potential of inhibiting this pathway as a way of weakening these pathogens. The goal of this part was to investigate the biochemical characteristics of two proteins involved in the biosynthesis of aminoarabinose in *B. cenocepacia* J2315. The first enzyme studied, the aminotransferase ArnB, was previously purified from *S. typhimurium* and *E. coli* and was identified as a cytoplasmic, PLP-dependent enzyme. *In vitro* studies have shown that the natural-product antibiotic cycloserine, could inhibit ArnB irreversibly.

Our second target was the putative *B. cenocepacia* undecaprenyl phosphate Ara4N flippase ArnG. This protein shows low sequence homology but high amino acids topology to two recently characterised *E. coli* inner-membrane proteins ArnE and ArnF. Both proteins have been reported to be necessary for the flippase activity in *E. coli* [98].

Recently, a study was undertaken to evaluate the antibacterial activity of eight cAMPs towards strains from the *Burkholderia cepacia* complex [117]. Of all the cAMPs used, only magainin II was reported to display a “moderate” activity against the different Bcc strains. This example highlights the difficult challenge remaining to eradicate bacterial infection caused by these organisms. New drugs and/or the combination of a mixture of antibiotics may decrease the resistance and virulence of pathogenic bacteria affecting CF patients.

Chapter 5: Characterisation of Enzymes Involved in Ara4N biosynthesis in *Burkholderia cenocepacia*.

5.1 Analysis of the *arn* Operon in *B. cenocepacia* J2315

The *arn* gene cluster (*arnTG*/*arnBCA*$_1$*A*$_2$*D*) is responsible for aminoarabinose biosynthesis and its attachment to lipid A in *Burkholderia cenocepacia*. The *arn* operon is present in a region spanning nucleotides 2128443 to 2135736 in chromosome 1 of *B. cenocepacia* strain J2315 (www.sanger.ac.uk/Projects/B_cenocepacia/). The sequence corresponding to this operon (and of the total genome, [91]) enabled us to design primers to clone the genes encoding the Arn enzymes from *B. cenocepacia*. Analysis of the J2315 strain suggests it has 7261 coding sequences, a large number for a Gram negative organism. The genes have been annotated with BCAL numbers.

Concerning the ArnB protein, previous studies from *E. coli* and *S. typhimurium* have shown that the protein (encoded by *pmrH*, BCAL 1931) is a pyridoxal 5'-phosphate (PLP)-dependent aminotransferase enzyme [95]. It catalyses the reversible transfer of the α-amine moiety from an amino acid donor (L-glutamate) to the C-4 position of UDP-Ara4O, generating UDP-L-Ara4N (Discussed later in this section). The reaction occurs via an enzyme-pyridoxamine 5'-phosphate (PMP) form. Sequence alignment of ArnB from *B. cenocepacia* with orthologs from *E. coli* K12, *S. typhimurium* and *P. aeruginosa* (PAO1) revealed similarities in sequences (Fig.5.1). Homology scores between the ArnB from *B. cenocepacia* and the three strains lie between 50% and 52%.

Structural studies of the ArnB from *S. typhimurium* revealed it to be a homodimer where the PLP cofactor is bound to the enzyme via a lysine residue, forming an internal aldimine [95]. This lysine residue is conserved through various bacteria species and is present at position 188 in the *S. typhimurium* homolog (Fig. 5.1). It could act as a catalytic acid/base entity involved in several steps of the enzyme reaction (Fig. 5.2 B). Moreover, two residues have been identified to be the selective filter for the amine donor, Lys241 and Arg229. If the Lys241 residue is also present in the alignment study for the *B. cenocepacia* strain the arginine 229 residue is missing (Fig 5.1). However, another arginine residue present at position 218 could be the missing residue of the selective filter for ArnB in *B. cenocepacia*.

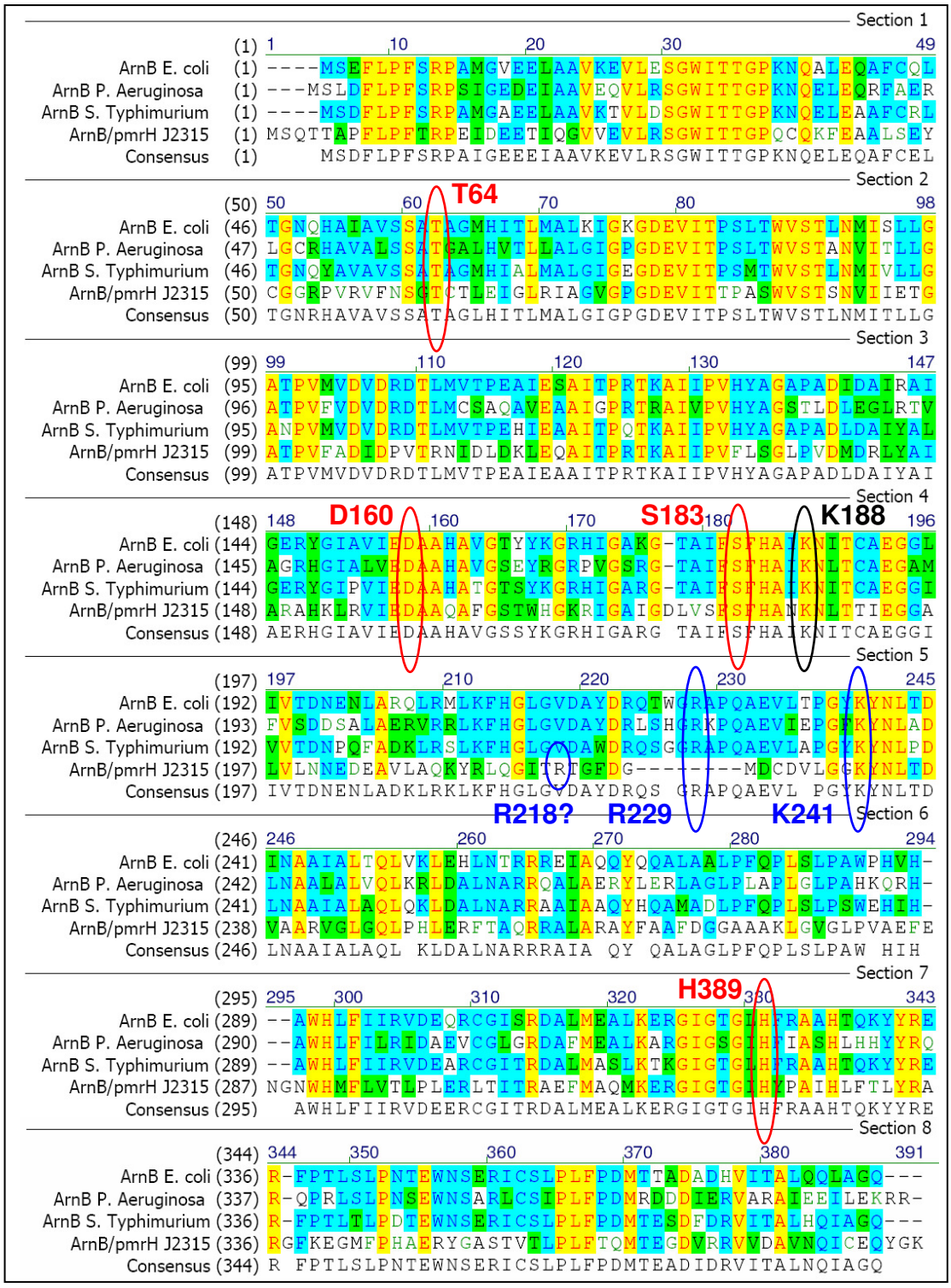

Figure 5.1 Sequence alignment of ArnB from *E. coli*, *P. aeruginosa*, *S typhimurium* and *B. cenocepacia* J2315. In blue are highlighted the residues involved in the selective filter for the amino donor substrate. Red circles represent some residues involved in the stabilisation of the PMP-cycloserine adduct (discussed in part 5.4).

The full reaction mechanism of ArnB is described in figure 5.2 and is directly adapted from the study mentioned above [95].

The first part of the reaction (Fig. 5.2 A) include the following steps: formation of an external aldimine via displacement of the lysine-PLP internal aldimine (holo-ArnB) by the incoming amino-acid substrate (L-glutamate); formation of a quinonoid intermediate by abstraction of the α-proton from the PLP-amino acid external aldimine; reprotonation of the quinonoid to form the ketimine 1 intermediate which hydrolysed to form the first product α-ketoglutarate and the reduced cofactor form PMP.

In the second part (Fig. 5.2 C), the UDP-LAra4O substrate reacts with PMP to form the ketimine 2 intermediate by abstraction of the α-proton; reprotonation of quinonoid 2 to form the external aldimine 2 intermediate; and finally release of the product UDP-L-Ara4N and regeneration of the enzyme PLP-internal aldimine.

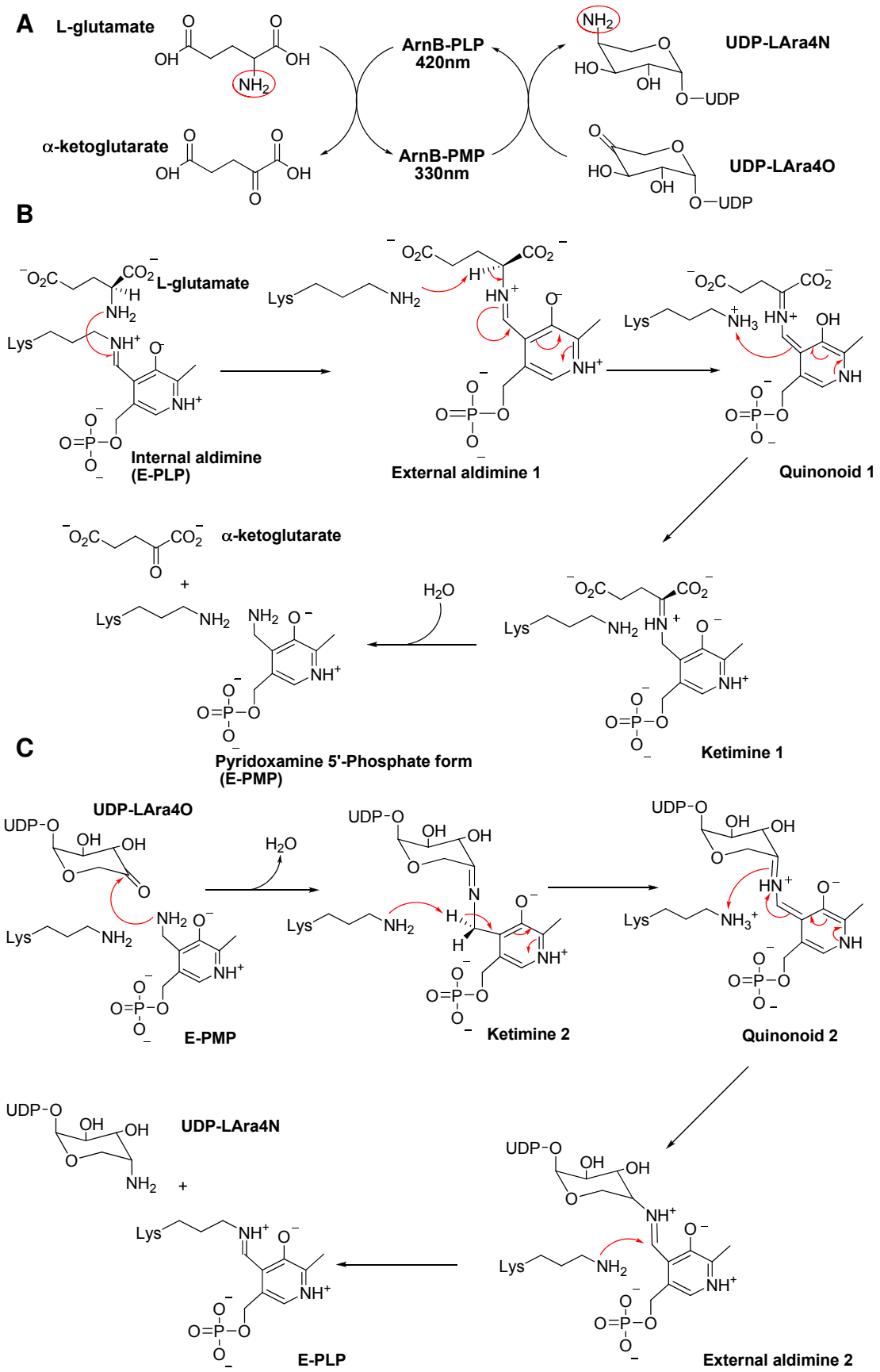

Figure 5.2. General (A) and detailed (B and C) mechanisms of transamination from glutamate to UDP-L-Ara4N by ArnB protein according to Noland *et al.*, 2002 [95].

The ArnG protein form *B. cenocepacia* (encoded by BCAL 1930) possesses a unique feature as it is encoded by one gene whereas the *E. coli* ortholog is encoded by two genes, *arnE* and *arnF* (previously termed *pmrL* and *pmrM* respectively). The *arnT* and *arnE/F* genes are located downstream of the *arnBCAD* genes in *E. coli*. In contrast, the *arnT* and *arnG* genes are situated upstream of the same genes in the *B. cenocepacia arn* operon. In *E. coli*, both ArnE and ArnF proteins have been shown to be indispensable for the flippase activity of undecaprenyl phosphate-aminoarabinose [98].

Despite low homology and sequence identity when comparing ArnG with ArnE and ArnF (22.1% and 27.4 % identity respectively), the amino acid characteristics are highly similar (Fig. 5.3). Topology prediction was also performed for ArnG in this study using the hidden Markov model topology predictor software (TMHMM v 2.0).

ArnG (123)

Amino Acid(s)	Number count	% by weight	% by frequency
Charged (RKHYCDE)	17	17.50	13.82
Acidic (DE)	3	2.81	2.44
Basic (KR)	6	6.51	4.88
Polar (NCQSTY)	25	21.49	20.33
Hydrophobic (AILFWV)	68	55.78	55.28

ArnE (128)

Amino Acid(s)	Number count	% by weight	% by frequency
Charged (RKHYCDE)	20	18.97	15.63
Acidic (DE)	3	2.52	2.34
Basic (KR)	7	6.59	5.47
Polar (NCQSTY)	25	19.49	19.53
Hydrophobic (AILFWV)	69	54.77	53.91

ArnF (111)

Amino Acid(s)	Number count	% by weight	% by frequency
Charged (RKHYCDE)	16	16.83	14.41
Acidic (DE)	1	1.04	0.90
Basic (KR)	7	7.81	6.31
Polar (NCQSTY)	21	18.69	18.92
Hydrophobic (AILFWV)	64	58.53	57.66

Figure 5.3 Amino acid topology of ArnE, ArnF and ArnG. The profile of charged, acidic, basic, polar and hydrophobic amino acids is very similar.

Figure 5.4 indicates that the protein could share a 4 transmembrane helical domain with both N and C-termini present in the cytoplasmic side of the membrane.

Predicted topology study for ArnE and ArnF also suggested that both proteins could share a 4 transmembrane helical domain and act as a heterodimer (Fig. 5.5 A) [98]. Hence we speculated that ArnG could also be active as a homodimer (Fig. 5.5 B).

Bioinformatic studies such as topology predictor software are informative tools allowing quick access to sets of data including the quantitative capability of a protein to be embedded in a membrane and the possible location of its N- and C-termini. However, the certainty of such approach remains improbable and despite recent progress in this area, the membrane proteome knowledge remains ill-defined.

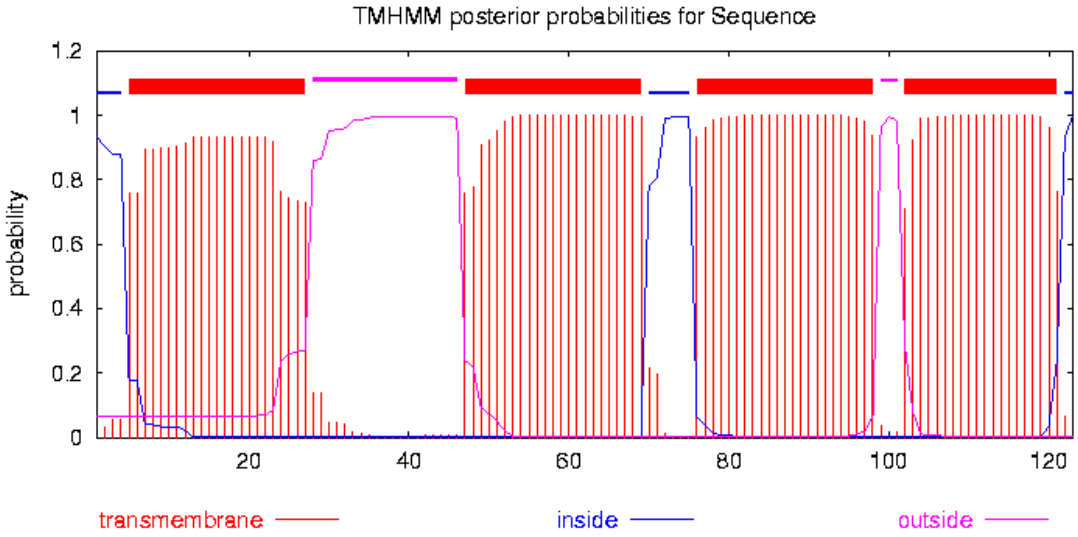

Figure 5.4 Topology prediction of ArnG from *B. cenocepacia* J2315 strain.

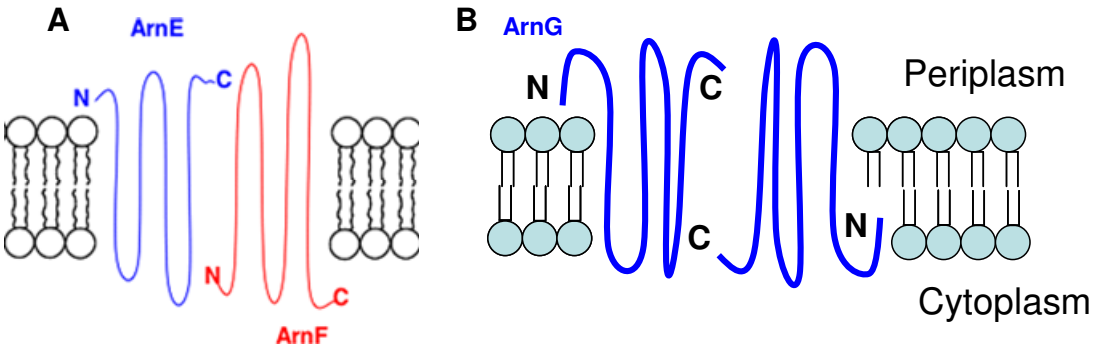

Figure 5.5 Proposed topography of the ArnE/ArnF heterodimer (A) [98] and ArnG homodimer (B).

Both proteins present interesting aspects. To start with, enzymes involved in the pathway of lipid A modification with aminoarabinose in *B. cenocepacia* appear to be ideal targets for therapeutic purpose. In fact, this pathway is one of the mechanism

that confers antibiotic resistance to such pathogenic bacteria but is also crucial for their viability. It is therefore interesting to exploit this paradox as it seems to be the Achille's heel of this bacterium.

ArnB, a PLP-dependent enzyme, can be tested with various inhibitors *in vitro* and *in vivo* in order to create a breach in the *B. cenocepacia* shield. ArnG, could be another key protein in the resistance mechanism in such bacteria. ArnG presents striking similarities with ArnE/F, two proteins which action is crucial for *E. coli* resistance against antibiotics. The inner membrane flippase activity demonstrated for ArnE/F could also be confirmed for ArnG in *B. cenocepacia*. Interestingly, ArnG sequence is unique to *Burkholderia* species as no homolog was found in other bacteria.

5.2 Cloning, Expression and Purification of ArnB from *B. cenocepacia*

The purification of ArnB from *S. typhimurium* for structural studies was carried out with a C-terminal hexa-histidine tag [95]. We decided to adopt the same strategy by including a histidine tag at the C-terminal end of the *arnB* sequence.

The gene was amplified by PCR using genomic DNA from *B. cenocepacia* J2315 as a template and ligated into pGEM-T Easy vector. DNA sequencing confirmed the exact gene sequence according to the published genome. Subsequently *arnB* gene was cloned into the pET22b vector (Novagen) where an extra LAAALEHHHHHH fusion tag sequence was added at the C-terminus resulting in expression plasmid pET22b-ArnB (Fig. 5.6).

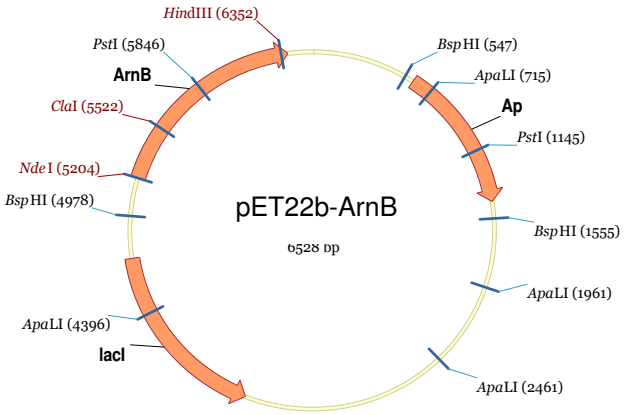

Figure 5.6 Plasmid map of pET22b-ArnB used for expression and purification of his-tagged ArnB.

After transformation of BL21(DE3) competent cells with pET22b-ArnB, bacterial cells were grown at 37 ºC in shake flasks and induced with 0.5 mM isopropyl-1-thio-β-D-galactopyranoside (IPTG) for 5 hours. These cells were then used as a source of soluble ArnB. Samples from each main step of purification were analysed by SDS-PAGE (Fig. 5.7).

Lane 1 and 2 in the gel represent respectively the cell-free extract before and after induction with IPTG. A band at around 43 kDa is revealed after induction corresponding to the theoretical mass of ArnB. After sonication, residual insoluble fractions from cells were removed by centrifugation and the supernatant was kept and further purified.

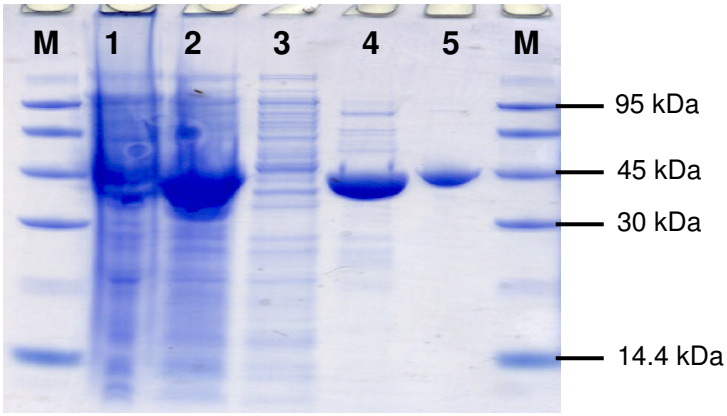

Figure 5.7 SDS-PAGE 12% gel showing the main steps of ArnB expression and purification; 1 and 2, cells before and after induction; 3, cell extract washed with 20 mM imidazole buffer; 4, protein elution with 100 mM imidazole buffer; 5, protein purification profile after SEC.

The soluble fraction was first purified by immobilised metal-affinity chromatography (IMAC) with a nickel resin. The ArnB cell lysate was poured onto a nickel resin column and washed with the binding buffer containing 20 mM imidazole (Fig. 5.7 lane 3). The protein was then eluted with 100 mM imidazole. The eluted ArnB protein is shown in band 4 with a thick distinct band at 43 kDa, but despite a dramatic increase in the sample purity, contaminants were still present at this stage. A second purification step was introduced with a size exclusion column (SEC) chromatography.

The protein was then loaded onto a Sephacryl High Resolution Column S200 for a higher level of purification. ArnB protein was eluted from the column and

fractions 12, 13 and 14 (Fig. 5.8) were pooled together and analysed by SDS-PAGE (Fig. 5.7, band 5). A well defined band at 43 kDa with no visible contaminants was obtained with purity greater than 95 % according to the gel profile. The elution profile of ArnB indicated that the protein was purified as a homodimer according to the calibration curve calculated from standard samples for this column (see Chapter 6, section 6.2.4.5).

The concentration of the purified ArnB protein was measured with the BCA™ assay and the final quantity of ArnB purified from 3 litres of *E. coli* cells was calculated to be ~25 mg. ArnB samples were eventually aliquoted in buffer containing 20 % glycerol and stored at -80ºC until further use.

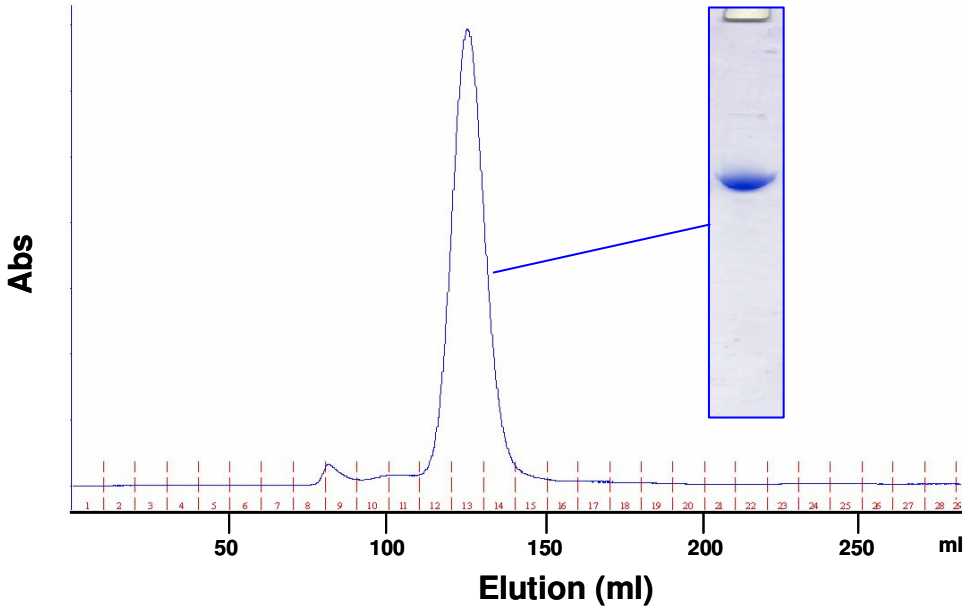

Figure 5.8. Sephacryl S200 High Resolution Column chromatograph of ArnB. In inlet is represented the SDS-PAGE gel profile of fractions 12 to 14.

A sample of freshly purified ArnB enzyme was analysed by high resolution FT-ICR MS. The mass spectrum (Fig. 5.9), shows an ion envelope and the calculated mass from the deconvoluted spectrum was 43,121 Da corresponding to a difference of 131 Da from the theoretical mass (43,252 Da) suggesting the loss of the starting amino acid methionine. The loss of the *N*-terminal methionine residue is a common phenomenon in the *E. coli* expression system.

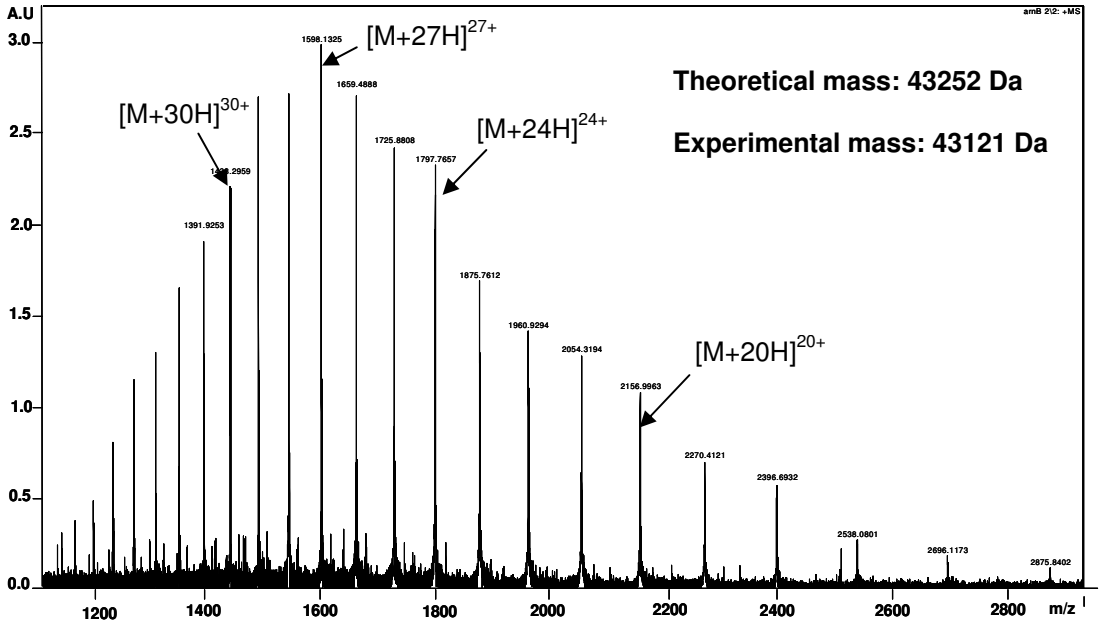

Figure 5.9. High resolution FT-ICR Mass Spectrometry of ArnB.

5.3 Spectroscopic Characterisation of ArnB

Prior to any further manipulation, the enzyme was dialysed overnight with an excess of fresh PLP followed by removal of unbound cofactor with a PD10 column.

The reaction catalysed by the ArnB aminotransferase is summarised in figure 5.2. The reaction consists of two main steps. In the first step, the complex enzyme-PLP is converted to enzyme-PMP form by activation with the amino donor. In the second step, the substrate, UDP-4'-ketopentose binds to the active site where the amine group is transferred to produce UDP-L-Ara4N. Here, we focused our attention on the reaction between of the co-substrate and ArnB-PLP. This reaction is called "half reaction" in the following. Freshly prepared ArnB was first characterised in its holo-form by UV-visible spectroscopy at a concentration of 10 µM (Fig. 5.10). The reaction was monitored by UV-visible spectrophotometry. A typical profile of PLP-dependent enzymes is shown on the spectrum as ArnB-PLP presents two characteristic peaks at 420 nm and 330 nm (Fig. 5.10). These two absorbances are the result of an equilibrium between tautomers of the external aldimine species; the ketoenamine and the enolimine forms.

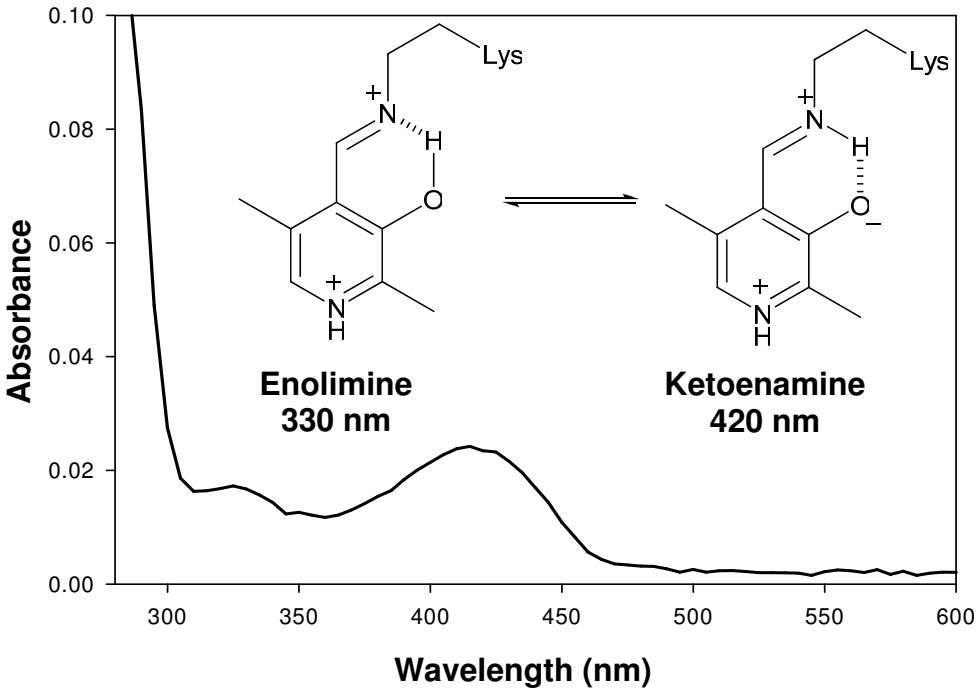

Figure 5.10 UV-visible spectrum of freshly purified ArnB (10 µM) in its holo-form (ArnB-PLP).

The first amino acid tested as the amine donor was the l-glutamate as it has previously been shown that it could be the physiological co-substrate for ArnB in *E. coli* and *S. typhimurium*. Increasing concentrations of l-glutamate (1 µM - 100 µM) was added to the enzyme ArnB-PLP and changes monitored by UV-visible spectrophotometry. The absorbance previously described and recorded at 420 nm for the holo-form decreases with the increasing amounts of l-glutamate while the signal intensity at 330 nm increases (Fig. 5.11). The peak at 330 nm represents the maximum of absorbance for the E-PMP species whereas ArnB E-PLP form possesses its maximum absorbance at 420 nm. The transfer of signal between the two species is observed as the reaction occurs. Increasing amount of l-glutamate favours the E-PMP form at 330 nm.

At 100 µM of l-glutamate, the reaction with ArnB-PLP was achieved within seconds. An isosbestic point is observed at around 360 nm (as shown by the red arrow in figure 5.11) suggesting that ArnB-PLP is transformed into ArnB-PMP without any absorbing intermediate species. This isosbestic point value is similar to the one published in the literature (363 nm, [95]).

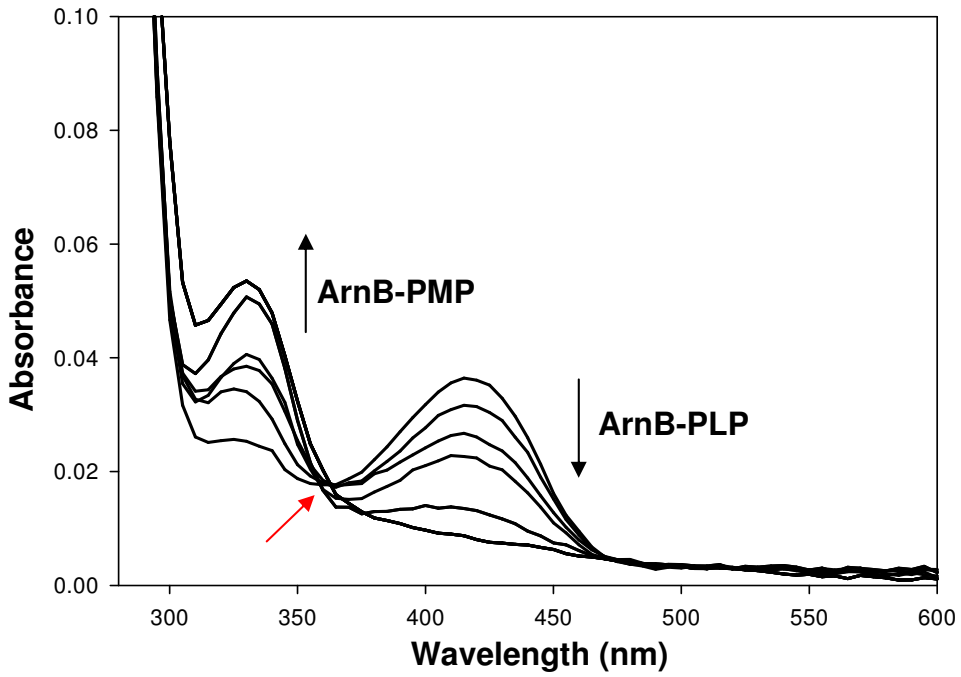

Figure 5.11. UV-visible spectra of the reaction between ArnB and increasing concentrations of l-glutamate (0 to 100 μM). Values were taken after 1 minute of reaction.

Six additional amino acids were tested as potential amine donor substrates; l-asparagine, l-aspartic acid, l-glutamine, l-methionine, l-serine and l-cysteine. Among the six amino acids tested, l-methionine, l-cysteine and l-glutamine were the only aminoacids capable of reacting efficiently with ArnB-PLP. However, l-asparagine, l-aspartic acid and l-serine demonstrated very little reactivity. If l-glutamate was the fastest amino acid tested, exceeding the limitation of our manual mixing studies (data not shown), l-glutamine was the second most reactive amino acid assayed. l-glutamine reached completion (full conversion to E-PMP) within few seconds in presence of 1 mM of amino acid (Fig. 5.12).

L-methionine and l-cysteine were independently incubated at saturating concentration of 1 mM in presence of 10 μM of enzyme and spectra were scanned every 5 minutes. The time course of the half-reaction of ArnB aminotransferase with l-methionine is shown in Figure 5.13. The conversion of ArnB from its PLP form to the E-PMP species is complete as the signal at 420 nm has disappeared for the 330 nm wavelength.

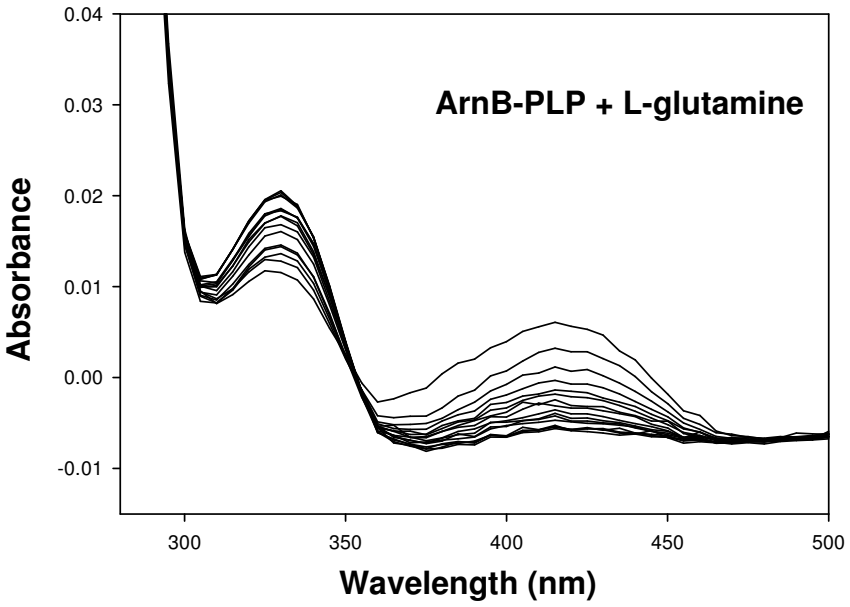

Figure 5.12. Formation of ArnB-PMP in the presence of l-glutamine (1 mM). Scans were recorded every 0.02 minute.

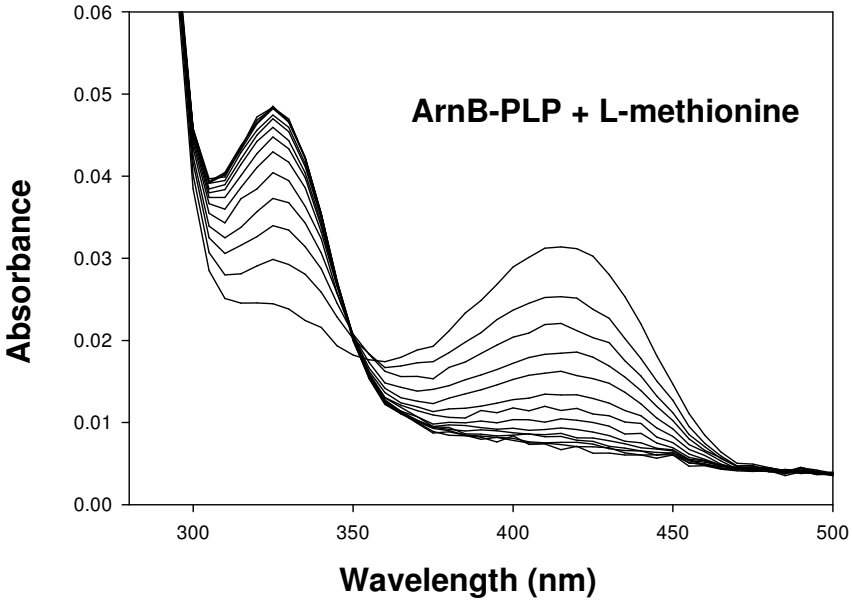

Figure 5.13. Formation of ArnB-PMP in the presence of l-methionine (1 mM). Scans were taken every 5 minutes.

We perform the same experiment in the presence of l-cysteine (data not shown). To quantitatively compare the reactivity of l-methionine and l-Cysteine towards ArnB-PLP, kinetics of ArnB-PMP formation obtained in the presence of both amino acids were plotted on the same graph and fitted to a single exponential decay function. (Fig. 5.14).

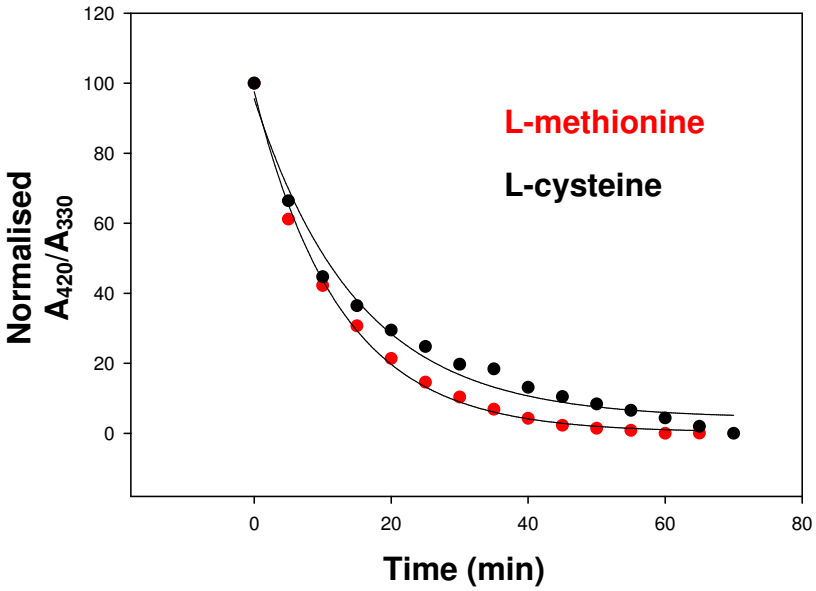

Figure 5.14. Reactivity of l-methionine (red dots) versus l-cysteine (black dots) with ArnB-PLP over time. Both amino acids were added to a final concentration of 1 mM

For each time points, the ratio A_{420}/A_{330} was calculated, normalised and plotted as function of time. Figure 5.14 shows the kinetics of ArnB-PMP formation in the presence of l-methionine (red) and l-cysteine (black). Solid curves are fits for a single exponential function (see chapter 6, section 6.2.5.2, equation 1). The observed rate constants for the l-methionine and l-cysteine were respectively 0.081 ± 0.0033 min^{-1} and 0.066 ± 0.0061 min^{-1}. The rate constant observed for the methionine is in agreement with the value reported for ArnB from *S. typhimurium* which was 0.051 ± 0.013 min^{-1} [95].

5.4 Assays of ArnB with Potential Inhibitors

In vitro inhibition tests of ArnB with various compounds were carried-out in order to screen potential inhibitors to perform *in vivo* studies consisting in killing assays towards various bacteria including pathogenic strains.

D-cycloserine (D-CS) and l-cycloserine (L-CS) were the first antibiotics to be tested since a previous study carried out analysis of the interaction of L-CS with ArnB from *S. typhimurium* [95]. The enzyme was incubated with 1 mM D-CS and monitored by UV-Vis. The reaction of D-cycloserine with the protein ArnB-PLP showed a different profile compared to those previously recorded with the L-amino acid substrates (Fig. 5.15).

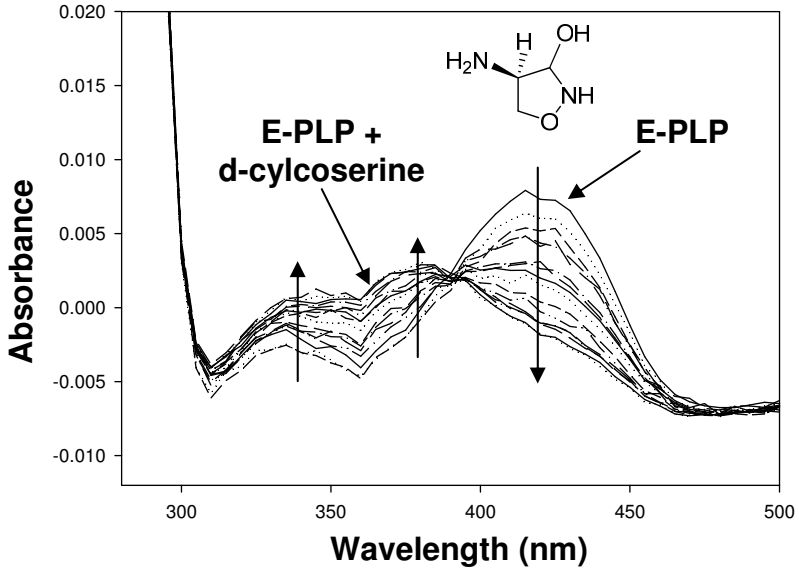

Figure 5.15. Time course of the reaction of ArnB with d-cycloserine (D-CS, 1 mM, scans were recorded every 12 seconds).

Upon incubation of *B. cenocepacia* holo-ArnB with D-CS the signal at 420 nm decreased immediately and a new peak appeared at around 370 nm with a broad shoulder between 330-360 nm (Fig 5.15). This suggested the formation of an inhibitor-ArnB complex. When 1mM l-glutamate was added to this reaction, the UV-visible spectrum of the enzyme with bound d-cycloserine remained unchanged (data not shown), suggesting that an alternative amino donor could not displace the product formed between D-CS and ArnB. The same incubation was also performed with the l-cycloserine enantiomer (Fig. 5.16).

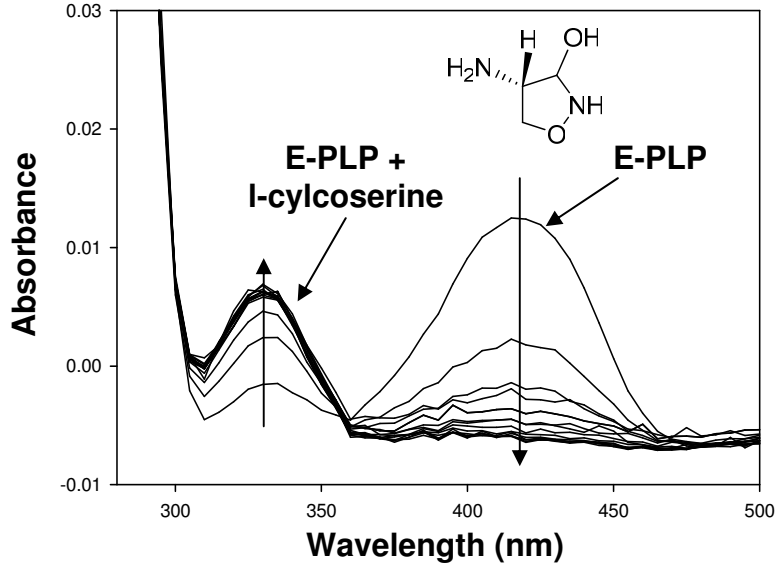

Figure 5.16. Time course of the reaction of ArnB with l-cycloserine (L-CS., 1 mM, scans were recorded every 6 seconds).

By monitoring the UV-vis spectrum it was immediately clear that the behaviour of the ArnB in the presence of the L-CS enantiomer was different to that of the enzyme in the presence of the D-enantiomer. In contrast to D-CS, L-CS caused a rapid disappearance of the peak at 420nm and the appearance of a peak at 320 nm. Unlike the case with D-CS which was not instantaneous (relatively slow), these rapid changes caused by L-CS addition could be monitored between 0-60 seconds. It appears that ArnB reacts differently, and at different rates with each cycloserine enantiomer. Of interest, in the study by Noland and colleagues of the ArnB from *S. typhimurium* the UV-vis data presented was that of ArnB incubated with only L-CS – this was similar to our data of *B. cenocepacia* ArnB with D-CS. However, according to the file recorded in the Protein DataBank (PDB code (1MDZ) Noland et al determined the x-ray structure of the ArnB in complex with D-CS at 2.07 Å resolution. They interpret the electron density of the PLP adduct as a hydroxyisoxazole-PMP and state that the α-carbon of D-CS has apparent sp^2 hybridisation, consistent with the abstraction of the α-H by the general base Lys188. They also suggest that the sp^2-hybridised α-carbon makes the cycloserine and PLP rings nearly co-planar in the adduct (see figure 5.17 below). However, it is interesting to note that in the rendered structure the α-H is still present in an oxazolidine adduct (rather than a hydroxyisoxazole) and the authors make no mention of this discrepancy.

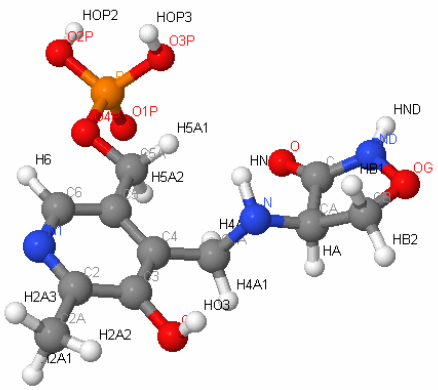

Figure. 5.17. The rendered J-mol structure of the *S. typhimurium* ArnB D-CS-PLP adduct taken from the ArnB 1MDZ.

Of further interest, Fenn and coworkers have reported that the two cycloserine enantiomers react with the PLP-dependent enzyme alanine racemase from *Bacillus stearothermophilus* (AR, EC 5.1.1.1) leading to the formation of the same PLP-

cycloserine adducts (the hydroxyisoxazole-PMP derivative) [118]. The UV-vis data presented in this study were very similar to what we observed between *B. cenocepacia* ArnB and L-CS (Fig. 5.16). In alanine racemase it is thought that the formation of the same product PLP-inhibitor adduct from the enantiomeric pair of inhibitors can be accomplished by the presence of a complementary acid and base pair of residues in the active site of this racemase. Fenn et al also determined the structures of alanine racemase in complex with D-CS (PDB code: 1EPV) and L-CS (PDB code: 1NIU). In both cases the authors suggest the cycloserine adducts are the hydroxyisoxazole-PMP and the α-carbon is sp^2 hybridised.

In our study, based on the UV-vis data of the *B. cenocepacia* ArnB, we suggest that the final products are likely to be the same derivatives to that found with *S. typhimurium* ArnB since the two enzymes share 51% amino acid sequence identity with the active site residues conserved (Fig. 5.1). However, our UV-vis data is also consistent with the excellent study of the alanine racemase by Fenn *et al*. There is uncertainty in assigning definitive structures of the adducts. The signal at 320 nm can be interpreted as being due to either PMP or PMP-cycloserine adducts since they both have a maximum absorbance at around 330 nm. However, the broad peaks extending out to beyond 400 nm suggest the presence of a PLP-isoxazole adduct. To account for the possible formation of PMP (i.e. cycloserine acting as an amino donor) and the PLP-isoxazole we have postulated two possible mechanisms outlined in figure 5.18.

The mechanism depicting the formation of the hydroxyisoxazole-PMP derivative is adapted from Fenn et al and describes the initial transamination of the cycloserine molecule from the internal aldimine (holo-form) to generate an external aldimine. The lysine residue (Lys 186 in *B. cenocepacia* ArnB equivalent to Lys188 in *S. typhimurium* ArnB) carries out a deprotonation at the α-carbon position generating a quinonoid intermediate that is rapidly converted to the ketimine form. From the ketimine, we speculate a different mechanism to that proposed by Fenn *et al* [119] that could lead to the formation of an ArnB-PMP form and "free" isoxazole derivatives by hydrolysis (Fig. 5.17, B, C and C').

The reaction mechanism for the formation of the hydroxyisoxazole-PMP derivative is the other route suggested. It begins with the ketimine form which is deprotonated at the β-carbon by the lysine residue leading to the formation of the product PMP-hydroxyisoxazole derivative A. This is the co-planar adduct observed

by Noland and coworkers in their crystal structure (Fig. 5.18, inset) [95]. Residues involved in the stabilisation of the PMP-cycloserine intermediate are highlighted in figure 5.18. The sequence alignment of ArnB from *Salmonella* and *Burkholderia* confirmed the presence of the same residues that stabilise the isoxazole PMP derivative; Thr64, Asp160, Ser183, and His329 (Fig.5.1 and 5.18).

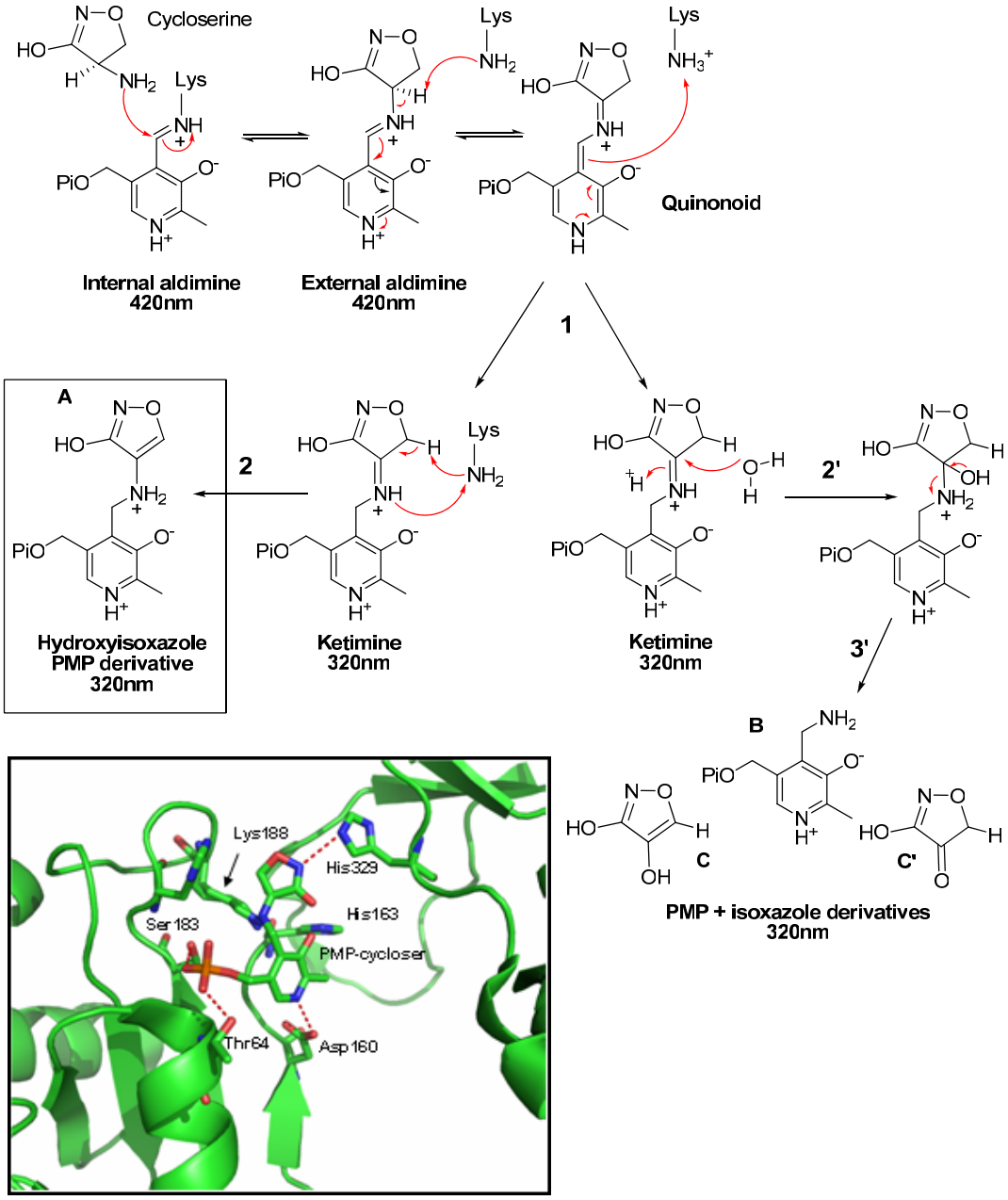

Figure 5.18. Proposed mechanisms of reaction between D-CS and ArnB. The structure is that of the *S. typhimurium* ArnB:hydroxyisoxazole-PMPcomplex (product A in box) (PDB code: 1MDZ).

The interesting data obtained with the CS inhibitors encourage us to explore two other potential inhibitors; gabaculine and ibotenic acid, which are two neurotoxins (Fig. 5.19). Gabaculine is a well-studied chemical compound and acts as potent irreversible inhibitor against GABA (γ-aminobutyrate) transaminase, a PLP-dependent enzyme [119]. Ibotenic acid is a neurotoxin found in mushroom from the genus *Amanita*. Unfortunately neither these two neurotoxins displayed any reactivity towards ArnB and after incubation with these compounds the UV-visible spectrum profile of the holo-form of the ArnB remained unchanged (data not shown).

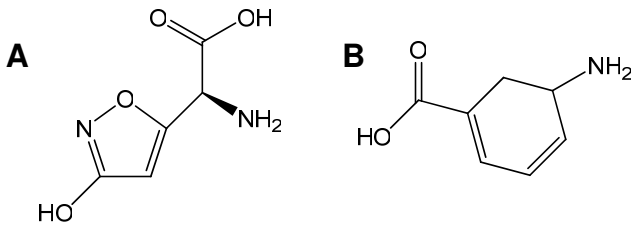

Figure 5.19. Chemical structures of ibotenic acid (A) and gabaculine (B)

It appears that although ArnB binds a range of amino acids and both CS enantiomers it does display some substrate selectivity.

5 5 *In vivo* Antimicrobial Assays of D-Cycloserine and Polymyxin B

Since d-cycloserine is a broad spectrum antibiotic used against tuberculosis (Seromycin, Lilly), and encouraged by the results obtained with the *in vitro* assays of recombinant *B. cenocepacia* ArnB we decided to perform antimicrobial tests with d-cycloserine on a range of *Burkholderia* species. For cost reasons only D-CS was used since it is ~30 times less expensive than L-CS. As a control we also used polymyxin PMB, a cationic AMP. We first assayed the two compounds separately and then simultaneously in order to evaluate respectively their antibiotic and synergistic potential. Therefore, the minimum inhibitory concentrations (MICs) of both compounds were determined against numerous bacteria including *E. coli*, *P. aeruginosa*, *B. multivorans* and *B. cenocepacia* (Table 5.1).

Within these four bacteria species, different strains were tested and the MIC values were given according to the concentration for which no growth could be observed on the plate. Concerning PMB, the MICs observed for *E. coli* and *P.*

aeruginosa were very low with no visible growth after 0.25 µg/ml while d-cycloserine MICs were calculated to be from 20 to 64 µg/ml. On the other hand, d-cycloserine displayed the lower MIC values towards both *Burkholderia* genomovars (II and III) with values ranging from 6 to 40 µg/ml while a majority of such strains were still resistant above 500 µg/ml of PMB.

It is interesting to note that for strains unable to modify their lipid A with aminoarabinose - *E. coli* and *P. aeruginosa* - the MICs value for PMB are very low. In contrast, *Burkholderia* strains where such modification is constitutively expressed, the PMB action has little effect as expected but interestingly, cycloserine displayed relatively low MIC values. Although D-CS is a broad-spectrum inhibitor that could inactivate many PLP-dependent enzymes, the differences observed in killing between bacterial species is quite striking.

Strain	MIC Polymyxin B (µg/ml)	MIC d-cycloserine (µg/ml)
E. coli		
K12 MG1655	0.125	30
P. aeruginosa		
PAO1	0.25	64
B. multivorans **(II)**		
C5393	>500	15
LMG 13010	>500	40
C1576	>500	6
CF-A1-1	>500	15
JTC	>500	15
C1962	250	12.5
ATCC 17616	250	15
B. cenocepacia **(III)**		
J2315	>500	40
K56-2	500	30
SAL-1	125	30

Table 5.1 Minimum inhibitory concentration (MIC) values for various strains of bacteria. MIC numbers given correspond to the first plate for which no growth could be observed.

The combined action of cycloserine with PMB was assayed by the disc diffusion method on isosensitive agar (ISA) plate containing increased concentrations of PMB (see Chapter 6, section 6.2.7.1). Different quantities of cycloserine were spotted on the disc (10, 50, 100 and 250 µg) and put on plate previously inoculated with cell culture. These assays were performed on *B. multivorans* (LMG 13010 and ATCC 17616) and *B. cenocepacia* strains (SAL-1 and J2315) (Fig. 5.20).

For all strains tested, a dose-response is observed as the killing zone increase with the concentration d-cycloserine. Moreover, the additional effect of cycloserine with increased concentrations of PMB was observed for *B. cenocepacia* SAL-1 and *B. multivorans* ATCC 17616 strains as the killing zone around the disc increases when PMB is more concentrated (Fig. 5.20).

The same effect was not observed for *Burkholderia* strains LMG 13010 and J2315 where the killing zones around the disc remain unchanged despite the increased concentration of PMB. Moreover, no synergistic effect was observed between PMB and cycloserine.

These antimicrobial assays were carried out with K. Bodewits, PhD student at University of Edinburgh.

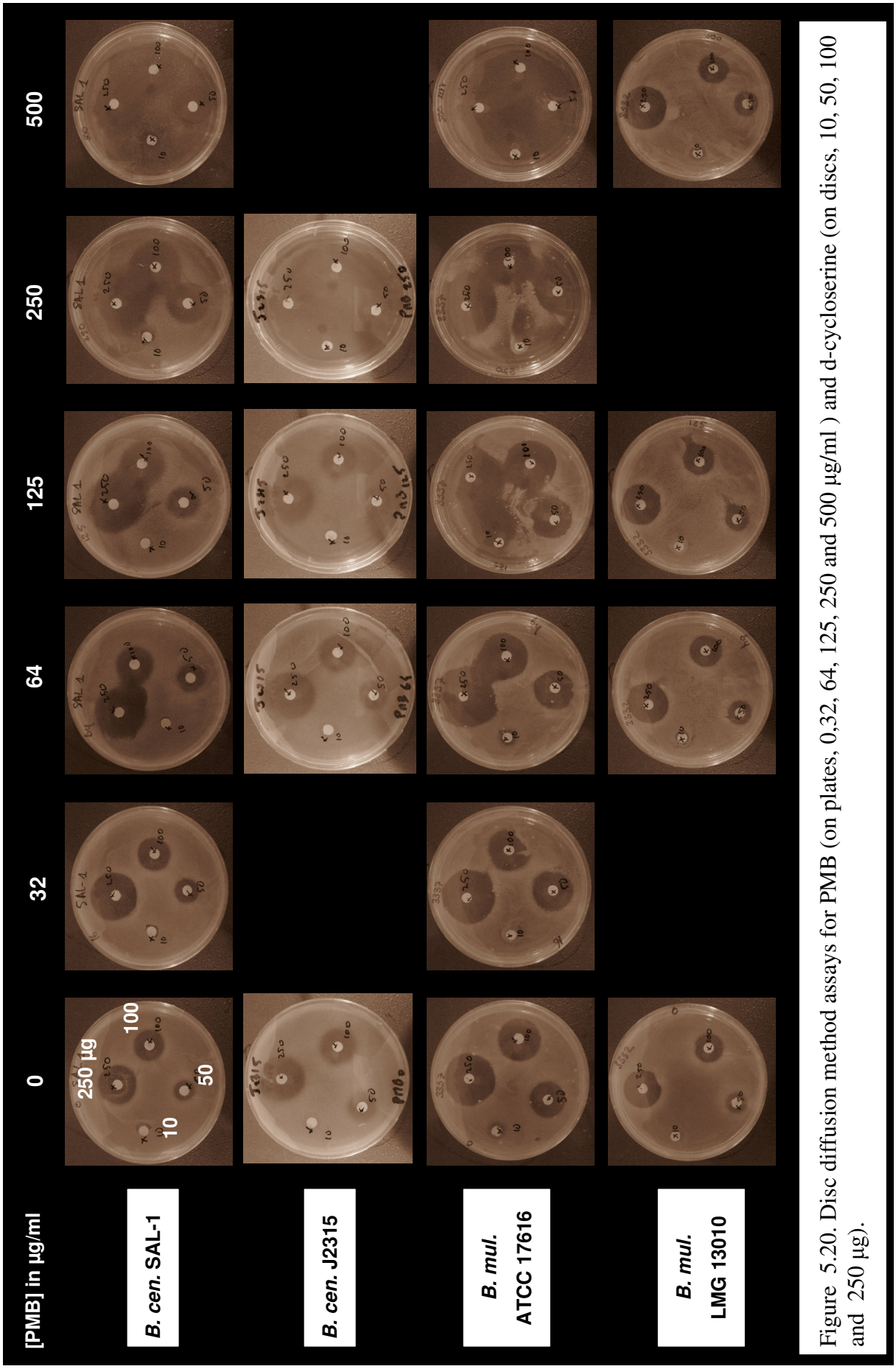

Figure 5.20. Disc diffusion method assays for PMB (on plates, 0,32, 64, 125, 250 and 500 µg/ml) and d-cycloserine (on discs, 10, 50, 100 and 250 µg).

5.6 Cloning, Expression and Purification of ArnG (BCAL 1930)

Since no structural data was available on the ArnG protein the initial strategy was to clone the *arnG* gene in pET28a in order to express and purify the protein either with a hexa-histidine tag at the C-terminal and at the N-terminal of the gene sequence.

A PCR amplification was carried out to amplify the *arnG* gene from the genomic DNA of *B. cenocepacia* J2315. Primers were designed to insert NcoI/XhoI and NdeI/XhoI restriction sites in order to clone the gene with respectively a C- and N-terminal hexa-histidine tag in the pET28a vector plasmid After ligation of *arnG* gene into the target plasmid, pET28a-ArnG-C_{His} and pET28a-ArnG-N_{His} (Fig. 5.21) were transformed into BL21(DE3)PlysS competent cells.

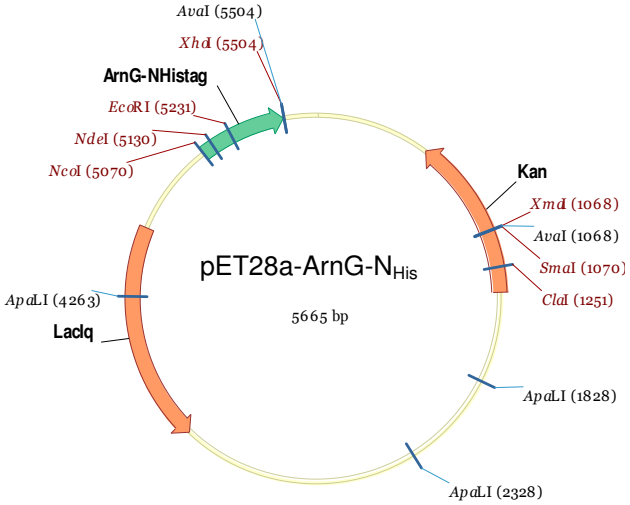

Figure 5.21. Plasmid map of pET28a-ArnG-N_{His} used to express and purify ArnG with a His-tag at the *N*-terminal.

After an overnight growth at 30ºC, cells were subcultured and further grown in universal tubes until the OD_{600} reached 0.6. Cells were induced with 0.5 mM IPTG for 6 hours and 1 mL of each sample was kept for Western-blot analysis. At this stage only the visualisation of ArnG expression was wanted. Attempts to detect ArnG expression by SDS-PAGE analysis failed as the level of expression for such proteins is very low. Therefore, a western-blot analysis was performed on ArnG expression with an anti-His tag antibody and shown in figure 5.22. Lane A and B represent respectively the expression of ArnG with a poly his-tag at the C-terminus before and after induction with IPTG. In parallel, the same analysis was carried out with arnG with an *N*-terminal His-tag (lane C and D). While no expression could be detected for

ArnG tagged at the C-terminus, the induced sample for ArnG with a histidine tag at the N-terminus could be visualised. These results suggest that the C-terminus sequence of ArnG could be embedded in the membrane, expression is very low, or the C-terminus is processed off in some way.

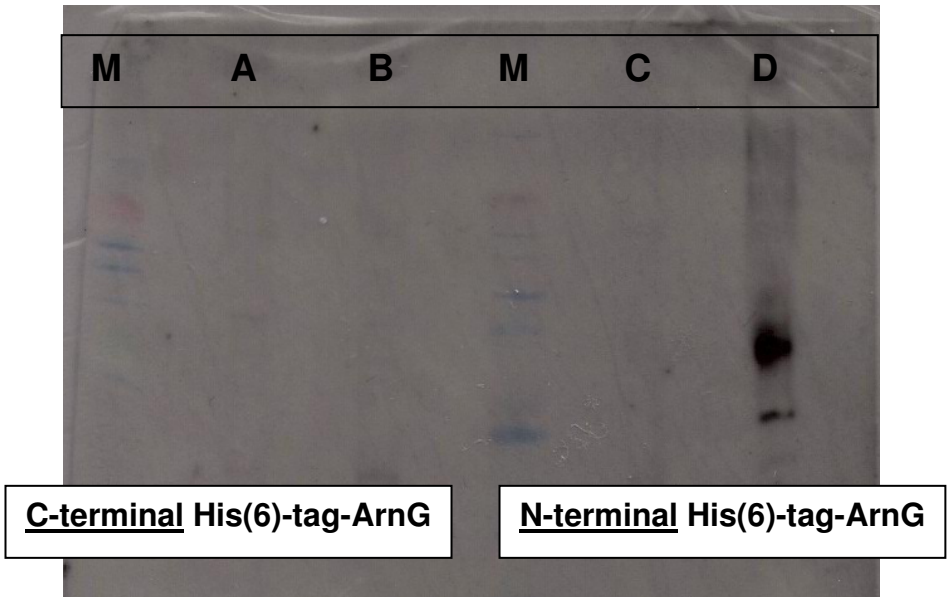

Figure 5.22. Detection of C-terminal versus N-terminal His tagged ArnG expression by the western-blot method. Lanes A and C represent the expression before IPTG induction, lanes B and D is the cell extract after induction.

Using the same strategy but with a different tag at the N-terminus *arnG* gene was cloned into pET29a plasmid leading to a construct where ArnG was cloned with an S-tag .The expression of ArnG was also detected on a western-blot (data not shown).

A small scale expression and purification (20 mL) was carried out with BL21(DE3)PlysS cells freshly transformed with the pET28a-ArnG-N_{His} plasmid. After 6 hours of induction with IPTG, the cell pellet was resuspended in 1% SDS buffer and centrifuged for 10 minutes at 13 Krpm at 4 ºC. The cell extract was incubated 4 hours with Ni-NTA resin in presence of 20 mM imidazole, washed, and eluted with 100 mM and 250 mM imidazole. The different steps of expression and purification were monitored by western blot after separation of proteins on a Tris-Glycine 16% precast gel (Fig. 5.23). Two samples were run side by side on the gel corresponding to a 0.5 mM and 1 mM IPTG induction. Induced samples were detected by western blot and two distinct bands could be visualised for both

inductions. Bands at around 15 kDa and 30 kDa which agree with the theoretical masses of the ArnG monomer and dimer were present after induction. After the washing step with 20 mM imidazole the sample was eluted with 100 mM imidazole revealing the two distinctive bands. No ArnG proteins could be detected after an elution step at 250 mM imidazole. Proteins present in the first elution sample were concentrated and run onto a Tris-Glycine 16% precast gel (Fig. 5.23, inlet). Two bands corresponding to those also detected by western blot are indicated by the two arrows. Contaminants were also present in the sample as shown in the higher section of the gel lane.

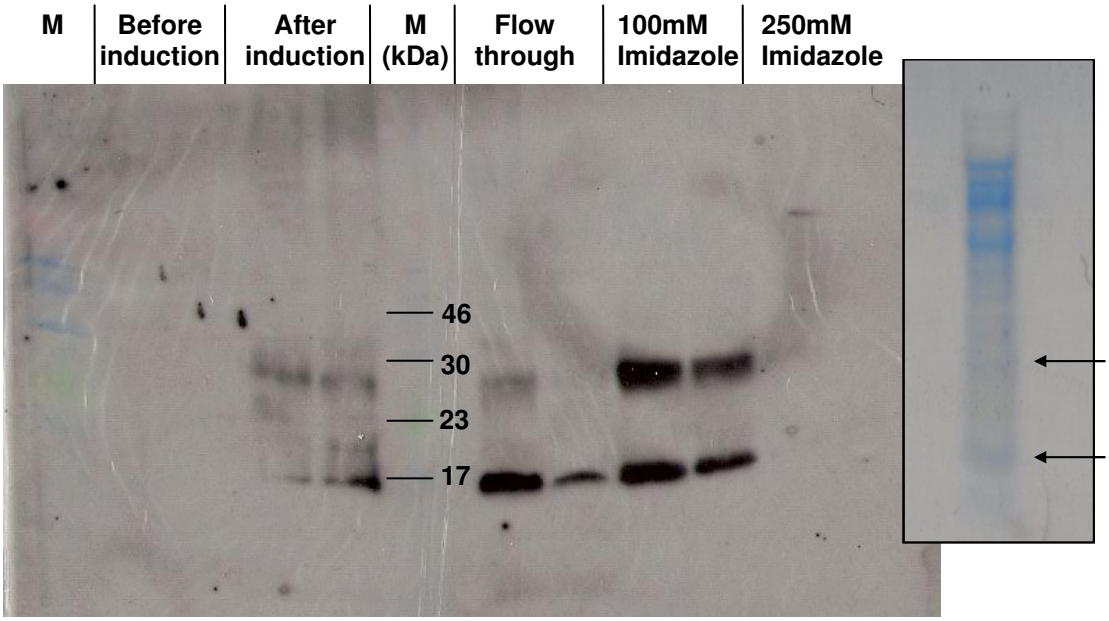

Figure 5.23. Western blot analyses of the different step of purification of ArnG. The insert shows the precast gel profile of the sample after Coomassie blue staining.

Our results suggest that ArnG is expressed at very low levels and is extremely difficult to isolate in high yield and purity, which is expected for an inner membrane protein. Nevertheless, our results suggest that this method could be optimised further to isolate ArnG for structural studies.

5.7 Complementation assay of ArnG in *E. coli* knock-out strains

In the paper published by Yan and coworkers in 2007 [98], the *E. coli* MST100 strain which is able to constitutively modify the lipid A moiety of LPS and therefore be resistant to polymyxin B (PMB) was modified in order to knock-out the genes

(*pmrL/M*) responsible for the flippase activity of the undecaprenyl phosphate-aminoarabinose. Hence, three new strains sensitive to PMB were created by replacing *arnE (pmrL)*, *arnF (pmrM)* and *arnE/F (pmrL/M)* genes with a kanamycin cassette (respectively named AY100, AY101 and AY102). Another gene, *arnT* (previously *pmrK*), was knocked-out, leading to the AY103 construct. The ArnT protein carries out the last step of modification pathway of lipid A by attaching the modified sugar (aminoarabinose) to the 1 and/or 4' phosphate of the lipid A moiety. The idea of the complementation assays was to transform the *B. cenocepacia arnG* gene in the different strains in order to restore the missing flippase activity in the *E. coli* mutants. Hence, successful complementation will restore the resistance towards PMB. The strains were kindly provided by Prof. Christian Raetz from Duke University Medical Center and analysed on agar plates (Fig. 5.24). If the MST100 strain was resistant to 15 µg/ml of PMB (plate A), none of the knocked-out strains were capable of growth under these conditions. On the contrary, all strains were able to grow on a kanamycin plate (20 µg/ml) with the exception of MST100 which doesn't contain the kanamycin resistance gene (plate B).

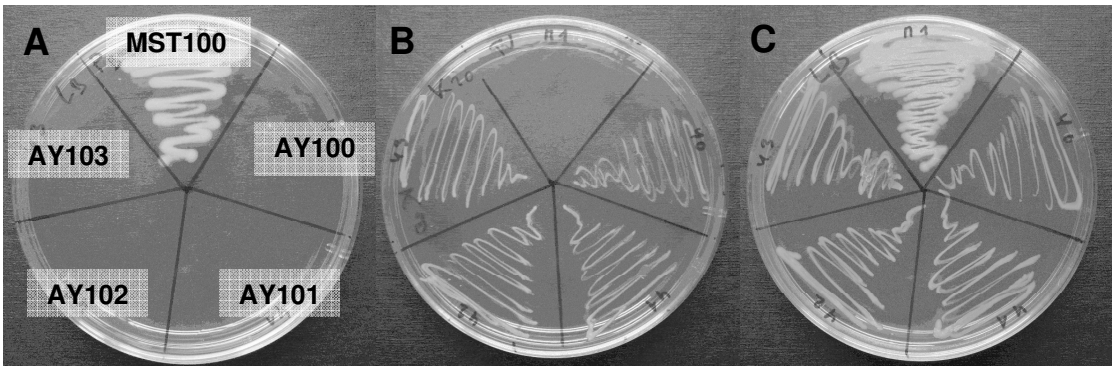

Figure 5.24. Strains provided by Raetz were tested on agar plates supplemented with 15 µg/ml of PMB (A), 20 µg/ml of kanamycin (B) and agar-only plate (C).

ArnG gene was cloned into the pTrc99a plasmid (ampicillin resistant) (Fig. 5.25) with no tag in order to avoid any negative artifacts due to the presence of a supplementary sequence. pTrc99a is a low-copy number plasmid and is optimised to express low amounts of the protein (10-20 per cell) compared to pET plasmids. It is convenient for complementation studies as its action is more physiologically relevant than plasmids optimised for overexpression and purification. Hence pTrc99a-ArnG was used to transform the three different strains, AY100, AY101 and AY102. After an overnight growth at 30 ºC in presence of adequate antibiotics, cells were

subcultured and grown for 5 hours. The different optical densities at 600nm were normalised and the cultures diluted 4 times to a 10^{-4} dilution. Three µl of each culture was spotted on 6 different plates of various PMB concentrations (0-15 µg/ml). In addition, the same protocol was applied to the three strains alone but also transformed with a pTrc99a-FbpA plasmid (P. Bilton, PhD, University of Edinburgh, which expresses a ferric binding protein FbpA) in order to compare the complementation tests with controls. The results concerning the double knock-out AY102 strain are shown on figure 5.26. The 3 samples displayed the same sensitivity towards the different PMB concentrations and same results were observed for AY100 and AY101 strains (data not shown) leading to the conclusion that ArnG did not complement the *E. coli* ArnE and ArnF knock-out strains under these conditions (Fig. 5.26).

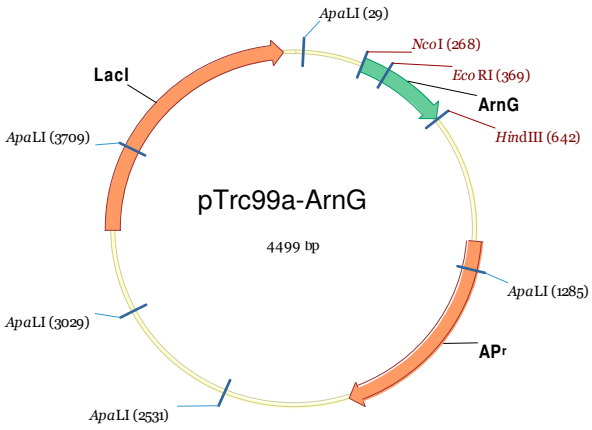

Figure 5.25. Plasmid map of pTrc99a-ArnG used for the complementation assays.

It appears that despite the fact that *B. cenocepacia* J2315 ArnG is present on the *arn* operon and bears resemblance to the *E. coli* ArnE and ArnF flippase proteins it cannot confer polymyxin resistance on *E. coli* strains in which these homologs have been knocked out. Sequence analysis of ArnG suggests it is a hydrophobic protein, but maybe *Burkholderia*-specific. It is interesting to note that the *arnG* gene is co-transcribed with ArnT in Burkolderia suggesting the Ara4N transfer to lipid A and flipping may be linked. It may be that functional ArnG expression in the *E. coli* membrane requires the presence of its ArnT partner.

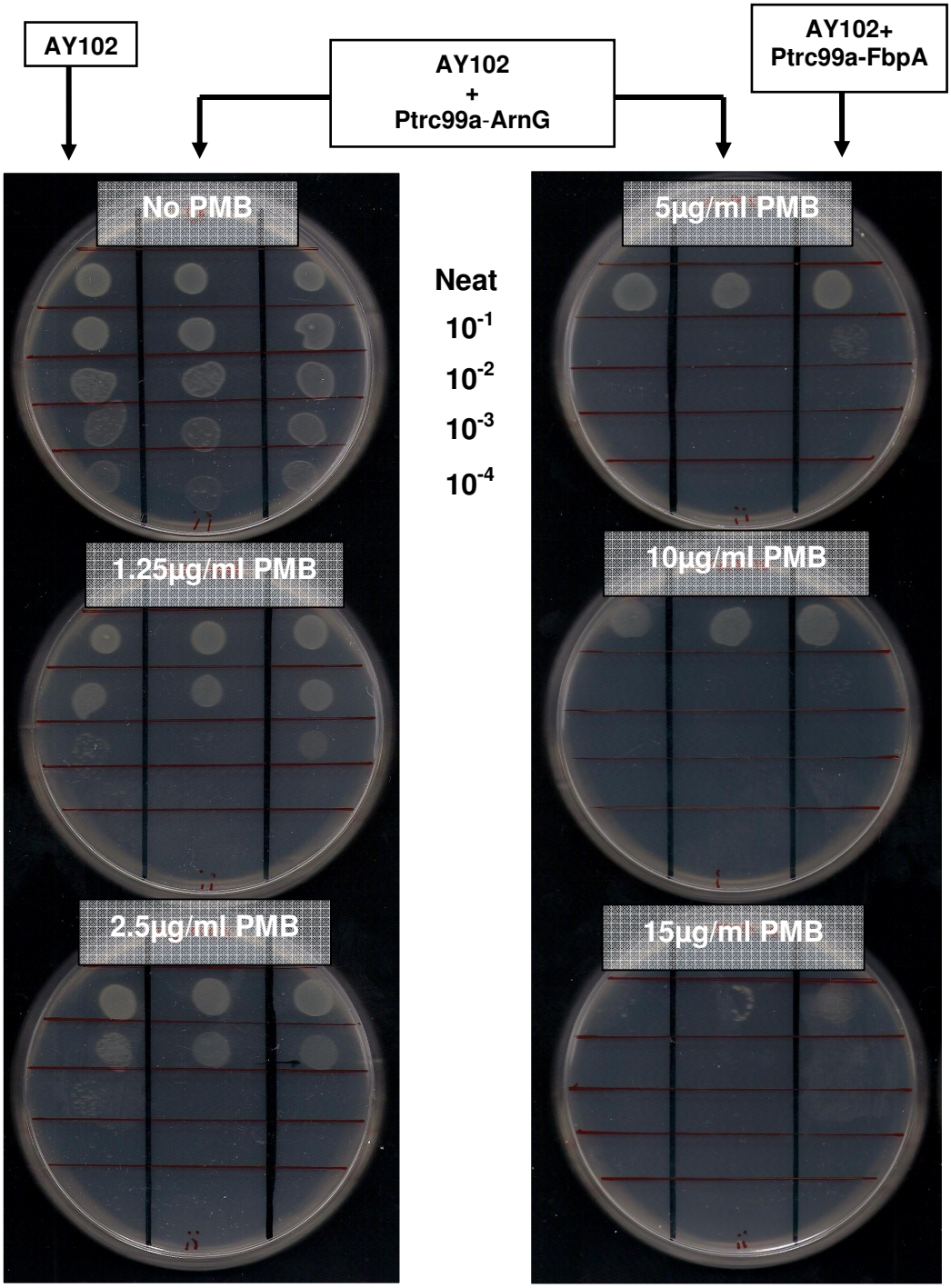

Figure 5.26. Complementation assays of AY102 transformed with pTrc99a-ArnG. Increasing concentrations of PMB (0 to 15 µg/ml) were used and a series of culture dilutions (neat, 10^{-1}, 10^{-2}, 10^{-3}, 10^{-4}) were spotted on plate as indicated on the figure.

5.8 Conclusions and Perspectives

In this study the biosynthesis of the amino sugar aminoarabinose (Ara4N) and its transfer to lipid A in *B. cenocepacia* J2315 was investigated by analysis of two important proteins. The enzyme ArnB (encoded by the gene pmrH) which is the third enzyme of the pathway, was cloned with a hexa-histidine tag, expressed in *E. coli* and purified in high yield using two steps – metal-affinity and size exclusion chromatographies. UV-visible spectroscopic analysis confirmed the enzyme was a PLP-dependent aminotransferase reacting with l-glutamate to form the ArnB-PMP species. ArnB was also able to react with various amino acids such as l-cysteine, l-methionine, l-glutamine but appeared not to use l-serine, l-asparagine and l-aspartic acid as substrates. In the well characterised *S. typhimurium* ArnB, Lys241 and Arg229 appear to be the residues selective for the amine donor. We suggest the equivalent residues in the *B. cenocepacia* ArnB are Lys232 and Arg218. l-glutamate and l-glutamine both share two methylenes in the side-chain. Therefore, the lysine and arginine residues could also act as selective "tweezers" discriminating the amine donor substrate according to its carbon backbone length. Despite the fact that in all in vitro studies, including those described here, l-glutamate is the most reactive substrate for ArnB, it remains to be proven as the physiological amine donor in the aminoarabinose lipid A modification pathway either for *E. coli*, *S. typhimurium* or *B. cenocepacia*.

We also incubated the recombinant *B. cenocepacia* ArnB protein in the presence of both the l- or d-enantiomers of cycloserine, a well-known inhibitor of many PLP-dependent enzymes. These generated different UV-visible spectra and reacted at different rates. By consideration of the previous work on *S. typhimurium* ArnB and the alanine racemase from *B. stearothermophilus* we propose two distinct mechanistic pathways leading to the formation of either a covalent hydroxyisoxazole-pyridoxal amine phosphate adduct or the PMP form of the enzyme and "free" hydroxyisoxazole adducts. The inhibitor complexes are non-covalently bound in the enzyme active site. Further work could apply x-ray crystallography and mass spectrometry techniques to capture these proposed molecules. Since amino arabinose metabolism appears to be essential for *Burkholderia*, an inhibitor of an aminoarabinose biosynthetic enzyme should be a potent antimicrobial agent against these species. *In vivo* antimicrobial assays have shown that d-cycloserine was more

efficient than the antimicrobial peptide polymyxin towards *Burkholderia* species and could be explored as a potential new therapy for Cystic Fibrosis sufferers infected by pathogens that are resistant to other antibiotics.

The increased potency of D-CS over PMB towards *Burkholderia* species could be due to the unique feature shared by such species which is the constitutive modification of lipid A by aminoarabinose moiety. This unique phenomenom could be the Achilles' heel of this and other pathogenic bacteria that cause lung damage and inflammation in cystic fibrosis patients. D-cycloserine targets ArnB, a key enzyme in this lipid A modification pathway. Moreover, these preliminary results open a new route for the development of promising therapeutics. However it appears that PMB is not a good candidate to use in combination with cycloserine. To date only three reported cases of cystic fibrosis patients with a "cepacia syndrome" survived after intravenous antibiotic therapy [120-122]. A mixture of different antibiotics including trimethoprim, tobramycin, meropenem and other antimicrobial compounds were necessary for the survival and recovery of these patients. Such chemical compounds could be tested alongside with cycloserine on clinical strains in order to evaluate a possible synergistic effect. So far the main clinical application of cycloserine is for the treatment of tuberculosis.

The second protein studied, ArnG, is an inner membrane protein which could act as a flippase of undecaprenyl phosphate-aminoarabinose just before the last step of the modification pathway of lipid A in *B. cenocepacia*. In *E. coli* two genes have been identified to be responsible for this flippase activity. *ArnE* and *arnF* have been shown to be critical for the translocation of the undecaprenyl phosphate through the inner membrane. Knock-out either or both of these two genes affected the resistance of the *MST100* strains towards polymyxin B in *E. coli*. Attempts to recover the resistance phenotype in these sensitive mutant strains with the ArnG from *B. cenocepacia*, a natural PMB-resistant microorganism, failed in our hands. The expression and purification of ArnG was performed on small-scale and expression was only detected if the protein was fused with an *N*-terminal His-tag using a His-tag specific antibody.

Small hydrophobic proteins such as ArnE, ArnF or ArnG have similarities to proteins found in the small multidrug resistance protein family (SMR family). SMR proteins are 100-140 amino acids length, share a 4 transmembrane α-helical domain and can act as homo- or hetero-oligomers. Moreover, SMR proteins are located in the inner membrane and confer resistance towards a variety of quaternary ammonium

molecules and cationic dyes [123]. Despite the fact that ArnG protein falls into the characteristics previously described, extreme care needs to be taken and further investigations to be performed to unambiguously attribute its function.

Future work should focus on investigating the synergistic effect of cycloserine with various partners in order to establish the most potent "mix" of antibiotics against diverse pathogenic bacteria. Concerning ArnG, a viable knock-out strain deleted for *arnG* gene in the *B. cenocepacia* J2315 genome will be very useful to repeat complementation assay with the plasmid used in this study. Moreover, the determination of the high resolution structure of such a protein may provide also highly valuable information about what role it plays in Ara4N biosynthesis and PMB resistance.

5.9 References Chapter 4 & 5

1 Andrès, E., and Dimarcq. J. L. (2004) *J. Intern. Med*. **255**, 519-520

2 Gordon, Y. J., Romanowski, E.G., and McDermott. A. M. (2005) *Curr. Eye Res*. **30**, 505-515

3 Yeaman, M. R., and Yount, N.Y. (2003) *Pharmacol. Rev*. **55**, 27-55

4 Cashman, K. A., Bayer, A. S., and Yeaman, M. R. (1998) 98th General Meeting for the American Society for Microbiology, May 17-21 Atlanta GA.

5 Nahaie, M. R., Goodfellow, M., Minnikin, D. E., and Hájek, V. (1984) *J. Gen. Microbiol*. **130**, 2427-2437

6 Peschel, A., and Collins, L.V. (2001) *Peptides* **22**, 1651-1659

7 Peschel, A. (2002) *Trends. Microbiol*. **10**, 1179-1186

8 Gross, M., Cramton, S. E., Götz, F., and Peschel, A. (2001) *Infect. Immun*. **69**, 3423-3426

9 Weidenmaier, C., Kokai-Kun, J. F., Kristian, S. A., Chanturiya, T., Kalbacher, H., Gross, M., Nicholson, G., Neumeister, B., Mond, J. J., and Peschel, A. (2004) *Nat. Med*. **10**, 243-245

10 Bayer, A. S., Prasad, R., Chandra, J., Koul, A., Smriti, M., Varma, A., Skurray, R. A., Firth, N., Brown, M. H., Koo, S. P., and Yeaman, M. R. (2000) *Infect. Immun*. **68**, 3548-3553

11 Shafer, W. M., Qu, X., Waring, A. J., and Lehrer, R. I. (1998) *Proc. Natl. Acad. Sci. U S A* **95**, 1829-1833

12 Andrade, A.C., Van Nistelrooy, J. G., Peery, R. B., Skatrud, P. L., and De Waard, M. A. (2000) *Mol. Gen. Genet*. **263**, 966-977

13 Kupferwasser, L. I., Skurray, R. A., Brown, M. H., Firth, N., Yeaman, M. R., and Bayer, A. S. (1999) *Antimicrob. Agents Chemother*. **43**, 2395-2399

14 Bengoechea, J. A., and Skurnik, M. (2000) *Mol. Microbiol*. **37**, 67-80.

15 Guina, T., Yi, E. C., Wang, H., Hackett, M., and Miller, S. I. (2000) *J. Bacteriol*. **182**, 4077-4086

16 Islam, D., Bandholtz, L., Nilsson, J., Wigzell, H., Christensson, B., Agerberth, B., and Gudmundsson, G. (2001) *Nat. Med*. **7**, 180-185

17 Galloway, S. M., and Raetz, C. R. (1990) *J. Biol. Chem*. **265**, 6394-6402

18 Rietschel, E. T., Kirikae, T., Schade, F. U., Ulmer, A. J., Holst, O., Brade, H., Schmidt, G., Mamat, U., Grimmecke, H. D., and Kusumoto, S., et al. (1993) *Immunobiology*. **187**, 169-190

19 Akashi, S., Ogata, H., Kirikae, F., Kirikae, T., Kawasaki, K., Nishijima, M., Shimazu, R., Nagai, Y., Fukudome, K., Kimoto, M., and Miyake, K. (2000) *Biochem. Biophys. Res. Commun*. **268**, 172-177

20 Rietschel, E. T., Kirikae, T., Schade, F. U., Mamat, U., Schmidt, G., Loppnow, H., Ulmer, A. J., Zähringer, U., Seydel, U., and Di Padova, F., et al. (1994) *FASEB. J*. **8**, 217-225

21 Raetz, C.R., and Whitfield, C. (2002) *Annu. Rev. Biochem*. **71**, 635-700.

22 Raetz, C. R., Reynolds, C. M., Trent, M. S., and Bishop, R. E. (2007) *Annu. Rev. Biochem*. **76**, 295-329

23 Kawasaki, S., Moriguchi, R., Sekiya, K., Nakai, T., Ono, E., Kume, K., and Kawahara, K. (1994) *J. Bacteriol.* **176**, 284-290

24 McClerren, A, L., Endsley. S., Bowman. J, L., Andersen, N. H., Guan, Z., Rudolph, J., and Raetz, C. R. (2005) *Biochemistry* **44**, 16574-16583

25 Mdluli, K. E., Witte, P. R., Kline, T., Barb, A. W., Erwin, A. L., Mansfield, B. E., McClerren, A. L., Pirrung, M. C., Tumey, L. N., Warrener, P., Raetz, C. R., and Stover, C. K. (2006) *Antimicrob. Agents Chemother*. **50**, 2178-2184

26 Barb, A. W., McClerren, A. L., Snehelatha, K., Reynolds, C. M., Zhou, P., and Raetz, C. R. (2007) *Biochemistry* **46**, 3793-3802

27 Karow, M., and Georgopoulos, C. (1993) *Mol. Microbiol*. **7**, 69-79

28 Polissi, A., and Georgopoulos, C. (1996) *Mol. Microbiol*. **20**, 1221-1233

29 Sperandeo, P., Dehò, G., and Polissi, A. (2009) *Biochim. Biophys. Acta*. **1791**, 594-602

30 Sperandeo, P., Pozzi, C., Dehò, G., and Polissi, A. (2006) *Res. Microbiol*. **157**, 547-558

31 Sperandeo, P., Cescutti, R., Villa, R., Di Benedetto, C., Candia, D., Dehò, G., and Polissi, A. (2007) *J. Bacteriol*. **189**, 244-253

32 Tran, A. X., Trent, M. S., and Whitfield, C. (2008) *J. Biol. Chem*. **283**, 20342-20349

33 Suits, M. D., Sperandeo, P., Dehò, G., Polissi, A., and Jia, Z. (2008) *J. Mol. Biol*. **380**, 476-488

34 Groisman, E. A., Kayser, J., and Soncini, F. C. (1997) *J. Bacteriol*. **179**, 7040-7045

35 Wosten, M. M., Kox, L. F., Chamnongpol, S., Soncini, F. C., and Groisman E. A. (2000) *Cell* **103**, 113-125

36 Gunn, J. S., and Miller, S. I. (1996) *J. Bacteriol*. **178**, 6857-6864

37 Gunn, J. S. (2008) *Trends. Microbiol*. **16**, 284-290

38 Soncini, F. C., and Groisman, E. A. (1996) *J. Bacteriol*. **178**, 6796-6801

39 Bader, M. W., Sanowar, S., Daley, M. E., Schneider, A. R., Cho, U., Xu, W., Klevit, R. E., Le Moual, H., and Miller, S. I. (2005) *Cell* **122**, 461-472

40 Roland, K.L., Martin, L.E., Esther, C.R., and Spitznagel J.K. (1993) *J. Bacteriol*. **175**, 4154-4164

41 Shafer, W. M., Martin, L.E., and Spitznagel J.K. (1984) *Infect. Immun*. **43**, 834-838

42 Paulus, H., and Gray, E. (1964) *J. Biol. Chem*. **239**, 865-871

43 Ashby, M. K. (2004) *FEMS. Microbiol. Lett*. **231**, 277-281

44 Trent, M. S., Ribeiro, A. A., Lin, S., Cotter, R. J., and Raetz, C. R. (2001) *J. Biol. Chem*. **276**, 43122-43131

45 Kanipes, M. I., Lin, S., Cotter, R. J., and Raetz, C. R. (2001) *J. Biol. Chem*. **276**, 1156-1163

46 Lee, H., Hsu, F. F., Turk, J., and Groisman, E. A. (2004) *J. Bacteriol*. **186**, 4124-4133

47 Gibbons, H. S., Kalb, S. R., Cotter, R. J., and Raetz, C. R. (2005) *Mol. Microbiol*. **55**, 425-440

48 Tamayo, R., Choudhury, B., Septer, A., Merighi, M., Carlson, R., and Gunn, J. S. (2005) *J. Bacteriol*. **187**, 3391-3399

49 Kim, S. H., Jia, W., Parreira, V. R., Bishop, R. E., and Gyles, C. L. (2006) *Microbiology* **152**, 657-666

50 Figueroa-Bossi, N., Lemire, S., Maloriol, D., Balbontin, R., Casadesus, J., and Bossi, L. (2006) *Mol. Microbiol.* **62**, 838-852

51 Tzeng, Y. L., Ambrose, K. D., Zughaier, S., Zhou, X., Miller, Y. K., Shafer, W. M., and Stephens, D. S. (2005) *J. Bacteriol*. **187**, 5387-5396

52 Gunn, J. S., Lim, K. B., Krueger, J., Kim, K., Guo, L., Hackett, M., and Miller, S. I. (1998) *Mol. Microbiol*. **27**, 1171-1182

53 Breazeale, S. D., Ribeiro, A. A., McClerren, A. L., and Raetz, C. R. (2005) *J. Biol. Chem*. **280**, 14154-14167

54 Guo, L., Lim, K. B., Gunn, J. S., Bainbridge, B., Darveau, R. P., Hackett, M., and Miller, S. I. (1997) *Science* **276**, 250-253

55 Bishop, R. E., Gibbons, H. S., Guina, T., Trent, M. S., Miller, S. I., and Raetz, C. R. (2000) *EMBO. J.* **19**, 5071-5080

56 Hwang, P. M., Choy, W.Y., Lo, E. I., Chen, L., Forman-Kay, J. D., Raetz, C. R., Privé, G. G., Bishop, R. E., and Kay, L. E. (2002) *Proc. Natl. Acad. Sci. U S A*. **99**, 13560-13565

57 Guo, L., Lim, K. B., Poduje, C. M., Daniel, M., Gunn, J. S., Hackett, M., and Miller, S. I. (1998) *Cell* **95**, 189-198

58 Bishop, R. E. (2005) *Mol. Microbiol*. **57**, 900-912

59 Reynolds, C. M., Ribeiro, A. A., McGrath, S. C., Cotter, R. J., Raetz, C. R., and Trent, M. S. (2006) *J. Biol. Chem*. **281**, 21974-21987

60 Trent, M. S., Pabich, W., Raetz, C. R., and Miller, S. I. (2001) *J. Biol. Chem*. **276**, 9083-9092

61 Gibbons, H. S., Lin, S., Cotter, R. J., and Raetz, C. R. (2000) *J. Biol. Chem*. **275**, 32940-32949

62 Gibbons, H. S., Reynolds, C. M., Guan, Z., and Raetz, C. R. (2008) *Biochemistry* **47**, 2814-2825

63 Kawasaki, K., Ernst, R. K., and Miller, S. I. (2004) *J. Biol. Chem*. **279**, 20044-20048

64 Geurtsen, J., Steeghs, L., Hamstra, H. J., Ten Hove, J., de Haan, A., Kuipers, B., Tommassen, J., and van der Ley, P. (2006) *Infect. Immun*. **74**, 5574-5585

65 Isshiki, Y., Kawahara, K., Zähringer, U. (1998) *Carbohydr. Res*. **313**, 21-27.

66 Shimomura, H., Matsuura, M., Saito, S., Hirai, Y., Isshiki, Y., and Kawahara, K. (2003) *Infect. Immun*. **71**, 5225-5230

67 (a) Hutchison, M. L., and Govan, J. R. (1999) *Microbes Infect*. **1**, 1005-1014 (b) De Soyza, A., Silipo, A., Lanzetta, R., Govan, J. R., and Molinaro, A. (2008) *Innate. Immun*. **14**, 127-144

68 Riordan, J. R., Rommens, J. M., and Kerem, B. S., Alon, N., Rozmahel, R., Grzelczak, Z., Zielenski, J., Lok, S., Plavsic, N., Chou, J.L., et al. (1989) *Science* **245**, 1066-1073

69 Rommens, J. M., Iannuzzi, M. C., and Kerem, B. S., Drumm, M.L., Melmer, G., Dean, M., Rozmahel, R., Cole, J.L., Kennedy, D., Hidaka, N., et al. (1989) *Science* **245**, 1059-1065

70 Riordan, J. R. (2008) *Annu. Rev. Biochem*. **77**, 701-726

71 Choi, J. Y., Muallem, D., Kiselyov, K., Lee, M. G., Thomas, P. J., and Muallem, S. (2001) *Nature* **410**, 94-97

72 Vankeerberghen, A., Cuppens, H., and Cassiman, J. J. (2002) *J. Cyst. Fibros*. **1**, 13-29

73 Ratjen, F., and Döring, G. (2003) *Lancet* **361**, 681-689

74 Gan, K. H., Veeze, H. J., van den Ouweland, A. M., Halley, D. J., Scheffer, H., van der Hout, A., Overbeek, S. E., de Jongste, J. C., Bakker, W., and Heijerman, H. G. (1995) *N. Engl. J. Med*. **333**, 95-99

75 Jilling, T., and Kirk, K. L. (1997) *Int. Rev. Cytol*. **172**, 193-241

76 Boucher, R. C. (2007) *J. Intern. Med*. **261**, 5-16

77 Govan, J. R., Brown, P. H., Maddison, J., Doherty, C. J., Nelson, J. W., Dodd, M., Greening, A. P., and Webb, A. K. (1993) *Lancet* **342**, 15-19

78 Burkholder, W. H. (1950) *Phytopathol*. **40**, 115-117

79 Goldmann, D. A., and Klinger, J. D. (1986) *J. Pediatr*. **108**, 806-812

80 Isles, A., Maclusky, I., Corey, M., Gold, R., Prober, C., Fleming, P., and Levison, H. (1984) *J. Pediatr.* **104**, 206-210

81 Parke, J. L., and Gurian-Sherman, D. (2001) *Annu. Rev. Phytopathol.* **39**, 225-258

82 Lessie, T. G., Hendrickson, W., Manning, B. D., and Devereux, R. (1996) *FEMS. Microbiol. Lett.* **144**, 117-128

83 Yabuuchi, E., Kosako, Y., Oyaizu, H., Yano, I., Hotta, H., Hashimoto, Y., Ezaki, T., and Arakawa, M. (1992) *Microbiol. Immunol.* **36**, 1251-1275

84 Vandamme, P., Holmes, B., Vancanneyt, M., Coenye, T., Hoste, B., Coopman, R., Revets, H., Lauwers, S., Gillis, M., Kersters, K., and Govan, J. R. (1997) *Int. J. Syst. Bacteriol.* **47**, 1188-1200

85 Vanlaere, E., Lipuma, J. J., Baldwin, A., Henry, D., De Brandt, E., Mahenthiralingam, E., Speert, D., Dowson, C., and Vandamme, P. (2008) *Int. J. Syst. Evol. Microbiol.* **58**, 1580-1590

86 Coenye, T., Vandamme, P., LiPuma, J. J., Govan, J. R., and Mahenthiralingam, E. (2003) *J. Clin. Microbiol.* **41**, 2797-2798

87 Mahenthiralingam, E., Baldwin, A., and Vandamme, P. (2002) *J. Med. Microbiol.* **51**, 533-538

88 Mahenthiralingam, E., Urban, T. A., and Goldberg, J. B. (2005) *Nat. Rev. Microbiol.* **3**, 144-156

89 Mahenthiralingam, E., Vandamme, P., Campbell, M. E., Henry, D. A., Gravelle, A. M., Wong, L. T., Davidson, A. G., Wilcox, P. G., Nakielna, B., and Speert, D. P. (2001) *Clin. Infect. Dis.* **33**, 1469-1475

90 Chen, J. S., Witzmann, K. A., Spilker, T., Fink, R. J., and LiPuma, J. J. (2001) *J. Pediatr.* **139**, 643-649

91 Johnson, W. M., Tyler, S. D., and Rozee, K. R. (1994) *J. Clin. Microbiol.* **32**, 924-930

92 Holden, M. T., Seth-Smith, H. M., Crossman, L. C., Sebaihia, M., Bentley, S. D., Cerdeño-Tárraga, A. M., Thomson, N. R., Bason, N., Quail, M. A., Sharp, S., Chevevach, I., Churcher, C., Goodhead, I., Houser, H., Holroyd, N., Mungall, K., Scott, P., Walker, D., White, B., Rose, H., Iversen, P., Mil-Homens, D., Rocha, E. P., Fialko, A . M., Baldwin, A., Dowson, C., Barrell, B. G., Govan, J. R., Vandamme, P., Hart, C. A., Mahenthiralingam, E., and Parkhill, J. (2009) *J. Bacteriol*. **191**, 261-277

93 Breazeale, S. D., Ribeiro, A. A., and Raetz, C. R. (2002) *J. Biol. Chem*. **277**, 2886-2896

94 Breazeale, S. D., Ribeiro, A. A., McClerren, A. L., and Raetz, C. R. (2005) *J. Biol. Chem*. **280**, 14154-14167

95 Noland, B. W., Newman, J. M., Hendle, J., Badger, J., Christopher, J. A., Tresser, J., Buchanan, M. D., Wright, T. A., Rutter, M. E., Sanderson, W. E., Müller-Dieckmann, H. J., Gajiwala, K. S., and Buchanan, S. G. (2002) *Structure* **10**, 1569-1580

96 Williams, G. J., Breazeale, S. D., Raetz, C. R., and Naismith, J. H. (2005) *J. Biol. Chem*. **280**, 23000-23008

97 Gatzeva-Topalova, P. Z., May, A. P., and Sousa, M. C. (2004) *Biochemistry* **43**, 13370-13379

98 Yan, A., Guan, Z., and Raetz, C. R. (2007) *J. Biol. Chem*. **282**, 36077-36089

99 Ortega, X. P., Cardona, S. T., Brown, A. R., Loutet, S. A., Flannagan, R. S., Campopiano, D. J., Govan, J. R., and Valvano, M. A. (2007) *J. Bacteriol*. **189**, 3639-3644

100 Loutet, S. A., Bartholdson, S. J., Govan, J. R., Campopiano, D. J., and Valvano, M. A. (2009) *Microbiology* **155**, 2029-2039

101 Kooi, C., Corbett, C. R., and Sokol, P. A. (2005) *J. Bacteriol*. **187**, 4421-4429

102 Mohr, C. D., Tomich, M., and Herfst, C.A. (2001) *Microbes Infect.* **3**, 425-435

103 Hutchison, M. L., Poxton, I. R., and Govan, J. R. (1998) *Infect. Immun*. **66**, 2033-2039

104 Tomich, M., Herfst, C.A., Golden, J.W., and Mohr, C.D. (2002) *Infect. Immun.* **70**, 1799-1806.

105 Moreira, L. M., Videira, P. A., Sousa, S. A., Leitão, J. H., Cunha, M. V., Sá-and Correia, I. (2003) *Biochem. Biophys. Res. Commun*. **312**, 323-333

106 Cheung, K. J. Jr, Li, G., Urban, T. A., Goldberg, J. B., Griffith, A., Lu, F., and Burns, J. L. (2007) *Microbes Infect*. **9**, 829-837

107 Khan, S. A., Everest, P., Servos, S., Foxwell, N., Zähringer, U., Brade, H., Rietschel, E. T., Dougan, G., Charles, I. G., and Maskell, D. J. (1998) *Mol. Microbiol*. **29**, 571-579

108 Shaw, D., Poxton, I. R., and Govan, J. R. (1995) *FEMS Immunol. Med. Microbiol*. **11**, 99-106

109 Silipo, A., Molinaro, A., Ieranò, T., De Soyza, A., Sturiale, L., Garozzo, D., Aldridge, C., Corris, P. A., Khan, C. M., Lanzetta, R., and Parrilli, M. (2007) *Chemistry* **13**, 3501-3511

110 Gronow, S., Noah, C., Blumenthal, A., Lindner, B., and Brade, H. (2003) *J. Biol. Chem*. **278**, 1647-1655

111 Vinogradov, E., Lindner, B., Seltmann, G., Radziejewska-Lebrecht, J., and Holst, O. (2006) *Chemistry* **12**, 6692-6700

112 Vinogradov, E. V., Lindner, B., Kocharova, N. A., Senchenkova, S. N., Shashkov, A. S., Knirel, Y. A., Holst, O., Gremyakova, T. A., Shaikhutdinova, R. Z., and Anisimov, A. P. (2002) *Carbohydr. Res*. **337**, 775-777

113 Vinogradov, E. V., Müller-Loennies, S., Petersen, B. O., Meshkov, S., Thomas-Oates, J. E., Holst, O., and Brade, H. (1997) *Eur. J. Biochem*. **247**, 82-90

114 Ortega, X., Silipo, A., Saldias, M. S., Bates, C. C., Molinaro, A., and Valvano, M. A. (2009) *J. Biol. Chem*. **284** 21738-21751

115 Vorachek-Warren, M. K., Ramirez, S., Cotter, R. J., and Raetz, C. R. (2002) *J. Biol. Chem*. **277**, 14194-14205

116 Ellis, C. D., Lindner, B., Anjam Khan, C. M., Zähringer, U., and Demarco de Hormaeche, R. (2001) *Mol. Microbiol*. **42**, 167-181

117 Thwaite, J. E., Humphrey, S., Fox, M. A., Savage, V. L., Laws, T. R., Ulaeto, D. O., Titball, R.W., and Atkins, H. S. (2009) *J. Med. Microbiol*. **58**, 923-929

118 Fenn, T. D., Stamper, G. F., Morollo, A. A., and Ringe, D. (2003) *Biochemistry* **42**, 5775-5783

119 Soper, T. S., and Manning, J. M. (1982) *J. Biol. Chem*. **257**, 13930-13936

120 Kazachkov, M., Lager, J., LiPuma, J., and Barker, P.M. (2001) *Pediatr. Pulmonol*. **32**, 338-340

121 Weidmann, A., Webb, A. K., Dodd, M. E., and Jones, A. M. (2008) *J. Cyst. Fibros*. **7**, 409-411

122 Grimwood, K., Kidd, T. J., and Tweed, M. (2009) *J. Cyst. Fibros*. **8**, 291-293

123 Bay, D. C., Rommens, K. L., and Turner, R. J. (2008) *Biochim. Biophys. Acta*. **1778**, 1814-1838

Chapter 6: Materials & Methods

6.1 Material and Methods for Chapters 2 and 3

6.1.1 General Materials

6.1.1.1 General Reagents

Solvents and chemicals were of the appropriate quality and were purchased from GE Healthcare, Sigma-aldrich, Promega, New England Biolabs, Pierce, BioRad, Vivascience, Anachem, Invitrogen, VWR International unless otherwise stated.

6.1.1.2 Solutions and Media for Peptide and Protein Expression

Buffers – All buffers were prepared fresh, as required, and were filtered with 0.2μm filter before use. Buffers contents are described in the text where appropriate.

Sterilisation of media – All media were autoclaved at 121 ºC for at least 15 min at 15 psi prior to use.

Agar plates – bacto-agar (15 g/L) was added to the specified media to prepare agar plates.

Luria Bertani (LB) – tryptone (10 g/l), yeast extract (5 g/l), sodium chloride (10 g/l); pH adjusted to 7.5 with sodium hydroxide.

2YT – tryptone (16 g/l), yeast extract (10 g/l), sodium chloride (5 g/l); pH adjusted to 7.5 with sodium hydroxide.

SOC – tryptone (20 g/l), yeast extract (5 g/l), sodium chloride (0.5 g/l), magnesium sulfate (5 g/l), glucose (3.2 g/l); pH adjusted to 7.5 with sodium hydroxide.

Isosensitest agar (ISA) – 31.4 g dissolved in 1L dH_2O (Oxoid Ltd.).

Isosensitest broth (ISB) – 23.4 g dissolved in 1L dH_2O (Oxoid Ltd.).

S-Gal/LB/Amp plates: a pack of S-GalTM/LB Agar blend (Sigma) was dissolved in 500 ml dH2O. After autoclaving, ampicillin was added before pouring the plates.

6.1.1.3 Minimum Media for ^{15}N-HBD2 Expression

Table 6.1 Composition of minimum media M9 used in this study

M9 medium	Final concentration in 3L total volume
Na_2HPO4	16 mM
KH_2PO4	7.4 mM
NaCl	2.8 mM
Fortification	
1 M $MgSO_5$	2 mM
50 mM $CaCl_2$	0.10 mM
50 mg/mL thiamine	0.12 mM
50 mg/mL biotin	0.16 mM
20% glucose	0.3%
2M $(^{15}NH4)_2SO_4$	7.6 mM
^{15}N-ISOGRO™	N/A (0.5 g/l)
1000 x trace metals mixture:	
50 mM $FeCl_3$ in 0.12 M HCl	50 µM
20 mM $CaCl_2$	20 µM
10 mM $MnCl_2$	10 µM
10 mM $ZnSO_4$	10 µM
2 mM $CoCl_2$	2 µM
2 mM $CuSO_4$	2 µM
2 mM $NiCl_2$	2 µM
2mM Na_2MoO_4	2 µM
2mM Na_2SeO_3	2 µM
2mM H_3BO_3	2 µM

6.1.2 Molecular Biology: DNA Manipulation

6.1.2.1 Bacterial Cell Lines

Table 6.2 Bacterial cell lines used in this study.

Strain	Genotype	Description/ Applications
BL21(DE3)	F^- omp Thsds$_b$ (r_B^- m_B^-) gal dcm (DE3)	General purpose expression host.
BL21(DE3)pLysS	F^- omp Thsds$_b$ (r_B^- m_B^-) gal dcm (DE3) pLysS (Cam^R)	Expression host for expression of ^{15}N-HBD2 in *E. coli*.

6.1.2.2 Oligonucleotide Primers for HBD2

The following oligonucleotide primers were used in this study.

Table 6.3. Oligonucleotide sequences used in this study.

Primers	Sequence 5'-3'
P1	CAGATGCTGATGGGTATCGGTGACCCGGTTACCTGCCTGAAATCC
P2	CGGACAGAAAACCGGGTGGCAGATAGCACCGGATTTCAGGCAGGT
P3	CCGGTTTTCTGTCCGCGTCGTTACAAACAGATCGGTACCTGCGGT
P4	GCAGCATTTGGTACCCGGCAGACCGCAGGTACCGAT
P5	ACCAAATGCTGCAAAAAATGACAGATGCTG
P6	CAGCATCTGTCACGGTTTTTTGCAGCATTTGGTACCCGG
M1A For	GCGGCAGCCATGCGCATACCCCAGAACACATC
M1A Rev	GATGTGTTCTGGGGTATGCGCATGGCTGCCGC
M126A For	GAATATTCACGCATGCCAGGCGCTGATGGGTATCGGTGAC
M126A Rev	GTCACCGATACCCATCAGCGCCTGGCATGCGTGAATATTC

6.1.2.3 Cloning of HBD2

Six overlapping primers (Table 6.3) with codons optimized for expression in *E. coli* were designed using the mature HBD2 amino acid sequence (also known as DEFB4, Genbank accession number, NM_004942). The reaction contained in a final volume of 100 µl: 10 µl (100 pmol) of the outermost 5' primers (P1 and P6) of each strand, 10

µl (10 pmol) of the internal primers (P2 – P5), 4 µl DMSO, 10 µl 10 x Herculase reaction buffer (Stratagene), 1 µl Herculase Hotstart DNA polymerase (Stratagene), 4 µl 25 mM dNTPs, 21 µl dH2O and was subjected to 30 PCR cycles of 95 ºC for 2 minutes, 40 ºC for 3 minutes and 72 ºC for 30 seconds. A second amplification was performed to confirm annealing of all six primers in a final volume of 50 µl: 5 µl primer P1 (50 pmol), 5 µl primer P6 (50 pmol), 2 µl template, 38 µl dH2O and 2 puRe Taq Ready-To-Go PCR beads were subjected to 30 PCR cycles of 95 ºC for 2 minutes, 40 ºC for 3 minutes, 72 ºC for 30 seconds and a final extension of 72 ºC for 10 minutes to add A overhangs. The PCR product containing the codon-optimized gene preceded by Met and flanking *Alw*N1 recognition sites was purified, cloned into pGEM-T Easy plasmid and a positive clone sequenced to confirm the fidelity of the insert. The target gene was then cut and ligated into the expression plasmid pET-31b (Novagen) to give pET-31b/HBD2. To incorporate a N-terminal His(6)-tag sequence, both pET-31b/HBD2 and pET-28a(+) vectors were cleaved by restriction enzymes *Nde*I and *Xho*I and the HBD2 fragment now containing the ketosteroid isomerase (KSI)-fused gene was cloned into pET-28a. To avoid CNBr cleavage at unwanted sites within the fusion residues Met 1 and 126 of KSI were replaced with Ala by site-directed mutagenesis to give plasmid pET-28a/HBD2. The fidelity of this clone was confirmed by DNA sequencing.

6.1.2.4 Cloning of HBD1

A codon-optimised, synthetic *HBD1* gene was purchased from CLONTECH and cloned alongside with the HisKSI sequence in the pUC19 vector. The HisKSI-HBD1 fragment was cloned into the pET28a vector using NcoI and XhoI restriction sites. The pET-28a/HBD2 plasmid was used as a template and replaced the HisKSI-HBD2 sequence with KSI-HBD1.

6.1.2.5 Transformation of *E.coli* Competent Cells

Competent cells were transformed according to the manufacturer's instructions. DNA (up to 40 ng) was added to an aliquot of competent cells and gently mixed. This was left on ice for 15 minutes before the cells were heat shocked at 42 °C for 30 secondes. The cells were then grown in 80 or 250 µl SOC medium at 37 °C for 1 hr. Finally, the cells were spread to dryness on selective agar plates and incubated at 37 °C overnight.

6.1.2.6 Storage of Bacterial Stocks

LB or 2YT medium containing the appropriate antibiotics were used for the short term storage of *E. coli*. Colonies of bacteria were stored on inverted agar plates at 4 °C for up to one month. For long term storage strains were frozen (-80 °C) in LB or 2YT media containing 20% glycerol.

6.1.3 Peptide Expression and Purification

6.1.3.1 Polyacrylamide Gel Electrophoresis (PAGE)

SDS-PAGE (15% (v/v) acrylamide) was used to analyse proteins at different step of purification process on the basis of their molecular mass. The technique used was the discontinuous buffer system of Laemmeli. Alternatively, proteins were analysed on precast 12% Bis-Tris Nu-PAGE gels (Invitrogen) according to manufacture's instructions. Gels were visualised using Coomassie blue.

6.1.3.2 Large Scale Expression of HBD2

Both pET-31b/HBD2 and pET-28a/HBD2 vectors were transformed into either BL21(DE3) or BL21(DE3)pLysS competent cells. After overnight growth on plate at 37 °C a single colony was added to 250 ml of 2YT supplemented with 100 µg/ml ampicillin (pET-31b/HBD2) or 30 µg/ml kanamycin (pET-28a/HBD2). This preculture was shaked overnight at 37 °C and 350 rpm. It was then used to inoculate 3 litres of fresh growth medium which was incubated until cells reached an absorbance A_{600} = 0.5 where the medium was supplemented with isopropyl-1-thio-β-D-galactopyranoside (ITPG) to a final concentration of 1 mM. After a further 6 to 7 hours the cells were harvested by centrifugation (5000 rpm for 15 minutes at 4 °C), and the supernatant discarded. The HisKSI-HBD2 expressing pellet (yellowish colour) was collected, weighed (7 to 12 g) and frozen at -20 °C before extraction and purification.

The same method was applied for the expression of HBD1.

6.1.3.3 Large Scale Expression of ^{15}N-HBD2

The *E. coli* strain BL21(DE3) containing the plasmid pET-28a/ HBD2 was grown in 6 x 6 mL of 2X YT medium containing 30 lg/ml kanamycin at 37 °C. Once the OD600

reached 0.6–0.8, cells were centrifuged (3000 rpm for 10 min, 4 °C) and the supernatant was removed. The pellet was washed and re-suspended in M9 minimal medium three times, and the combined suspensions were added to 3 L fortified M9 minimal medium with 30 μg/ml kanamycin. The summary of the components used in the fortified minimal medium is presented in Table 6.1. The 3 L of culture were divided into 6 x 1 L flasks with approximately 500 mL in each and shaken at 30 °C. When the A_{600} reached 0.5, protein expression was induced by 1 mM isopropyl-b-D-1-thiogalactopyranoside (IPTG) and the cells were further incubated for 6 h. Cells were isolated by centrifugation (5500 rpm for 12 min, 4 °C). From 3 L of culture, approximately 7 g of wet weight *E. coli* paste was obtained.

6.1.3.4 Purification and Solubilisation of Inclusion Bodies

All centrifugation steps were carried out for 20 minutes at 11000 rpm and 4 ºC. The cell pellet containing highly expressed HisKSI-HBD2 was suspended in 5 mL/g in re-suspension buffer (50 mM Tris, 25% sucrose, 1 mM EDTA, 0.1% sodium azide, 10 mM DTT, pH 8.0), before addition of 50 mg/mL lysozyme, 500 mM $MgCl_2$ and 10μl DNase. After incubation for 30 minutes at room temperature, lysis buffer (50 mM Tris, 1% Triton X-100, 100 mM NaCl, 0.1% sodium azide, 10 mM DTT, pH 8.0) was added (5 mL/g wet weight original pellet) and incubated for 45 minutes at room temperature. To this cloudy suspension, EDTA (500 mM) was added to give a final concentration of 1 mM, and the sample was snap-frozen in liquid N2 before immediately thawing for 30 minutes in a 37 ºC water bath. To this thawed extract, MgCl2 (500 mM) was added to give a 1 mM final concentration and the sample was incubated at room temperature for 1 h to allow the viscosity to decrease before centrifugation. The supernatant was discarded and the pellet from this step was re-suspended in an appropriate volume of buffer (50 mMTris, 1% Triton X-100, 100 mM NaCl, 1 mM EDTA, 0.1% NaAzide, 1 mM DTT, pH 8.0), sonicated for 4 x 30 second blasts and centrifuged. The resulting pellet was then washed in 1 M Guanidine HCl buffer (1 M GuHCl, 50 mM Tris, 1% Triton X-100, 100 mM NaCl, 1 mM EDTA, 0.1% sodium azide, 1 mM DTT, pH 8.0), sonicated with 4 x 30 second bursts and centrifuged. The resulting pellet (inclusion bodies containing highly enriched KSI-HBD2) was re-suspended in ~ 50ml 6 M GuHCl binding buffer (6 M GuHCl, 50 mM Tris, 10 mM imidazole, 500 mM NaCl, 5 mM β-mercaptoethanol, pH 8.0).

Concerning the preparation with the pET-31b plasmid (KSI-HBD2), after resuspension with 6 M GuHCl (no imidazole), the solution was directly supplemented with CNBr (see next chapter). For HisKSI-(^{15}N-)HBD2 sample, the re-suspended solution was added to 10 ml pre-equilibrated nickel-nitrilotriacetic acid (Ni-NTA, Qiagen) agarose affinity resin, mixed by rotation for 1 h at 4 °C, then decanted into an empty 25 ml column reservoir. The packed resin was washed with 6 M GuHCl binding buffer (50 ml) and then eluted with 25 ml of elution buffer (6 M GuHCl, 50 mM Tris, 120 mM imidazole, 500 mM NaCl, 5 mM -mercaptoethanol, pH 8.0). This elution step with 120 mM imidazole was then repeated to give 50 ml of purified HisKSI-HBD2. The eluted fusion protein was dialyzed (Snakeskin dialysis tubing 3 kDa cut-off from Pierce) against 25 mM Tris buffer, pH 8.0 overnight at 4 ºC which caused precipitation of the fusion protein.

The same protocol was applied for HBD1 purification.

6.1.3.5 CNBr Cleavage of the Fusion Tag

The fusion was recovered by centrifugation and the pellet was re-suspended in 6 M GuHCl, 25 mM Tris buffer, pH 8.0. To this HCl (5 M stock) was added until the pH was ~1.0. Solid CNBr was added to give a final concentration of 250 mM and cleavage was allowed to proceed for 24 h in the absence of light and under nitrogen. The cleaved mixture was evaporated at 42 ^{o}C using a rotary evaporator to remove any unreacted CNBr, and the concentrated sample was dialyzed against 25 mM Tris buffer, pH 8.0 overnight at 4 ^{o}C to cause precipitation of the KSI. The precipitate was removed by centrifugation and the supernatant containing the peptide was filtered (0.45 μM) and purified by FPLC or RP-HPLC.

6.1.3.6 Purification of HBD2 by FPLC

FPLC was performed on an Amersham Biosciences AKTA purifier 900. Samples were run onto a strong cationic Mono S 5/50 GL column (Amersham biosciences). A linear gradient was applied from 100 % 25 mM Tris buffer, pH 8.0 to 100 % 25 mM Tris, 1 M NaCl buffer, pH 8.0 at a flow rate of 0.5 ml/min.

6.1.3.7 Purification of Defensins by Semi-Preparative RP-HPLC

Semi-preparative RP-HPLC on a Jupiter™ Proteo column was performed with a Waters 600 control pump fitted with a photodiode array 996 detector using Millenium

32 software. The HBD2 isolated from the CNBr cleavage step was applied to the column in 3-4 ml batches, the column was washed with 5% acetonitrile (ACN) then a linear gradient of 5-55% acetonitrile over 50 minutes at a flow rate of 3 mL/minute was used to elute the HBD2. Fractions were analysed by SDS-PAGE and those containing HBD2 were pooled and analysed by ESI-mass spectrometry as described in section 6.1.4.4.

6.1.3.8 Oxidation of Recombinant HBD2

The HBD2 recovered by semi-prep-HPLC was freeze-dried then reconstituted in 25 mM Tris, pH 8.0, with 20 mM tris(2-carboxyethyl)phosphine (TCEP) added to convert the peptide to the fully reduced form before re-purification by prep-HPLC using identical conditions as above. Fractions containing HBD2 were freeze-dried then dissolved in 50 mM Tris, pH 8.0, 3 mM cysteine, 0.3 mM cystine and stirred for 4 h at room temperature. The reaction was followed by analytical RP-HPLC and analysed by ESI-mass spectrometry to confirm that the HBD2 was present in the oxidized form (elution at 40 mins). The final yield of oxidized β-HBD2 is 3-6 mg from 3 litres of *E. coli* culture (based on 10 preparations).

6.1.4 Peptide Characterisation

6.1.4.1 BCA Assay

The concentration of defensins was calculated using a BCA™ protein Kit Assay (Pierce) according to the manufacturers instructions. Breiefly, this assay is a detergent-compatible formulation based on bicinchoninic acid (BCA) for the colorimetric detection and quantification of total protein. A standard curve was assayed with different concentrations of bovine serum albumin (BSA) and the sample was referenced from this standard curve. The concentration of BSA and sample was read at 562 nm.

6.1.4.2 Iodoacetamide Modification of HBD2

Iodoacetamide assay is used to assess the ability for modification of free thiols in proteins and peptides. Iodoacetamide is a sulfhydryl alkylating reagent with a prosthetic group that irreversibly and covalently modifies cysteine residues.

The assay was performed as follows: Iodoacetamide (4ul, 1 M made up in 1 M NaOH) was added to 200 µl of peptide sample (0.5 mg/ml) and incubated for 30 minutes in the dark at room temperature. Excess of iodoacetamide was removed by PD10 column chromatography (GE Healthcare) with Tris 25 mM buffer, pH 8. the sample was further analysed by LC-ESI-MS.

The iodoacetamide modified peptide yields a 57 Da mass increased on LC-ESI-MS.

6.1.4.3 Protease Digestion and Peptide Mass Mapping of Defensins

Chemotrypsin and trypsin (0.5 mg/ml each) were used for the enzymatic digestion of 50 µl of HBD2 (1 mg/ml). The reaction was performed overnight at 37 ^{o}C in 50 mM Tris buffer containing 0.005% Triton X-100 and 20 mM NaCl, pH 8.3. TFA 0.05 % was then added to terminate the reaction and the cleaved product injected onto a Phenomenex Jupiter 4µ Proteo 90A column (250 x 2.00 mm) coupled with an ESI-MS spectrometer. The gradient used was 10 to 35 % ACN at a flow rate of 0.2 ml/min.

The two-disulfide bridged peptide fragment was extracted, freeze-dried and subjected to one-step manual Edman degradation. The peptide was re-suspended in 200 µl water/pyridine (1:1) and 10 µl of PITC was supplemented. The solution was incubated 30 min at 50 °C to remove the solvent and 100 µl of TFA was then added to cleave the N-terminal residue(s). The cleavage reaction proceeded at 50 °C for 15 min, followed by removal of TFA under vacuum and re-suspension in 100 µl water. Pentane/ethyl acetate (4:1) was used to wash (extract) the reaction mixture, and the aqueous phase was analyzed by LC-ESI-MS. The Edman degradation protocol was based on previous study from ref. [102].

6.1.4.4 Liquid Chromatography-Electrospray Ionisation Mass Spectrometry (LC-ESI-MS).

LC-MS was performed on a MicroMass Platform II quadrupole mass spectrometer equipped with an electrospray ion source with a cone voltage ramped from 40 to 70 V. The source temperature was set at 140 °C and peptide samples were separated with a Phenomenex Jupiter C18 reverse phase column (5 µm, 250 x 4.6 mm). Typically, separation was achieved using a 20-50% acetonitrile (containing 0.01% TFA)

gradient at a flow rate of 1 ml/min over 60 min. The total ion count in the range 600-2000 m/z was scanned at 0.1 s interval. The scans were accumulated, spectra combined and the molecular mass determined by the MaxEnt and Transform algorithms of the Mass Lynx software (Micromass, U. K.).

6.1.4.5 Fourier Transform-Ion Cyclotron Resonance (FT-ICR)

Characterisation of the recombinant ^{15}N HBD2 peptide was performed using the accurate mass capabilities of a 9.4 T Apex III Fourier transform ion cyclotron resonance (FT-ICR) mass spectrometer (Bruker Daltonics, Billerica, MA). Nano-ESI was performed using a TriVersa Nanomate running in infusion mode and operated in the positive mode. Prior to analysis, peptides were reconstituted to a final concentration of 5 μM in 50:49:1 MeOH: water: formic acid. The isotopic abundance was predicted using published methods within the XMASS and DataAnalysis software (Bruker).

6.1.4.6 NMR Spectroscopy

One mg of oxidized HBD2 was dissolved in 20 mM sodium acetate buffer, pH 4.0 at 25 ^{o}C and 10% D_2O (v:v) was added to give to a final peptide concentration of 0.46 mM.

The 1D ^{1}H NMR Spectrum of HBD2 was recorded on a Bruker AVANCE spectrometer equipped with a cryoprobe operating at 600 MHz and 25 °C. 128 scans were taken with a sweep width of 15 ppm and 8000 complex points. For water suppression double-pulsed gradient spin echo was used. The same protocol was used for HBD1.

^{15}N labelled HBD2 (0.5 mg) was dissolved in 0.45 mL 20 mM sodium acetate buffer and 0.05 mL D_2O to a final concentration of 0.23 mM and final pH of 4.7. All NMR spectra were recorded on a 600 MHz Bruker AVANCE instrument equipped with a cryoprobe and operating at 25 ^{o}C. For 1D spectra, 128 scans were taken with a spectral width of 15 ppm and 8000 complex points. Double pulsed field gradient spin echo was used for water suppression. For the ^{1}H–^{15}N HSQC experiment, 8 scans were taken for each increment, using acquisition times of 125 ms to sample both F1 and F2 dimensions. For both the 3D HSQC-TOCSY and 3D HSQC-NOESY, spectral widths of 11, 17 and 17 ppm were used in ^{1}H (indirect), ^{15}N and ^{1}H (direct) dimensions, respectively. WATERGATE suppression was used for both experiments. For both

spectra, 192 and 2048 complex points were acquired in F1 and F3, respectively. In F2, 48 and 40 complex points were collected for the TOCSY and NOESY experiments, respectively. The relaxation delay was set to 1.3 s for both and the mixing time was 70 ms for the TOCSY and 150 ms for the NOESY.

6.1.4.7 Antimicrobial Activity Assay

The purified, oxidized HBD2 was dissolved into 0.01% acetic acid and centrifuged (13000 rpm for 10 minutes, 25 °C) to remove precipitate. The HBD2 was concentrated (Vivaspin 0.5 ml concentrator, 3000 MWCO PES) to 1 mg/ml and stock HBD2 solutions of concentrations 15, 30, 60, 125, 250 and 500 µg/ml were prepared. Antimicrobial assays were carried out according to the method set out in our previous study [36]. Briefly, a laboratory strain of *E. coli* K-12 MG1655 was grown to midlogarithmic phase (OD at 600 nm = 1.0). From this 90 µl of *E. coli* (~1.0 x 10^5 cells) culture was incubated with 10 µl of each stock of HBD2 solution and as a negative control 90 µl *E. coli* was incubated with 10 µl of sterilised water containing 0.01% acetic acid. These samples were incubated at 37 °C for 2 hours. Then 10-fold serial dilutions of the incubation mixture were plated on Iso-Sensitest plates, incubated at 37 °C, and the CFU was determined the following day. Colonies were counted and the LD50, LD90 (Lethal Dose: amount of peptide required to kill 50% and 90% of viable cells) and the $MBC_{99.99}$ (Minimum Bactericidal Concentration at 99.99%) values were calculated from the resulting killing curve. The same antimicrobial assays were performed with *Pseudomonas aeruginosa* (PAO1), a Gram-positive strain *Staphylococcus aureus* (ATCC 25923) and a fungus, *Candida albicans* (J2922). In parallel, the same strains were used with the antimicrobial agent Polymyxin B (PMB) as a control. All the killing assays were performed at least 3 times for each strain and the values were obtained by taking the mean of at least 3 experiments.

6.1.5 Surface Plasmon Resonance (SPR)

6.1.5.1 Preparation of SPR Samples

All lipids were purchased from Avanti Polar Lipids. Lipids vesicle were prepared as follows; typically, appropriate amount of lipids (in powder form) were re-suspended in 100% chloroform with the exception of POPE/Kdo2 lipid A mixture which was re-

suspended in chloroform and methanol (8:2, v/v). Chloroform and/or methanol were evaporated under a gentle stream of nitrogen gas for 2 hours and then placed under vacuum pump overnight to remove any trace amounts of solvent. Dried lipids were re-suspended in 10 mM HEPES buffer containing 50 mM NaCl and 1 mM EDTA, pH 7.5. The solution was vortexed for 1 min and the lipid suspension was extruded with an Avanti mini-extruder through a 100 nm polycarbonate membrane according to the manufacturer's instructions.

HBD2 peptide was re-suspended in filtered water and aliquots of 1.25, 2.5, 5 and 10 μM were prepared.

6.1.5.2 SPR Experiments

SPR was performed on a BiaCore T100 instrument with a L1 sensor chip (BiaCore). The "desorb and sanitize" protocol was used to clean the system with a maintenance chip and then allowed to run overnight with water. The L1 chip was docked in the system and first washed with an injection of 5 μl of 20 mM nonionic detergent (Octyl β-D-glucopyranoside) at a flow rate of 5 μl/min in order to clean the chip surface. The extruded lipid solutions were then applied to all three flow cells on the chip surface simultaneously with injections of 80 μl at a low flow rate of 2 μl/min. In order to remove any mutilamellar structures from the lipid surface and to stabilize the baseline, 30 μl of 10 mM NaOH was injected at 50 μl/min. The peptide solution (100 μl) was then injected onto the model membrane surface at a flow rate of 30 μl/min, having a total injection time of 200 seconds. On completion of injection, buffer flow continued to allow a dissociation time of 600 s. All binding experiments were carried out at 30 °C. All solutions were freshly prepared, degassed, and filtered through a 0.2 μm filter. Each sample was run in duplicate.

6.1.6 Solid Phase Peptide Synthesis of HBD1

The chemical synthesis of HBD1 was carried out on an Applied Biosystems model 433A peptide synthesizer using a pre-loaded Fmoc-Lys(Boc) NovaSyn®TGT resin. Fmoc amino acids were purchased from Novabiochem. LC-Mass spectra confirming the identity and purity were obtained on a Micromass Quattro LC mass spectrometer. Semi-preparative HPLC was performed using a Phenomenex Luna C18 column and a gradient of 5-95% acetonitrile (containing 0.1% TFA) over 45 minutes

(flow rate of 3 ml/min). All other chemical reagents were obtained from Aldrich. Automated solid-phase peptide synthesis was carried out on a 0.05 mmol scale using 0.5 mmol of each Fmoc amino acid per coupling reaction and HBTU/HOBt as coupling reagents. The coupling time was 30 minutes. Peptide products were cleaved from the resin by exposure to 95 % TFA, 2.5% ethanedithiol, 2.5% water for 3 h. After this time, the resin was filtered-off, washed with TFA, and the filtrate was poured into diethylether (10 volumes). The precipitated peptide was then collected by centrifugation (3000 rpm, 15 minutes). The precipitate was re-suspended in ether (5 volumes) and collected by centrifugation once again (3000 rpm, 15 minutes). The crude peptide was dissolved in water and loaded directly onto a semi-preparative HPLC column. Fractions containing the peptide products were identified by mass spectrometry and lyophilised to obtain the purified products as fluffy white powder.

6.2 Material and Methods for Chapter 5

6.2.1 General Materials (see section 6.1.1)

6.2.2 Molecular Biology: DNA Manipulation

6.2.2.1 Bacterial Cell Lines

Table 6.4. Bacterial cell lines used in this study.

Strain	Genotype	Description/Applications [ref.]
Top 10™	F'mcrA D(mrr-hsdRMS-mcrBC) Φ80lacZΔM15 ΔlacX74 deoR recA1 araD139 Δ(ara-leu)7697 gal/U gal/K rpsL endA1 nupG	Used For transforming DNA ligations.
DH5α	F- φ80*lac*ZΔM15 Δ(*lac*ZYA-*arg*F) U169 *rec*A1 *end*A1 *hsd*R17 (rk-, mk+) *gal- pho*A *sup*E44 λ- *thi*-1 *gyr*A96 *rel*A1	Used for plasmid DNA expression
BL21(DE3)	F^- omp Thsds$_b$ (r_B^- m_B^-) gal dcm (DE3)	General purpose expression host.
BL21(DE3)pLysS	F^- omp Thsds$_b$ (r_B^- m_B^-) gal dcm (DE3) pLysS (Cam^R)	Expression host for expression of ^{15}N-HBD2 in *E. coli*.
MST100	W3110, Δ*lacU169 gal490* λ*cl857* Δ(*cro-bioA*) *pmrA*^{c}	[98]
AY100	MST100, Δ*pmrL*::*kan*, Kan^r	Complementation assays [98]
AY101	MST100, Δ*pmrM*::*kan*, Kan^r	Complementation assays [98]
AY102	MST100, Δ*pmrLM*::*kan*, Kan^r	Complementation assays [98]
AY103	MST100, Δ*arnT*::*kan*, Kan^r	[98]

6.2.2.2 Plasmids

Table 6.5. Plasmids used for cloning and expression in this study

Plasmid	Characteristics	Source/reference
pGEM-T-Easy	Cloning vector (Amp^R)	Promega
pET22b	Expression vector (Amp^R)	Novagen
pET28a	Expression vector (Kan^R)	Novagen
pET29a	Expression vector (Kan^R)	Novagen
pTrc99a/FbpA	Complementation vector, low copy number. Ap^r P_{trc} *rrnB* T_1T_2 *ori* (pBR322) *lacI*^{q}	P. Bilton

6.2.2.3 Oligonucleotide Primers

The following oligonucleotide primers were used in this study. Restriction sites are highlighted in bold character.

Table 6.6. Oligonucleotide sequences used in this study. Mutant codons and restriction sites are shown in bold.

Primers	Sequence 5'- 3'
arnB For (NdeI)	CGCCATTACAGGCCAAACGCG**CATATG**AGC
arnB Rev (HindIII)	CAAGGTGACTCATGTACGC**AAGCTT**TCCGTATTG
arnG For (NcoI)	**CCATGG**ACCCCGTTTCGTTCGTCTGCATCGT
arnG Rev (XhoI)	**CTCGAG**GCTGCGCGCGAGCACGAGCACA
arnG For (NdeI)	TGATCGTCGAGAAACCGCAATCGTAAGGACGCCTCC **CATATG**
arnG Rev (XhoI*stop*)	**CTCGAG***TCA*GCTGCGCGCGAGCACGAGCACACCGAT
arnG Rev (HindIII*stop*)	CG**AAGCTT***TCA*GCTGCGCGCGGAGCACGAGCACA

6.2.2.4 Gene Amplification

The PCR was carried out using two puReTaq Ready-To-Go beads (GE Healthcare), 5µl of each primer, 3 µl J2315 chromosomal DNA and 37 µl H_2O. Samples were amplified for 25 cycles at 95 °C 1 min., 65 °C 1 min., 72 °C 2 min., with the initial

cycle of 95 °C 2 min. and final cycle 72 °C 10 min. (using a Perkin Elmer DNA thermal cycler).

6.2.2.5 Gel Electrophoresis of DNA

To make a 1% agarose gel, 1 g Agarose (Fisher Scientific) was added to 100 ml TAE buffer (Tris-Acetic acid-EDTA; 1X TAE buffer (50X stock diluted in H_2O) containing 40 mM Tris-HCl, 20mM Acetic acid, 1M EDTA, adjusted to pH 8.3) and boiled by heating in a microwave until totally dissolved. The solution was then cooled before the addition of ethidium bromide (10 µl). The gel was poured into a casting mould and allowed to set at room temperature.

Added into the first well was 7.5 µl molecular DNA marker hypperladder I (Promega), 2.5 µl DNA 5 X loading buffer (Bioline) was added to 10 µl PCR products, which was added to the adjacent well. The gel was run at 100V until markers showed sufficient separation.

DNA purification from the agarose gel was carried out following a QIAprep® Gel Extraction kit from Qiagen according to the manufacturer's instructions.

6.2.2.6 Cloning

The purified DNA PCR product (3 µl) was then ligated with 1 µl pGEM T-Easy plasmid in 5 µl of 2X ligation buffer and 1 µl T4 DNA ligase. It was left overnight at 4 °C.

The ligated product (2 µl) was used to transformed suitable competent cells. SOC buffer (80 µl) was inoculated with transformed cells and the broth was shaked at 37 ^{o}C for one hour at 250 rpm and then spread on an S-Gal/Amp plate and left at 37 °C overnight.

White colonies were picked from plate and inoculated with 5 ml LB broth, 5 µl ampicillin and grown overnight at 37 °C at 250 rpm.

The cells were spin down by centrifugation (using accuSpin™ Micro centrifuge). The plasmid DNA from the overnight culture was purified using QIAprep® Spin Mini-Prep kit from Qiagen according to the manufacturer's instructions.

6.2.2.7 Digestion of DNA with Restriction Endonucleases

The required amount of DNA (0.5-1 µg) was incubated with the appropriate amount of endonuclease and with the relevant buffer for at least 2 hours at 37 °C. The sample was then subjected to electrophoresis on agarose. The gels were viewed and photographed under UV-light.

6.2.2.8 Cloning into Plasmid Vectors

The DNA fragment cut with suitable restriction enzymes (13 µl), the host vector cut with suitable restriction enzymes (4 µl), 10x T4 DNA ligase buffer (2 µl), and T4 DNA ligase (2 µl) were gently mixed and incubated overnight at room temperature. 2 µl of the reaction mixture was used to transform suitable competent cells.

6.2.2.9 DNA Sequencing

The different cloned plasmids were sequenced according to a PCR-based method using BigDye®Terminator v3.1 (Apllied Biosystems). Each sequencing reaction typically contained: 5 µl plasmid DNA, 1 µl forward or reverse primer, 2 µl BigDye and 2 µl of 5X sequencing buffer. The reaction was performed on an Eppendorf Mastercycler Personal hot-lid DNA thermal cycler and cycled 30 times at 94 °C for 30 sec, 45 °C for 15 sec and 60 °C for 4 min. The reaction was submitted to the Institute for Cell and Molecular Biology service (ICMB) at University of Edinburgh for sequencing. Sequence data was analysed using Contig Express within the Vector NTI Advance™ V9 software package (Invitrogen).

6.2.3 Cells Competency

Two methods were used to make AY100, AY101 and AY102 strains competent. All buffers and disposable plasticwares were previously cooled down on ice.

6.2.3.1 Chemical Competent Cells

Freshly prepared LB broth (100 ml) was supplemented with the appropriate antibiotic and inoculated with 1 ml of overnight pre-culture. Cells were grown at 37 ^{o}C until OD_{600} reached 0.6 and then cooled down on ice for 30 minutes. They were then transferred to 50 ml falcon tubes and centrifuged at 6000 x g for 10 minutes at 4 ^{o}C.

Cell pellet was re-suspended in ice cold 10 mM Tris with 50 mM NaCl (pH 8.0) and pelleted again. The pellet was re-suspended in 50 ml (half of the original LB broth volume) 30 mM $CaCl_2$ and placed on ice for 20 minutes. Cells were centrifuged and gently re-suspended in $1/20^{th}$ of the original volume of 30 mM $CaCl_2$. Finally, aliquots of 200 µl were immediately flash frozen in liquid nitrogen and store at -80 ^oC until further use.

6.2.3.2 Electro-Competent Cells

Freshly prepared 2YT broth (200 ml) was supplemented with the appropriate antibiotic and inoculated with 2 ml of overnight pre-culture. Cells were grown at 37 ^oC until OD_{600} reached 0.6 and then cooled down on ice for 30 minutes. They were then transferred to 50 ml falcon tubes and centrifuged at 6000 x g for 10 minutes at 4 ^oC. The pellet was washed 3 times with ice cold sterile dH_2O and transferred to a 15 ml falcon tube. Cells were further washed with sterile dH2O containing 10 % glycerol (v/v) and centrifuged (6000 x g for 10 minutes at 4 ^oC). Finally, cells were gently re-suspended in 5 ml of sterile dH_2O with 10 % glycerol (v/v). Aliquots of 200 µl were immediately snap frozen and store at -80 ^oC until further use.

6.2.3.3 Electroporation

Two to three µl of plasmid DNA was placed in a 0.2 cm cuvette (Sigma-aldrich) and 100 to 200 µl of appropriate competent cells were added. The cuvette was then placed in the electroporator (EasyjecT plus, EQUIBIO, Flowgen) and cells subjected to electroporation (2500 V, 25 µF, 99 Ω). SOC (500 µl) was added immediately and the mixture was shaked for 1 hour at 30 ^oC. The culture was then spread onto LB agar plate containing the appropriate antibiotics and incubated overnight at 30 ^oC.

6.2.4 Peptide Expression and Purification

6.2.4.1 Polyacrylamide Gel Electrophoresis (PAGE)

SDS-PAGE (15% (v/v) acrylamide) was used to analyse proteins at different step of purification process on the basis of their molecular mass. The technique used was the discontinuous buffer system of Laemmeli. Alternatively, proteins were analysed on precast 16% Tris-Glycine Precast gels (Invitrogen) according to manufacture's instructions.

6.2.4.2 Large Scale Expression of ArnB

Two µl of pET22bArnB plasmid was transformed into *E. coli* BL21(DE3) competent cells and left on ice for 30 minutes. The mix was heat shocked at 42 °C for 30 seconds and then put back on ice for 2 min. SOC media (80µl) was added to the cells and shaked for 1 hour at 37 °C at 250 rpm. The cells were then spread on an ampicillin plate and left overnight at 37 °C. A colony was picked, added to 200 ml LB broth and grown overnight at 37 °C.

The overnight pre-culture was added to 3L LB broth with a starting OD of 0.1. Cells were grown at 37 °C until an optical density (OD_{600}) of 0.6-0.7 was achieved. The cells were induced with 0.5 mM IPTG for 5 hours and then spun down by centrifugation at 7000 rpm for 10 minutes at 4 ºC resulting in 10 g of cell pellet.

6.2.4.3 Purification of ArnB

Cell pellet was resuspended in 50 ml binding buffer (20 mM Kphos, 150 mM NaCl, 25 µM PLP, 15 mM imidazole, pH 8.0) as approximately 4 ml of binding buffer per gram of pellet is required. A Protease Inhibitor Tablet (Roche diagnostic, GmbH complete EDTA free) was added and left to dissolve. After 30 minutes on ice, cells were sonicated (Soniprep 150) for 15 minutes with 30 seconds on and off. The split cell was centrifuged at 14 krpm for 1 hour (DuPont Instruments). The cell free extract (CFE) was then filtered with a 0.45 µm filter.

Nickel Sepharose resin (Amersham Biosciences) was prepared by resuspending the resin in the stored solution. The slurry (4 ml) was centrifuged for 5 minutes at 3000 rpm and the supernatant discarded. The resin was washed with 10 ml water and centrifuged for 5 minutes at 3000 rpm with the supernatant being removed. This step was repeated once and the beads were resuspended in 20 ml of binding buffer (20 mM Kphos, 150 mM NaCl, 25 µM PLP, 15 mM imidazole, pH 8.0), centrifuged for 5 minutes at 3000 rpm and supernatant removed.

The cell free extract was then added to the Nickel Sepharose beads, loaded into the column (Qiagen Polypropylene Column) and washed with 20 ml of binding buffer at 1 ml/min using a peristaltic pump (Minipuls3, Gilson). Three eluting buffers were used to isolate the protein, 20 ml of eluting buffer 1 (20 mM Kphos, 150 mM NaCl, 25 µM PLP, 50 mM imidazole, pH 8.0) was added to the column. Then 20 ml eluting buffer 2 (20 mM Kphos, 150 mM NaCl, 25 µM PLP, 100 mM imidazole, pH

8.0) was added to elute the protein. Finally the column was flushed with 40 ml of eluting buffer 3 (20 mM Kphos, 150 mM NaCl, 25 μM PLP, 500 mM imidazole, pH 8.0).

Fractions from the 3 eluting buffers and the binding buffer were collected but only fractions from eluting buffer 2 and 3 were dialysed overnight (using BioDesign Dialysis Tubing, 8k MWCO) against 20 mM of dialysis buffer (20 mM KPhos, 150 mM NaCl, 25 μM PLP, 0.1 mM EDTA, pH 7.5).

6.2.4.4 Size Exclusion Chromatography (SEC)

Protein fractions eluted from buffer 2 and 3 were concentrated to 4ml by centrifuging at 3 krpm for 20 minutes (Denley BR401 centrifuge) in a 10000 MWCO filter tube (Vivascience, vivaspin). The Sephacryl S200 Hiprep 26/60 column (GE healthcare) was used to obtain a higher level of purification of ArnB. The column was equilibrated with 1 L 20 mM Phosphate buffer (20 mM KPhos, 150 mM NaCl, 25 μM PLP, 0.1 mM EDTA, pH 7.5) and the 5ml protein sample was then injected via a superloop. The column was run at a 1 ml/min flow rate with an isocratic gradient using the same buffer for equilibration and 10 ml fractions were collected.

6.2.4.5 Sephacryl S-200 Column Calibration

A calibration was performed with low and high molecular weight calibration kits (GE Healthcare) according to the manufacturer's guide lines. The column was pre-equilibrated with 20 mM Tris buffer containing 150 mM NaCl, pH 7.5 and then run with Blue Dextran 2000 (1 mg/ml). Its elution volume was referred as the void volume, V_0. Mixture of low and high molecular weight standards (5 mg/ml each) were successively run and the elution volumes noted V_e. The gel phase distribution coefficient (K_{av}) of the protein was calculated as $(V_e - V_0)/(V_t - V_0)$, where Vt is the total volume of the column (320 ml). K_{av} was plotted against log(Mw) of each sample injected (Fig. 6.1) and a linear equation was fitted by Sigmaplot software (Systat Software Inc., figure 6.1 inset).

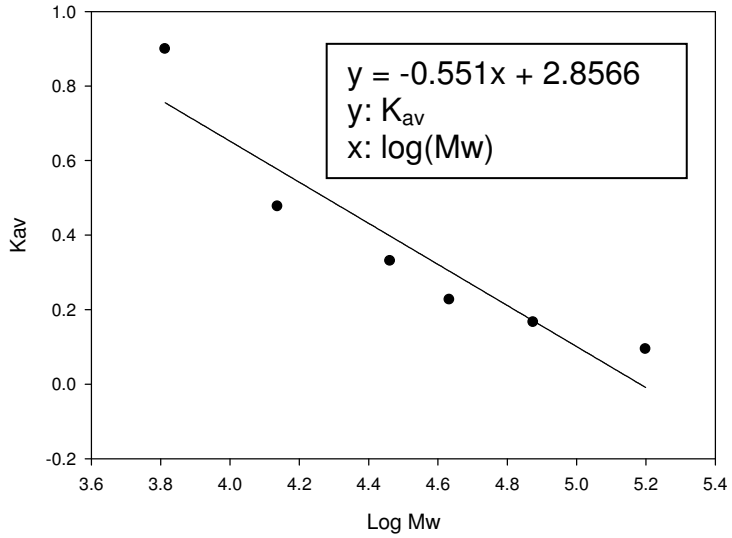

Figure 6.1 Calibration curve of Sephacryl S200 Hiprep 26/60 column.

6.2.4.6 Small Scale Expression of ArnG

ArnG expression was performed with, pET28a-ArnG-N_{His}, pET28a-ArnG-C_{His} and pET29a-ArnG vectors. Dna plasmid was transformed in BL21(DE3)PlysS competent cells. A single colony was added to 20 ml LB media supplemented with kanamycin (30 µg/ ml) and grown overnight at 30 °C and 250 rpm. The overnight pre-culture was added to 20 ml LB broth with a starting OD of 0.1. Cells were grown at 30 °C until an optical density (OD_{600}) of 0.6-0.7 was achieved and induced with 0.5 mM or 1 mM of IPTG for 6 hours. One ml of each sample (induced and non induced) was pelleted and re-suspended in 1 ml of SDS buffer (1.5 M Tris, 2 ml 100% (v/v) glycerol, 2 ml 0.05% (w/v) bromophenol Blue, pH 8.0) and agitated overnight at 4 °C. Cell extracts containing ArnG were run on gel and detected by western blot (see 6.2.4.8).

6.2.4.7 Purification of ArnG

ArnG expressing pellet was re-suspended in 25 mM HEPES buffer containing 500 mM NaCl, 0.1 mM EDTA, 20 % glycerol (v/v), 1 % sodium dodecyl sulphate (SDS) and 20 mM imidazole, pH 8.0. The re-suspended pellet was stirred at 120 rpm at 4 ^{o}C for 2 hours and then centrifuged at 13000 rpm at 4 ^{o}C for 1 hour and the supernatant kept.

Nickel-NTA resin (Qiagen) was prepared as mentioned in section 6.2.4.3. The resin was re-suspended in 5 ml of binding buffer (20 mM HEPES, 500 mM NaCl, 20 mM imidazole, and 0.1 % of SDS, pH 8.0), centrifuged for 5 minutes at 3000 rpm and

the supernatant removed. Cell extract containing the protein was then incubated with the prepared resin for 2 hours at 4 ^{o}C in a shaker at 120 rpm. The preparation was then loaded onto the column (Qiagen Polypropylene Column) and a peristaltic pump was then used to elute the protein.

Three eluting buffers were used to isolate the protein; 20 ml of eluting buffer 1 (25 mM HEPES, 500 mM NaCl, 20 mM imidazole, 0.1% n-Dodecyl-β-maltoside (DDM), pH 8.0) was added to the column. Then 20 ml eluting buffer 2 (25 mM HEPES, 500 mM NaCl, 100 mM imidazole, 0.1% DDM, pH 8.0) was added to elute the protein. Finally the column was flushed with 40 ml of eluting buffer 3 (25 mM HEPES, 500 mM NaCl, 250 mM imidazole, 0.1% DDM, pH 8.0).

Western blot technique was used to determine fractions containing ArnG.

6.2.4.8 Western Blot

After SDS-PAGE, the gel was disposed with a piece of nitrocellulose membrane (Hybond^{TM}-ECL^{TM}, Amersham) of similar size in a transfer buffer for 10 mins at room temperature and under agitation. Six pieces of filter paper (Whatman) of slighty longer size than the gel were soaked in the transfer buffer and placed back to back (3 each) with the gel and the membrane in the Trans-Blot$^{®}$Semi-Dry Transfer Cell (Bio-Rad). The membrane was blotted at 15 V and 120 mA for 45 minutes. The membrane was then placed in blocking solution (25 ml 1 x PBS, 0.01% (v/v) tween, 5% (w/v) dried skimmed milk) overnight at 4 ^{o}C under agitation.

The membrane was placed in washing solution (PBS, 0.01% tween) and washed 3 x 5 mins followed by 3 x 10 mins under agitation. Then, an anti-His antibody solution (25 ml PBS, 0.01% (v/v) tween, 5% (w/v) dried skimmed milk, 2.5 µl anti-His antibody (GE Healthcare) was added and left for 1 hour at room temperature under agitation. The wash step was repeated and the membrane was then placed in an anti-IgG antibody solution (25 ml PBS, 0.01% (v/v) tween, 5% (w/v) dried skimmed milk, 2.5 µl anti-mouse IgG-Hrp-linked antibody (Cell Signalling Technology)). After a last wash step, the membrane was dried and soaked in an ECL Plus Western Blotting solution (GE Healthcare) for 2 minutes. The membrane was then covered by a cling film before being developed on a KODAK BioMax Xar film in a Hypercassette^{TM} (Amersham) for 30 s to 15 minutes.

6.2.5 Protein Assays

6.2.5.1 Spectroscopic Measurements

All UV-visible spectra were recorded on a Varian's Cary 50 UV-Vis spectrophotometer and analysed using Cary WinUV software (Varian). All assays were carried out at 30 °C. All chemicals were purchased from Sigma-Aldrich with the exception of ibotenic acid (Ascent scientific).

Before every spectroscopic experiment, the enzyme was reconstituted with PLP by dialysing it overnight at 4 °C against 20 mM potassium phosphate (pH 7.5) containing 150 mM NaCl and 25 μM PLP. Unbound PLP was then discarded by passing the reconstituted protein through a PD-10 desalting column (Sephadex G-25M, GE Healthcare). The final concentration of recombinant ArnB-PLP was 10 μM. Typically assays contained 10 μM ArnB (Calculated with the BCA assay – see section 6.1.4.1) in 20 mM potassium phosphate (pH 7.5) and were carried out in a 500 μL quartz cuvette (1 cm path length).

6.2.5.2 ArnB Aminotransfer and Inhibition Assays

Varying amounts of amino acids were used to assay the protein (0-1 mM). With the exception of L-glutamate (0-100 μM), all the amino acids tested were added in large excess (1 mM) compared to ArnB-PLP. After addition of the substrate, the reactants were mixed and the reaction monitored immediately. For L-glutamate spectra, small baseline changes were corrected using Sigma Plot software. For L-methionine and L-cysteine assays, the ratio A_{420}/A_{330} was calculated and plotted against time. Resulting time course were fitted to a single exponential function (Equation 1) using Sigma Plot software:

$$Y_{obs} = ((Y_0 - Y_\infty)e^{-kt}) + Y_\infty \quad (1)$$

The Y_{obs} is the observed ratio A_{420}/A_{330}, Y_0 is the ratio A_{420}/A_{330} at time zero and Y_∞ is the ratio A_{420}/A_{330} at the end of the reaction. K is the pseudo first order rate of the reaction and t is the time.

6.2.6 Antibacterial Assays

6.2.6.1 Disk Diffusion Tests

Single colonies of *B. cenocepacia* strain J2315, - SAL-1, - *B. multivorans* ATCC 17616, - LMG 13010, *P. aeruginosa* PAO1, *E. coli* K12 MG1655, and *S. aureus* were picked and grown in 5 ml IS broth at 37°C overnight. The A_{600} was measured and the cultures were diluted in IS broth to an A_{600} of ~ 0.2. Two ml of diluted liquid culture of each strain was equally spread onto ISA plates containing different concentrations of polymyxin B (0-, 0.06-, 0.12-, 0.25-, 0.5-, 1-, 2-, 4-, 8-, 16-, 32-, 64-, 125-, 250-, 500-, 1000- μg). After ~30 s, the remaining fluid was suctioned, and the plates were dried for 1 hour.

D-cycloserine was dissolved in dH_2O, and sterile Whatman filter paper disks were dotted with 250 μg, 50 μg, and 10 μg by adding 4 μl of stock solutions of different concentrations. The filter disks were then directly placed on top of the agar plates. The plates were incubated for 24 hours at 37°C.

6.2.6.2 Minimal Inhibitory Concentration (MIC)

MIC data was generated as in the JAC guidelines [1]. Single colonies of the strains listed in table 5.1 (Section 5.5) were picked and grown overnight in 10 ml nutrient broth + 0.5% yeast extract. The next day, the overnights were diluted 1/10 in fresh broth and grown for an additional 2 h. at 37 ºC (mid-log phase). All strains were diluted 10 times in Saline (NaCl). This dilution was used as inoculum for the multipoint inoculator. This gives the recommended inoculum of 10^4 cfu/spot.

The plates, containing different concentrations of antibiotic ranging from 0 to 500 μg/ml (0, 1, 2, 4, 6, 8, 10, 12.5, 15, 20, 30, 40, 50, 75, 100, 125, 175, 200, 250, 300, 400, 500), were inoculated, allowed to dry, and incubated at 37 ^{o}C for 18 hours.

MICs values were taken according to the concentration of antibiotic where no growth could be observed.

6.2.7 Complementation Assays of ArnG in *E. coli* Knock-out Strains

E. coli knock-out strains AY100, AY101 and AY102 were made either chemically competent or electrocompetent. Cells were electroporated or transformated with the pTrc99a-ArnG vector. Systematically, the pTrc99a/FbpA plasmid (P. Bilton, PhD,

Ferric binding protein A) was also used as a control for the complementation tests. After transformation, cells were grown on plate with the appropriate antibiotic (kanamycin and/or ampicillin). One single colony was used to inoculate 10 ml of LB broth overnight at 30 ºC. This growth was then subcultured in 10 ml LB and further grown for 6 hours. The different cultures were then normalised at A_{600} and diluted as follows; 10^{-1}, 10^{-2}, 10^{-3} and 10^{-4}. Cells were spotted (3 µl) on PMB plate (0-15 µg/ml) and incubated overnight at 30 ºC.

6.2.8 Reference

1 Andrews, J. M. (2001) *J. Antimicrob. Chemother.* **48 Suppl**, 5-16

Appendix: Publications